UNIVERSITÀ DEGLI STUDI DI MILANO

Agriculture, Environment and Bioenergy
XXXV cycle

Department of Agricultural and Environmental Sciences - Production, Territory, Agroenergy

CARBON SEQUESTRATION UNDER CONSERVATION AGRICULTURE
STUDY AND MODELLING OF CARBON DYNAMIC

AGR-02

TOMMASO TADIELLO

prof. MARCO ACUTIS
prof.ssa ALESSIA PEREGO

COORDINATORE DEL DOTTORATO prof. PIERO ATTILIO BIANCO

A.A.
2021-2022

Table of Contents

1. Introduction

Why soil organic carbon is so important?

Soil organic carbon (SOC) is regarded as a crucial ecological indicator of soil health. Its presence in soils is essential for the active role in sustaining soil fertility (Smith et al., 2018) and mitigating the effect of climate change. Soil organic carbon sequestration can be a possible solution to mitigate climate change because of the long-lived atmospheric CO_2 conversion into soil carbon (Minasny et al., 2017). This phenomenon significantly reduces greenhouse gas emissions, so guidelines have been adopted worldwide to quantify changes in these emissions from agricultural soils, land-use changes and forestry (Lugato et al., 2014). Thus, studies of SOC sequestration are mandatory for decisions making on sustainability (Dai et al., 2014, Panagos et al., 2013).

In addition, soil organic carbon sequestration provides considerable benefits for agricultural soils because of its positive effect on soil health, resilience, and crop productivity (Mueller et al., 2010). The SOC importance in agricultural soils is due to the fact that SOC is the main component of soil organic matter (SOM) that supports key soil functions as it is critical for the stabilization of soil structure, retention and release of plant nutrients, and allowing water infiltration and storage in soil. In fact, the loss of SOC indicates a certain degree of soil degradation (FAO, 2017). Thus, the SOC impact on agricultural soil is strongly related to ensuring global food security, which is one of the greatest challenges of this millennium because of the increased food demand of over 9 billion people estimated for the year 2050 (Pravalie et al., 2021).

Which are the best management practices to increase the SOC stock?

To deal with these incoming challenges, it is fundamental to identify the best soil management to increase the SOC stock, especially in agricultural soils (Smith et al., 2015). In the recent decades, the scientific community has studied the different effects of several management techniques on soil. Paustian et al., (2016) estimated from recent scientific publications that different types of management such as afforestation, conversion to pasture, organic amendments, residue incorporation, no or reduced till and crop rotation are related to different SOC accumulation rates. In fact, soil C sequestration rate can greatly vary in agricultural land,

where it ranges between 0.1–1 Mg C ha^{-1} $year^{-1}$ as a function of land-use history, soil or climate conditions, and the combination of management practices applied (Ogle et al., 2005). The scientific research on different management practices allowed to define an ensemble of techniques that should help farmers increase the SOC stock amount in their soils. This group of best practices has been clearly defined by FAO (2017), and it is called "Conservation Agriculture" (CA). Its definition includes three different practices that have to be applied together:

- **Minimum mechanical soil disturbance** (i.e. no tillage) through direct seed and/or fertilizer placement. This reduces soil erosion and preserves soil organic matter;
- **Permanent soil organic cover** with crop residues and cover crops;
- **Species diversification** through varied crop sequences and associations involving at least three different crops.

Appling all these practices together allows to increase soil organic matter but also to reduces soil erosion, suppresses weeds, preserve soil moisture, avoids compaction of the soil and promotes good soil structure (Topa et al., 2021, Mondal et al., 2020, Blanco-Canqui and Ruis, 2018, FAO, 2017, Cooper et al., 2016).

Besides all these positive CA effects, there is still much more to understand about its impact on agricultural soil. In particular, there is a lack of knowledge on the actual CA benefit at greater soil depths (Minasny et al., 2017), its different impact across different climate conditions (Sun et al., 2020), on its minimum period of implementation to get positive results (Baker et al., 2007) or on its impact on soil gas emission (Haddaway et al., 2017). Besides comprehending the different CA mechanisms and the consequences of the CA application, the future climate-smart agriculture programmes will rely on the capacity to quantify the impact of specific practices across different pedo-climatic conditions. Most of all, knowing the uncertainties related to a specific agricultural practice evaluation will allow payments based on the level of uncertainty, and it will likely be part of programmes with financial incentives (Andrieu et al., 2019, Paustian et al., 2016). The scientific community will be part of this process if it can provide a reliable methodology to estimate or forecast different variables (e.g., C stock sequestration or crop production) across different pedo-climatic and temporal scenarios.

What is an effective approach to evaluate different management practices and their effects on SOC?

Process-based models consist of a set of mathematical equations representing physically based or (semi)empirical processes that describe plant development and growth as well as soil conditions as affected by weather, soil characteristics and crop management. Crop models are widely used to study, understand, and optimize crop production in current and future environments (Wallach et al., 2021). Process-based models are then likely to provide the most robust framework for estimating soil SOC dynamics (Paustian et al., 2016) for three main reasons: (1) process-based agroecosystem models simulate soil organic carbon dynamic as a function of climate, soil properties (soil organic matter content and nitrogen availability), crop residue production (type and quantity), and agronomic management (tillage, planting date, fertilization, irrigation) (Basso et al., 2015); (2) they, therefore, integrate multiple processes at the same time being able to represent also interaction between each other; (3) process-based agroecosystem models allow overcoming the temporal and physical peculiarity of the agronomical field research. For these reasons, process-based models are predictive and are likely to be the most appropriate tool when predicting different variables under present or future scenarios (Sándor et al., 2020, Smith et al., 2012, Ogle et al., 2010).

In addition to the process-based model's prediction capacity, these models are largely used to understand and study the impacts of many different pedo-climatic conditions on soil processes such as net mineralisation, spatio-temporal patterns of C fluxes or to estimate harvested phytomass (Sándor et al., 2020). So, their implementation and continued improvement are a priority for the current scientific research. At the same time, outputs from different models often differ, presenting a range of possible impacts and adaptation responses (Sándor et al., 2016). So, it has recently been shown that comparing different model at the same time may reduce the uncertainties of the simulations across contrasting soil and climate conditions in comparison with single models utilization (Ehrhardt et al., 2018). Therefore, the improvement of an already existing model, as it will be presented in this work, can be also evaluated within a comparison with other models. This gives the advantage of (1) checking how a new model release behaves according to measured data in comparison with other models and (2) compensating the errors across models allows as broader comprehension of model processes (Martre et al., 2015).

Purpose of the PhD

This PhD work aims to improve the existing modelling tools that allow quantifying and evaluating the CA impact on SOC sequestration with a specific link to the ARMOSA cropping system model (Valkama et al., 2020, Perego et al., 2013)

This model has been used in several regional and European projects (LandSupport, HelpSoil, GENESIS, MACSUR) because it is a versatile tool to represent the carbon and nitrogen fluxes and the influence of high levels of agroecosystem processes varying in response to agricultural management and pedoclimatic conditions. At regional to national scale, the capability of depicting multi-crop rotation in a medium to long-term perspective allows quantification of crop production and environmental aspects in response to varying market and policy needs (e.g., organic farming, greening, and healthy diet habits).

The PhD intends to improve the ARMOSA capability to reproduce the effect of different soil management on soil organic carbon sequestration with particular attention to the CA practices. To reach this goal, the PhD activities have been organized as follows:

1. **CHAPTER 1: Soil Organic Carbon Sequestration Under Conservation Agriculture In Mediterranean And Humid Subtropical Climates: A Meta-Analysis.**

OBJECTIVE: understand how CA impacts soil organic carbon sequestration in areas that can benefit the most from this agricultural technique.

RESULT: I analyzed worldwide data to quantify the CA effect on SOC sequestration through a meta-analysis.

2. **CHAPTER 2: Computation of total soil organic carbon stock and its standard deviation from layered soils.**

OBJECTIVE: the meta-analysis highlighted some weakness in the way SOC data are collected and analyzed. To prevent any bias in the summary and interpretation of the results we want to solve these problems.

RESULT: I developed a specific tool that allows a correct computation of carbon stock and its standard deviation (SD) from the product between SOC concentration and bulk density or the sum of SOC stocks of multiple correlated sub-layers.

3. **CHAPTER 3: A new module to simulate surface crop residue decomposition: description and sensitivity analysis.**

OBJECTIVE: based on the results of the first activity (chapter 1), I identify the ARMOSA weaknesses in representing the CA impact on SOC in agricultural soil. The objective is to improve the ARMOSA capacity to simulate the CA practices based on what learn from the first activity.

RESULT: I developed and tested a new ARMOSA release that specifically improves the quality and reliability of the output concerning the SOC dynamic. I developed a new module to be integrated into ARMOSA that precisely reproduces the superficial crop residue decomposition.

4. **CHAPTER 4: Simulation of the new SOM fractions**

OBJECTIVE: Based on the improved ARMOSA capacity to represent the CA management and the new scientific achievement about SOM dynamics we want to redefine the way ARMOSA represents soil organic matter dynamics.

RESULT: I developed a new ARMOSA release that redefines how the organic matter is simulated and represented.

Chapter 1. Soil Organic Carbon Sequestration Under Conservation Agriculture In Mediterranean And Humid Subtropical Climates: A Global Meta-Analysis

This is the official draft submitted to the European Journal of Soil Science and currently under peer review.

Authors:

Tommaso Tadiello[a*], Marco Acutis[a], Alessia Perego[a], Calogero Schillaci[b], Elena Valkama[c]

Affiliation:

[a]DiSAA, Department of Agricultural and Environmental Sciences, University of Milan, Italy

[b]European Commission, Joint Research Centre (JRC), Ispra, Italy

[c]Natural Resources Institute Finland (Luke), Bioeconomy and Environment, Sustainability Science and Indicators, Tietotie 4, 31600 Jokioinen, Finland

**Corresponding author (tommaso.tadiello@unimi.it, DiSAA, Department of Agricultural and Environmental Sciences, University of Milan, Italy)*

Abstract

Conservation agriculture (CA) is an agronomic system based on minimum mechanical soil disturbance (i.e., no-tillage, NT), permanent soil cover and species diversification. Since the 2000s, the effects of NT on soil organic carbon (SOC) changes have been summarized in several meta-analyses, conducted mostly on a global scale, which drew somewhat inconsistent conclusions. There is a knowledge gap in relation to the Mediterranean and humid subtropical climates. Therefore, by using a weighted meta-analysis we summarized the results of 47 studies (between 1998 and 2020) all around the world in these climates. To increase precision of SOC stock computation, we included only studies with measured carbon stocks or where carbon concentration and bulk density were reported. We examined different sources of variation in SOC responses to CA, such as soil characteristics (clay and sand content, SOC levels under conventional agriculture), agricultural management (N fertilization levels, the duration of CA practice, crop diversification, the proportion of high-residue crops in rotations), climate and geography.

The overall effect of CA on SOC accumulation in the plough layer (0-0.3 m) was 12% (95% CI 8-17%, n = 47) greater in comparison to conventional agriculture. However, the response was 20% (95% CI 12-28%, n = 22) in soils which had < 40 Mg C ha^{-1} ("Low" SOC level) under conventional agriculture, while it was only 7% (95% CI 3-11%, n = 25) in soils that had > 40 Mg C ha^{-1} ("High" SOC level). Furthermore, splitting the dataset into these two groups enabled us to detect specific effects of agronomic and environmental factors within each group. In soils with "Low" SOC level, the response increased with the longer duration of CA practice and with the increasing proportion of crops in a rotation with high residue biomasses. In soils with "High" SOC level, the duration of CA practices and clay content were the main factors influencing the magnitude of SOC increases. Climate and geography had specific effects on SOC accumulation due to CA, depending on the SOC level under conventional agriculture. We conclude that the greatest benefits from CA application in terms of SOC increase can be reached in agricultural soils with low SOC content and located in the middle latitudes or in the dry conditions of Mediterranean and humid subtropical climates.

1.1 Introduction

Soil organic carbon (SOC), the major component of soil organic matter, has a great impact in all soil processes. SOC dynamics are regulated by climatic variables, geographical characteristics, soil physico-chemical properties, quantity and quality of C inputs into the soil and management practices, as well their interactions (Haddaway et al., 2017; Lal, 2004; Lorenz and Lal, 2018; Ogle et al., 2019; Paustian et al., 1997; West and Post, 2002). Playing an important role in modifying the SOC dynamics (Lorenz and Lal, 2018), conservation agriculture (CA) is being promoted by FAO as an approach for achieving sustainable land management, environmental protection and climate change adaptation and mitigation (Pisante et al., 2015). Conservation agriculture utilizes three agronomic principles: [1] minimum soil disturbance, avoiding soil inversion, i.e., no-tillage (NT) or minimum tillage or vertical tillage; [2] permanent soil cover that is guaranteed by retaining crop residues or by cover crop adoption; and [3] the integration of crop rotations involving at least three different crops (FAO, 2017b).

Since the 2000s, the effects of NT on SOC changes have been summarized in nine meta-analyses conducted mostly on a global scale, but with a few on regional or national scales. These analyses have drawn somewhat inconsistent conclusions (Table 1). Most of the meta-analyses revealed a range of SOC sequestration increases attributable to NT from 8 to 18 % in the 0-0.25/0.3 m soil layer, when log response ratio was used as the index of effect size. In contrast, for temperate climates, Mondal et al. (2020) reported a 40% and a 5% of SOC increases in the 0-5 and 5-10 cm soil depths, respectively, while there was a significant decrease in deeper soil layers, resulting in a slight overall increase of 1.1% in the 0-0.6 m soil layer (Table 1). The meta-analyses that used mean difference as an index of effect size reported discrepancies in outcomes too, since Haddaway et al. (2017) found a SOC sequestration almost twice as large as that reported by Luo et al. (2010) and by West and Post (2002). In addition, different meta-analyses demonstrated inconsistent outcomes for the effects of pedo-climatic factors on SOC accumulation under NT management (Table 1). For example, regarding the soil texture, the effect of NT varied from study to study: increasing effects were only reported in silty and sandy soils within the 0-0.3 m layer (Li et al., 2020), or in loamy and clay soils within the 0-0.1 m layer (Mondal et al., 2020). Sometimes there were no effects of the texture class (Haddaway et al., 2017; Sun et al., 2020). Moreover, Li et al. (2020) reported that conservation tillage practices increased SOC stock in humid or perhumid (Thornthwaite, 1948) climate conditions, but not in semi-humid. Mondal et al. (2020) highlighted that in tropical and subtropical climates, the effect was positive and significant only up to 10-cm depth, whereas in temperate climates, changes were significant but negative further down the profile. However, Sun et al., (2020) stated that CA adoption

is recommended in arid regions, while other meta-analyses did not report a significant effect of climate (Haddaway et al., 2017; Luo et al., 2010; Virto et al., 2012).
On the other hand, the impact of carbon input into soil, which has been considered as a key factor involved in SOC accumulation, was confirmed by many meta-analyses (Table 1). It is also common to refer to the effect of experiment duration to explain the variability of SOC responses across the studies. In this case, five out of nine meta-analyses demonstrated the importance of the NT management duration on SOC accumulation, finding greater effects when the duration of the experiment was longer. Nevertheless, Luo et al. (2010) and Sun et al. (2020) found no consistent relationships with the duration of NT practice.

The reason of such inconsistencies mainly stems from the different methodologies or even erroneous approaches applied in the nine meta-analyses. For instance, three meta-analyses included studies in which bulk densities were not originally measured but were estimated from pedotransfer functions to compute SOC stocks from SOC concentrations. The potential uncertainty which can arise by applying a pedotransfer function developed in a particular area and which is then applied on different sites (Schillaci et al., 2021) can seriously impact the final results. Another problem occurs when multiple observations are extracted from a single experiment or from different time points throughout a study, as for example, in studies by Li et al. (2020) and by Mondal et al. (2020), who extracted 1928 and 4,131 pairs of data points from 243 and 522 studies, respectively. Such "relaxed" approach (all effect size observations from each experiment, derived from multiple observation, for example, over time or over soil depths) may overestimate the significant outcome of the meta-analysis by narrowing the confidence intervals that do not overlap with zero indicating a control (Hungate et al., 2009). Lastly, 7 out of 9 meta-analyses were weighted by sample size or not weighted at all. This may produce seriously biased estimates of the overall effects by exaggerating the results from small and imprecise studies (Gurevitch et al., 2018; Koricheva et al., 2013). Within one meta-analysis, weighting by sample size or with no weight gave comparable estimates that were often larger than weighting by the inverse of the variance (Hungate et al., 2009).

In addition to the shortcomings listed above, reviewing the existing meta-analyses on SOC sequestration under NT also indicated a knowledge gap for a specific climate, in particular for areas characterized by mild winters and hot summers (Bouma, 2005; Hernandez-Ochoa and Asseng, 2018). Therefore, the integrated outcomes related to SOC sequestration in such climates are limited since only one meta-analysis summarizing 33 studies on herbaceous crops was conducted in similar

climatic conditions (Aguilera et al., 2013). After more than eight years from their publication, an update of the results related to carbon sequestration could be helpful to integrate new findings.

In this type of climate, found in areas mainly characterized by temperate and Mediterranean climates (Köppen sub-types Cfa, Csa, Csb, Csc), SOC mineralization rates are accelerated because of unfavorable climatic conditions (Álvaro-Fuentes and Paustian 2011; Pravalie et al., 2021) and soils usually have quite low SOC content (FAO, 2017a; Jones et al., 2005). Predicted climate change is expected to accentuate human-induced desertification processes (Ruiz et al., 2020; Spinoni et al., 2015; Underwood et al., 2009).

Based on these considerations, deduced from a scientific literature screening, a robust meta-analytic approach could highlight the possibility of CA adoption to mitigate soil C depletion by increasing the low soil C content in these climatic regions, in which agriculture is usually based on intensive traditional plough-based crop production systems (Mazzoncini et al., 2016).
Therefore, the present study aims to summarize studies on the effects of CA on SOC sequestration capability in the plough layer (0-0.3 m) in Mediterranean and humid subtropical climates (from all over the world) by using a weighted meta-analysis. To overcome the weaknesses of the previous meta-analyses, we used a rigorous approach that relies on including studies with measured bulk density (when carbon stock was not already reported) and utilizing no pedotransfer functions to compute the carbon stock; the computation of a single effect size per study/site; and weighting by inverse variance. We examined different sources of variation in SOC responses to CA across the studies, such as climate, geography, soil characteristics (clay and sand content, SOC levels under conventional tillage) and agricultural management (N fertilization levels, duration of CA practice, crop diversification, proportion of high-residue crops in rotation).

Table 1. Description of meta-analyses studying the effects of no-tillage on SOC stock compared to conventional tillage published during the last 20 years.

		Li et al. (2020)	Sun et al. (2020)	Mondal et al. (2020)	Aguilera et al. (2013)	Haddaway et al. (2017)	Luo et al. (2010)	West and Post (2002)	Virto et al. (2012)	Angers and Eriksen-Hamen (2008)
	Origin	global	global	global	Mediterranean	global	mostly USA and Canada	global	global	global
	Type of effect size	log response ratio	log response ratio	log response ratio	log response ratio	mean difference	mean difference	mean difference	non-standard metrics	non-standard metrics
	No till overall effect[1]	+13% (§ 3.1)[2]	+ 8% (Fig. 4)	+1.1% (Fig. S6)	+18.2% (§ 3)	+ 4.6 Mg ha^{-1} (Fig. 35)[2]	+ 2.8 % (p. 228)	+ 16% (p. 1943)	+ 7% (p. 21)	+ 5% (p. 1373)
	Soil depth range (m)	0-0.3	0-0.3	0-0.6	0-0.25	0-0.3	0-1	0-0.3	0-0.3	0-0.9
	Crops	herbaceous crop	herbaceous crop	cereal and legume	cereals, horticulture	herbaceous crop	herbaceous crop	herbaceous crop	herbaceous crop	mainly cereal
	Bulk density	measured	pedotransfer	measured	pedotransfer	measured	pedotransfer	measured	measured	measured
Effect of moderators	**Climate**	no effect in semi-humid climate (Fig. 7)	positive effect in dry region (Fig. 4)	the effect dependent on climate and soil depth interaction (Table 3)	-	no effect (p. 22)	no effect (Fig. 5a, b)	-	no effect (Fig. 1a/b/c)	-
	Soil	positive effect with sandy and silty soils (Fig. 6)	no effect of clay and sand (Fig. 1)	loamy and clay texture positively affects only 0-0.1 m layer (Table 3)	-	no effect (p. 22)	-	-	no effect (Fig. 1d)	-
	C input	positive effect regardless of tillage intensity (§ 3.1)	the most important management factor (decision tree, Fig. 1)	effect only in upper layers (§ 4)	positive (§ 4)	-	-	-	positive (Fig. 2)	-
	Experiment duration	positive (§ 3.4)	no effect (Fig. 1)	positive effect only 0-0.1 m layer (Table 3)	-	positive (p. 22)	no effect (Fig. 5c)	peak sequestration rates in 5 to 10 yr (Fig. 5)	-	positive (Fig. 2)
	N° of studies[3]	**not declared for SOC under no till (243 in total)**	**115**	**not declared for SOC under no till (522 in total)**	**33**	**29**	**69**	**74**	**37**	**24**

(1) Related to the selected soil depth range; (2) Effect size is weighted by inverse variance (3) N° of studies that evaluated the effects of no-tillage on SOC stock compared to conventional tillage.

1.1 Materials and Methods

1.1 Systematic search and data extraction from literature

The database creation for the final statistical analysis involved three different steps: (1) primary studies collection from different online database resources, (2) selection of studies with several inclusion criteria to match the research purpose and (3) data extraction.

1.1.1 Studies collection

We found the articles by searching for keywords with a nested query (Supplemental file 1) in Web of Science and Scopus databases, obtaining two different datasets. The query was based on four different parts related to conservation agriculture, conventional tillage, SOC and the list of the 67 countries that belong to Mediterranean and humid subtropical climates (i.e., that have at least one correspondence with the Cfa, Csa, Csb, Csc sub-types) of the Köppen classification (Chen and Chen, 2013; Peel, 2007). Finally, the Bibliometrix R package (Aria and Cuccurullo, 2017) was utilized to merge the resulting two databases, excluding the duplicated studies. The outcome of this search consisted of 960 studies.

1.1.2 Inclusion criteria

To be included in the final database, a study had to meet the following criteria:

1. the study was conducted on herbaceous field crops;
2. the study coordinates belong to Cfa, Csa, Csb or Csc;
3. the study had an appropriate control group (conventional agriculture): inversion/mixing tillage (moldboard/disk plowing, disk harrow or chisel plowing) in spring, autumn or in both, residues incorporated and no cover crop utilization. Within the single study, the rotation with the least number of crops was selected;
4. the study had an appropriate treatment group (conservation agriculture): no tillage management, residues retained on the top of the soil (chopped or not) and with or without cover crops. Within the single study, the rotation with the largest number of crops was selected;
5. the study assessed the effect of CA on SOC stock or concentration in the plough layer reported either for a single soil layer (e.g., 0-0.30 m or 0-0.2 m) or for multiple soil layers (e.g., 0-0.15 m and 0.15-0.30 m);
6. along with SOC concentration, the study reported bulk density (BD) measured separately for control and treatment;

7. at the end of experiment, SOC was recorded as means for treatment (CA) and control (conventional agriculture), with sample sizes and standard deviations (SD) or standard errors (SE), or statistical analysis references (e.g., P(F) or LSD value from the ANOVA table) to compute SD.

1.1.3 Data extraction

The data extraction method is crucial to deal with the non-independence of the observations that can lead to underestimates of the standard error of the mean effect and therefore liberal evaluations of the statistical significance of effects (Gurevitch and Hedges, 1999; Nakagawa et al., 2017).

To avoid problems with non-independence of the effect sizes, only one pair comparison corresponding to the last sampling date was extracted from a study. If an article reported results from different experimental sites with different pedo-climatic characteristics, those sites were considered as independent studies and were included in the database. However, if several articles referred to the same experimental site with the same pedological characteristics, the article with the longest experimental duration was chosen.

Several articles treated factorial experiments, in which tillage treatments were studied in combination with different fertilization or cover crops. In the case of different fertilization levels, the second one from the top was chosen for both control and treatment. Legume cover crops were selected as a first choice when available.

Data were extracted from tables and digitized from figures using WebPlotDigitizer software (Rohatgi, 2020). Standard errors were converted to standard deviations ($se = \frac{SD}{\sqrt{n}}$ where n is the number of replicates) where necessary. When no measure of variability was provided, we extracted the SD from the ANOVA table using the EX-TRACT tool (Acutis et al., 2021a, Acutis et al., 2021b). This tool allows the estimation of the experimental error (i.e., standard deviation and standard error of treatments mean) associated to statistical analysis results of published articles (i.e., estimated from the LSD, P(F) values or even from the letters assignment indicating differences among means based on the results of a multiple comparison test).

1.2 Database creation

The final database used for this study consisted of 47 studies (Fig. 1S, Supplemental file 1) published in 41 articles in peer-reviewed scientific journals (Table 2 and Supplemental file 3).

No restrictions were set about the articles` publication date: those selected were published between 1998 and 2020. The final number of studies was only 5% of that obtained by searching for keywords.

Studies were located in North America (n=19), South America (n=9), Europe (n=10), Asia (n=8) and Africa (n=1) between 23° and 36° S and 19° to 45° N of latitude (Table 2). The soils mainly belonged to the clay, loam and silt loam texture classes, and annual precipitation ranged from 331 to 1850 mm. The major climate sub-types were Cfa (n = 33) and Csa (n = 13), while only one study referred to Csb, and no studies referred to Csc.

The soil management of the controls included different soil inversion techniques of which the fall/spring moldboard ploughing was the most frequent (71% of the studies). In all cases, control and treatments included nitrogen fertilization, weed control (without soil mechanical disturbance for the treatments) and no grazing. These main agronomic features were kept the same during the entire duration of experiments, ranging from 2 to 51 years. At least three different crops in the rotation of the treatment were reported in 11 studies, and monocropping in 9 studies. Four studies did not report any information on crop rotation.

Table 2. Studies included in the meta-analysis on the effect of conservation agriculture on soil organic carbon sequestration in Mediterranean and humid subtropical climates.

Study ID	*Authors*	*Year*	*Country*	*Site*	*Crops*[1]	*Duration (year)*	*Rainfall (mm year^{-1})*	*Clay (%)*	*Sand (%)*	*SOC*[2]	*Plough layer (cm)*[4]
1	Loopez-Garrido et al.,	2011	Spain	Alange-Badajoz	1	3	500	22	38	stock	25
2	Loopez-Bellido et al.,	2019	Spain	Cordoba (Malagon)	-	29	549	69	12	stock	30
3	Plaza-Bonilla et al.,	2010	Spain	Agramunt (AG-1)	1	2	430	21	24	stock	30
4	Plaza-Bonilla et al.,	2010	Spain	Agramunt (AG-17)	2	17	430	18	30	stock	30
5	Lopez-Bellido et al.,	2010	Spain	Cordoba	2	20	584	69	22	stock	30
6	Alvaro-Fuentes et al.,	2008	Spain	Selvanera	3	18	475	17	36	stock	30
7	Lopez-Garrido et al.,	2011	Spain	Alange-Badajoz	3	4	485	24	58	stock	30
8	Cid et al.,	2014	Spain	Alameda del Obispo farm	2	5	536	13	47	stock	30
9	Fiorini et al.,	2020	Italy	Luignano	1	8	914	13	61	stock	30
10	Badagliacca et al.,	2018	Italy	Pietranera experimental farm	-	23	572	52	26	concentration	30
11	Khorami et al.,	2018	Iran	Zarghan Field Station	2	3	331	38	22	concentration	30
12	Celik et al.,	2019	Turkey	Çukurova Agricultural Research Station	3	10	642	49	18	concentration	30
13	Jemai et al.,	2012	Tunisia	Mateur	2	7	560	28	34	stock	30
14	Higashi et al.,	2014	Japan	-	2	9	1154	10	32	stock	30
15	Wang et al.,	2019	China	Yangtze Plain	1	11	1360	40	36	stock	30
16	Xionghui et al.,	2011	China	Changsha County	1	3	1500	NA[3]	NA[3]	stock	30
17	Li et al.,	2010	China	Wuxue City	2	3	1360	33	10	concentration	20
18	Cheng-Fang et al.,	2012	China	Wuxue City	2	3	1360	47	3	stock	20
19	Xu et al.,	2013	China	Ningxiang	1	4	1358	NA[3]	NA[3]	stock	30
20	Costa de Campos et al.,	2011	Brazil	FUNDACEP research center	3	25	1774	53	24	stock	30
21	Babujia et al.,	2010	Brazil	Embrapa Soja experimental station	2	20	1651	71	20	stock	30
22	Boddey et al.,	2010	Brazil	Passo Fundo	3	17	1750	64	22	stock	30
23	Machado et al.,	2003	Brazil	Londrina	3	20	1622	76	22	stock	30
24	Dieckow et al.,	2009	Brazil	Santo Angelo	2	25	1850	71	5	stock	20

25	Dieckow et al.,	2009	Brazil	Eldorado do Sul	2	18	1440	22	54	stock	20
26	Freixo et al.,	2002	Brazil	Centro Nacional de Pesquisa do Trigo	3	11	1746	59	22	stock	30
27	Bono et al.,	2008	Argentina	Anguil Experimental Station	4	5	664	20	53	stock	25
28	Noellemeyer et al.,	2013	Argentina	Dorila	6	16	703	10	32	stock	15
29	Scopel et al.,	2005	Mexico	La Tinaja	1	5	525	15	61	stock	20
30	Salvo et al.,	2010	Uruguay	Experimental Station Mario A. Cassinoni	7	10	1224	29	27	stock	20
31	Siri-Prieto et al.,	2007	United States	Alabama Agricultural Experiment Station	4	3	1400	7	78	concentration	20
32	Minoshima et al.,	2007	United States	Long Term Research in Agricultural Systems site	2	2	394	33	10	concentration	30
33	Terra et al.,	2005	United States	Alabama Agricultural Experiment Station	3	2	1330	17	55	stock	30
34	Hendrix et al.,	1998	United States	Horseshoe Bend (LTE experiment)	4	17	1300	17	37	stock	20
35	Hendrix et al.,	1998	United States	Griffin	2	3	1300	10	32	stock	25
36	Hendrix et al.,	1998	United States	Horseshoe Bend (STE experiment)	2	3	1300	17	37	stock	25
37	Blanco-Canqui et al.,	2011	United States	Hutchinson	3	23	889	17	37	stock	30
38	Olson,	2010	United States	Dixon Springs Agricultural Research Center	2	20	1255	13	35	stock	15
39	Puget and Lal,	2005	United States	Don Scott Experimental Farm	2	8	995	33	10	stock	25
40	Gal et al.,	2007	United States	Agronomy Center for Research and Education	-	27	1083	33	10	stock	30
41	Blanco-Canqui and Lal,	2008	United States	Jackson	3	12	1082	13	35	concentration	30
42	Blanco-Canqui and Lal,	2008	United States	Canal Fulton	2	15	1006	17	37	concentration	30
43	Blanco-Canqui and Lal,	2008	United States	Troy	1	20	1081	17	37	concentration	30
44	Mishra et al.,	2010	United States	Western Agricultural Research Station	1	44	952	20	15	concentration	30
45	Sainju et al.,	2008	United States	Alabama Agricultural Experimental Station	-	10	1562	27	15	stock	20
46	Dou et al.,	2008	United States	Brazos River floodplain	3	20	978	43	43	stock	30
47	Burgos Hernandez et al.,	2019	United States	Wooster	2	51	1018	13.5	35	stock	30

[1] Number of crops in the rotation; [2] all carbon data were converted into stock; [3] NA: data not available; [4] soil depth considered in the present study.

Most of the studies (38) report the bulk density while the standard deviation was not always reported: 27 studies did not report SD or SE. For the remaining articles (20) no additional computation was required to obtain a measure of variability.

1.3 Soil organic carbon computation

The results for SOC changes in the plough layer for controls and treatments were reported as stock (Mg ha^{-1} or kg m^{-2}) in 37 studies or as concentration (g kg^{-1} or %) and bulk density (BD) that were converted to stock in 10 studies. Studies that reported C concentrations with no measured BD were excluded from the final database. Moreover, to avoid false computation due to ignoring the differences in soil BD between treatments (Du et al., 2017; Toledo et al., 2013), only studies with BD measured separately for treatment and control were considered.
SOC was reported for a single topsoil layer (e.g., 0-0.30 m or 0-0.2 m) in 29 studies and for multiple soil layers (e.g., 0-0.15 m and 0.15-0.30 m) in 18 studies (see Supplemental file 2). Nowadays, to assess different agronomic practices, it is usually required to report SOC as mass per unit area (Mg ha^{-1} or kg m^{-2}) for a single soil layer (e.g., 0-0.3) and the associated standard deviation. Nevertheless, sometimes data were not directly reported as mass per unit area, or multiple layers were included. To deal with these kinds of data, we developed a specific methodology to compute a mean of SOC for a single soil layer and its SD from a product of two normally distributed variables (C concentration and BD, being correlated variables) or from a multiple correlated layer sum, when SOC results for several layers were reported (Tadiello et al., 2022). This method allows considering the correlation coefficient between C concentration and BD or/and between multiple sub-soil layers for a better estimation of the SD of the single stock soil layer.

1.4 Explanatory variables

To explain the variation in SOC stock due to the CA application in the plough layer, we included pedo-climatic and management-related explanatory variables (moderators) listed in Table 3.
Latitude and longitude were expressed as decimal degrees; latitude moderator was expressed as the absolute value (e.g., 30° and -30° refer to the same latitude, indicating an equal distance from the equator).

Table 3. Categorical and continuous explanatory variables (moderators) included in the meta-analysis.

Type	Moderator	Group or range
Climate	Köppen classification	Cfa, Csa, Csb
	Rainfall (mm year^{-1})	331 - 1850
	Average annual temperature (°C)	10-21
Geography	Continent	Asia, Africa, Europe, North America, South America
	Longitude (degree)	-121 - 139
	Latitude (degree absolute value)	19 - 45
Soil	SOC level under conventional agriculture (Mg ha^{-1})	18 - 102
	SOC level under conventional agriculture (Mg ha^{-1})	low (<= 40), high (> 40)[1]
	Clay (%)	7 - 76
	Sand (%)	3 - 78
Agronomic management	N fertilization level (kg N year^{-1})	0 - 390
	Experiment duration (years)	2 - 51
	Number of crops in treatment rotation	<3, >= 3
	Proportion of crops with high residue biomass (%)[2]	0 - 100

[1] based on Lugato et al. (2014); [2] grain maize, sorghum, cotton, rice.

If annual average annual rainfall or temperature were missing in a study, we used the value available from World Bank Group (World Bank Group, Climate change knowledge Portal, 2021). When only the textural class of the soil was available, we used the central values of clay and sand of the given textural class as continuous moderators.

Based on the SOC in control (SOC_{ctrl}) in the plough layer (0-0.3 m) measured at the end of the experiment, we created two different studies groups (i.e., "Low" SOC level and "High" SOC level). A single study (x) was then assigned to one of the groups following this formula:

$$\begin{cases} if\ (SOC_{ctrl}/layer\ depth) * 0.3\ <=\ 40 & Then\ \ x\ \in\ "Low"\ SOC\ level\ group \\ if\ (SOC_{ctrl}/layer\ depth) * 0.3\ >\ 40 & Then\ \ x\ \in\ "High"\ SOC\ level\ group \end{cases}$$

where layer depth is expressed in meters.

The threshold was selected based on the paper by Lugato et al. (2014), who reported that, in the Mediterranean area, frequently the topsoil SOC stock values were below 40 Mg C ha^{-1}.

We included the number of crops in a treatment rotation as an explanatory variable, because the presence of at least three different crops is one of the three CA principles defined by FAO (2016). Moreover, we included the proportion of crops with high residue biomass (grain maize, sorghum, cotton, rice) in a rotation as an indicator of C input to the soils.

1.5 Meta-analysis

Meta-analyses were conducted in R (R Core Team, 2018) with the "metafor" package (Viechtbauer, 2010, see Supplemental file 4 for the code used).

Quantitative meta-analysis involves calculating an effect size (i.e., the magnitude of the treatment effect) that can be averaged across independent studies. Since two experimental groups have been compared, the response ratio (r) was computed for the response variables as an index of the effect size:

$$r = \bar{X}_{CA}/\bar{X}_C \quad [1]$$

where $\bar{X}_{CA}$ and $\bar{X}_C$ represent the means for treatments (conservation agriculture) and for control (conventional agriculture), respectively, averaged for experimental replicates or samples.
Since the distribution of r is skewed, performing statistical analyses in the metric of the natural logarithm of r is usually preferred due to its much more normal distribution in small samples than that of r (Hedges et al., 1999):

$$\ln(r) = \ln(\bar{X}_{CA}/\bar{X}_C) = \ln(\bar{X}_{CA}) - ln(\bar{X}_C) \quad [2]$$

We calculated the variance of ln(r) as:

$$V_{\ln(r)} = \frac{(SD_{CA})^2}{n_{CA}(\bar{X}_{CA})^2} + \frac{(SD_C)^2}{n_C(\bar{X}_C)^2} \quad [3]$$

where SD_{CA} and SD_C are the corresponding standard deviations, and n is the sample size.

We assumed that studies do not share the same effect sizes and consequently we used a random effects model to combine estimates across the studies. The application of this kind of model accounts for experimental method differences between studies (that are considered only a random sample of possible effect sizes) which may introduce variability ("heterogeneity", τ^2) among the true effects.
We calculated the weighted mean of the log response ratio for all studies as:

$$\overline{\ln(r)} = \frac{\sum_{i=1}^{n} w_i \ln r_i}{\sum_{i=1}^{n} w_i} \quad [4]$$

where lnr_i is the log response ratio for study i, n is the number of studies, and w_i is the weight for study i, defined as:

$$w_i = \frac{1}{V_i + \tau^2} \quad [5]$$

where V_i is the variance of the study i and τ^2 denotes the amount of residual heterogeneity (between-study variance). Because the variance of the effect sizes is a function of the sample size (Eq. 3), studies with a larger sample size had lower variances and received heavier weights.

The τ^2 parameter is considered the variance of the true effect size. Since is it not possible to compute it from the entire population of the effect size, the τ^2 is an estimation from the observed effect:

$$\tau^2 = \frac{(Q - df)}{C} \quad [6]$$

where

$$Q = \sum_{i=1}^{k} w_i(Y_i - M)^2, df = n - 1, C = \sum w_i - \frac{\sum w_i^2}{\sum w_i}$$

where w_i is the study weight, Y_i is the study effect size, M is the summary effect, and n is the number of studies. The τ^2coefficient is in the same metric (squared) as the effect size itself and reflects the absolute amount of variation in that scale (Borenstein et al., 2009). To describe the distribution of the effect size it is more useful to use its "standard deviation" measurement expressed as:

$$\tau = \sqrt{\tau^2} \quad [7]$$

that is on the same scale as the effect size itself but, while τ^2 is a squared value, τ is not.

The *rma* function has been used to compute the random model and the maximum-likelihood estimator ("ML") to estimate the amount of heterogeneity (Raudenbush, 2009). When a moderator was taken into account in the model to explain at least part of the total heterogeneity, a mixed-effect model was fitted.

The Cochran's Q-test (Hedges and Olkin, 1985) was used to test the null hypothesis $H_0 : \tau^2 = 0$ that examines the between-group heterogeneity, while an omnibus test (that excludes the intercept β_0) of all the model coefficients was conducted when moderators were included in the model (test of moderator, model (Q_M) heterogeneities). Weighted meta-regressions were run to study the effect of continuous explanatory variables, with ln(r) as the dependent variable and the continuous variables as independent ones.

For the outliers' identification we used the backward search algorithm specifically developed for meta-analysis (Mavridis et al., 2017). Backward search algorithms start with the full data set and remove sequentially outlying observations until all outliers have been removed. This method can be useful when there are a few outlying studies (Mavridis et al., 2017).

Moreover, the descriptive I^2 statistic (%) was reported for the overall effect size. This coefficient is useful to explain the estimated amount of heterogeneity as the inconsistency across the studies (Borenstein et al., 2009), and it is expressed as the ratio between the true heterogeneity and the total variance:

$$I^2 = \frac{\tau^2}{\tau^2 + V_Y} * 100 \quad [8]$$

where V_Y is the within study variance.

As an additional parameter, the metafor package also computed the R^2 statistic (Raudenbush, 2009) as the ratio:

$$R^2 = \frac{\hat{\tau}^2_{RE} + \hat{\tau}^2_{ME}}{\hat{\tau}^2_{RE}} \quad [9]$$

where $\hat{\tau}^2_{RE}$ refers to the random model τ^2 (total amount of heterogeneity) while $\hat{\tau}^2_{ME}$ to the estimated value of τ^2 based on the mixed-effect model. The R^2 coefficient defines the amount of heterogeneity accounted for by the moderator inclusion in the model. This coefficient does not take into account the within-study variance and, for this reason, it cannot be compared to the classical R^2 referred to *OLS (ordinary least square)* regression.

Results were back-transformed, except for meta-regression, and reported in the text and figures as percentage changes from the controls:

$$Response(\%) = [EXP(\ln(r)) - 1] * 100 \quad [10]$$

The percentage difference between the control and the treatment is a straightforward way to show the increment/decrement of SOC due to the conservation agriculture technique.

The p-value and the 95%CI were used to identify the significant effect of continuous and categorical moderators, respectively (Hedges et al., 1999).

To detect possible publication bias in the meta-analysis we first used a graphical method based on two funnel plots (Nakagawa et al., 2021; Nakagawa et al., 2017; Sterne and Egger, 2001). The x-axis displays the ln(*r*), and the y-axis is the sample size and the standard error respectively in the two funnel plots. When the standard error (SE) was used as the vertical axis, it had the zero placed at the top (i.e., standard error 0 at the top). In this way, the largest studies have the smallest standard errors, and they are placed at the top of the graph. When present, the diagonal lines show the expected 95% confidence intervals around the summary effect.

Moreover, we checked the funnel plots asymmetry with the Egger's regression test for the mixed-effects model reported by Viechtbauer (2010) and implemented in the "regtest" function.

To assess the robustness of the observed effects the fail-safe number (Nfs) has been computed for both "Low" and "High" SOC groups to estimates the number of non-significant, unpublished, or missing studies need to be added to a meta-analysis to change its results from significant to non-significant. Specifically, we used the Rosenthal method (Rosenthal, 1979) that estimates how many missing studies we would need to retrieve and incorporate in the analysis before the p-value became non-significant (Borenstein et al., 2009).

1.3 Results

1.3.1 Overall effect and SOC levels

For the entire database, the CA effects on SOC was highly variable, ranging from -9% to 99% compared to the controls, with a weighted summarized effect of 12% (95% CI 8-17%, n = 47, Fig. 1).

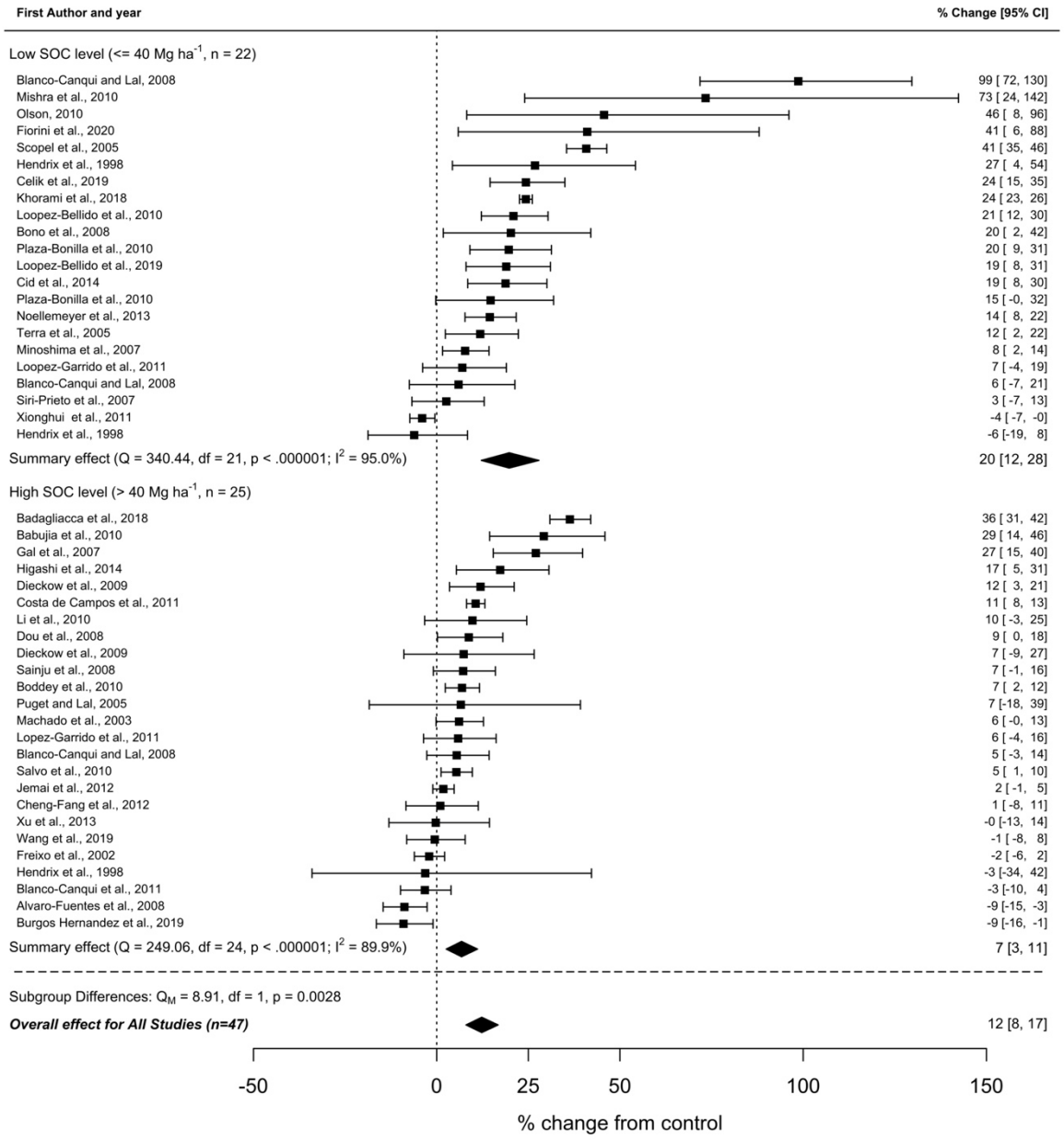

Figure 1. *Forest plot showing the results of 47 studies examining the effect of conservation agriculture on SOC sequestration. The diamonds are centred on the summary effect, which was estimated for the "Low" and "High" SOC level separately. The overall effect diamond (n = 47) is also displayed at the bottom of the plot. Lateral tips of diamonds represent the 95% confidence intervals. Numbers in the right-hand column are summary effect estimates for each study [lower 95% CI, upper 95% CI]. Dotted vertical line indicates conventional agriculture (control).*

Across 47 studies, the SOC levels under conventional agriculture (control) were highly variable, ranging between 18 and 102 Mg C ha^{-1} in the plough layer. Unequal controls may cause a "noise" in meta-analysis, confounding the effects of explanatory variables, such as pedo-climatic factors and management practices. Therefore, we ran a weighted meta-regression between SOC levels and the response to CA. The meta-regression indicated that increasing SOC levels reduced linearly the response to CA, and an increase of 1 Mg ha^{-1} in SOC stock was associated with a 0.22% decrease in the response (R^2 = 13.4; Q_M = 5.98, P = 0.014, n = 47; Fig. 2). For example, when soils had 30 Mg C ha^{-1} the application of CA increased the SOC amount by 16% (ln(*r*) = 0.15). However, on more fertile soils that had 60 Mg C ha^{-1}, the SOC increase due to CA was only 9% (ln(*r*) = 0.08) and no response can be expected on soils reaching 100 Mg C ha^{-1}.

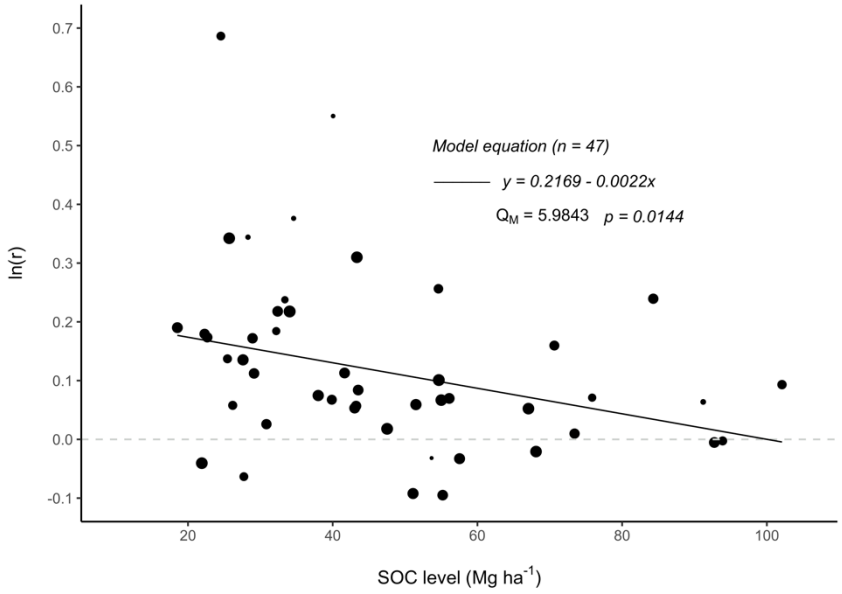

***Figure 2**. Weighted meta-regression between SOC changes due to CA expressed as ln(r) and the SOC level under conventional agriculture (control) for the entire database. Point size represents study weight in the analysis as expressed in the eq. [5]. The dotted line represents the control. For back-transformation of ln(r), see Eq.10.*

To eliminate the effect of unequal controls, we subdivided the database into "Low" and "High" SOC level groups with a threshold value of 40 Mg C ha^{-1}. Compared to the controls, the weighted summarized effect was a 20% (12-28%, n = 22) of SOC increase in the "Low" group, and only a 7% (95% CI 3-11%, n = 25) in the "High" group (Fig. 1). However, the first group had a larger variability of responses (τ = 0.14), compared to the latter (τ = 0.08).

Since within each group no associations between SOC levels and the response to CA were found (P = 0.93 and P = 0.70 for the "Low" and "High" groups, respectively), this allowed us to study the effects of pedo-climatic factors and management practices within each group.

1.3.2 The source of variation across studies

The effects of five different moderators were significant in at least one of the two SOC level groups (Table 4). The R^2 coefficient varied significantly from one moderator to another, indicating that the SOC response variability is strictly dependent on specific moderators. For instance, the largest R^2, about 25-40%, was recorded for rainfall and latitude, while the smallest was for clay and experimental duration (16-18%).

Table 4. The effect of pedo-climatic and geographical factors and management practices on SOC changes due to conservation agriculture in "Low" and "High" SOC level groups.

Variable category	Explanatory variables	"Low" SOC level						"High" SOC level					
		n	R^2 (%)	p (Q_M)	df (Q_M)	Figure	Outliers (study ID)	n	R^2 (%)	p (Q_M)	df (Q_M)	Figure	Outliers (study ID)
PEDO-CLIMATIC AND GEOGRAPHICAL	Clay (%)	21	0.00	0.980	1	3A	-	23	16.35	**0.047**	1	3A	14
	Sand (%)	21	0.00	0.829	1	-	-	24	4.86	0.312	1	-	-
	Rainfall (mm $year^{-1}$)	21	43.07	**0.007**	1	3B	42	23	33.28	**0.021**	1	3B	10, 40
	Temperature	22	6.28	0.092	1	-	-	25	3.10	0.431	1	-	-
	Latitude (degree absolute value)	21	24.91	**0.018**	1	3C	29	23	39.31	**0.007**	1	3C	10, 40
	Longitude (degree)	22	5.32	0.310	1	-	-	25	0.01	0.991	1	-	-
	Continent	22	3.28	0.839	3	4A	-	24	4.88	0.807	3	4B	-
	Köppen climate	21	0.00	0.75	1	4C	-	25	0.63	0.793	1	4D	-
AGRONOMIC MANAGEMENT	Experiment duration (years)	22	17.76	**0.020**	1	5A		24	17.46	**0.047**	1	5A	47
	Proportion of crops with high residue biomass (%)	19	35.06	**0.013**	1	5B	16, 42	22	0.00	0.999	1	5B	-
	Number of crops in rotation (treatment)	22	8.25	0.175	1	4E	-	25	0.56	0.746	1	4F	-
	Nitrogen fertilization level (kg N $year^{-1}$)	12	4.45	0.476	1	-	-	15	4.13	0.411	1	-	-

"n" is the number of studies; "R^2" estimates the amount of heterogeneity accounted for by the moderators included in the model; "p(Q_M)" is the P-value of the heterogeneity test; "df(Q_M)" are the degrees of freedom of the residual heterogeneity test. P-values highlighted in bold are significant ($P < 0.05$). Outliers was identified by backward search algorithm (Mavridis et al., 2017).

1.3.3 Pedo-climatic and geographical factors

In the “Low” group, a change in clay or sand percentage (within the range of this study) did not lead to a different response to the CA adoption, while in the "High" group an increased clay content was positively correlated with the magnitude of the response (Table 4 and Fig. 3A). For example, at 60% of clay the SOC increase due to CA adoption was 12% (ln(r) = 0.10) compared to conventional agriculture, while no response was found (ln(r) = 0.0) at 8% of clay.

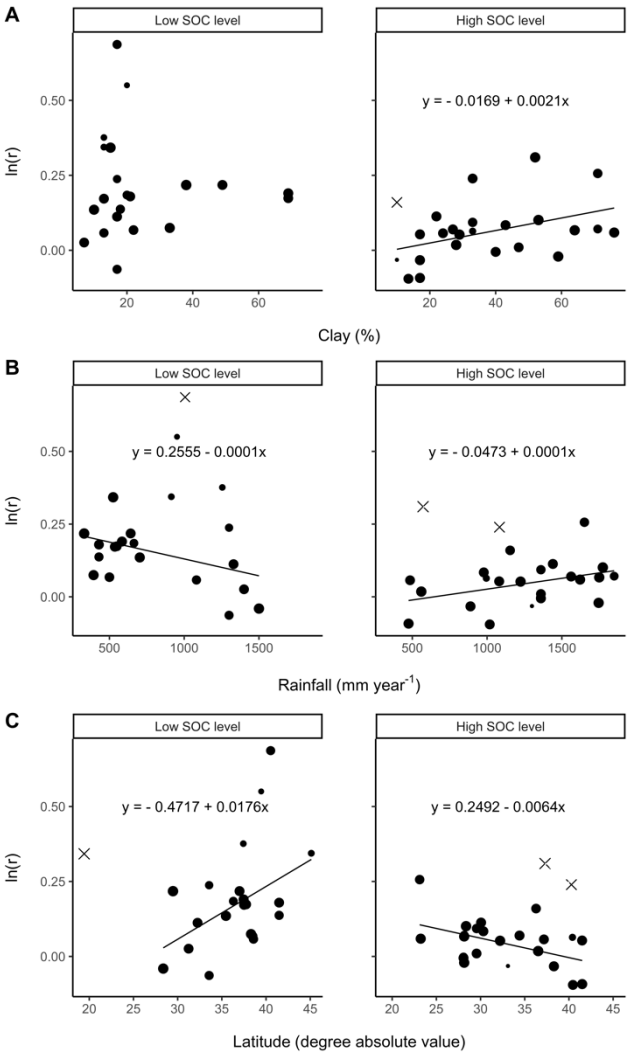

***Figure 3**. Weighted meta-regressions between SOC changes due to conservation agriculture expressed as ln(r) and clay (A), rainfall (B) and latitude (C) in the soils with "Low" and "High" SOC levels under conventional agriculture. The point size represents the study weight in the analysis as expressed in eq. [5]. Statistics for meta-regressions and ID of studies identified as outliers (crosses) appear in Table 4. For back-transformation of ln(r), see Eq.10.*

The meta-regressions indicated that rainfall was an important factor governing the response to CA in both groups (R^2 = 33% and 43%, Table 4). The relationship was negative in the “Low”

SOC group, and positive in the “High” group (Fig. 3B). In both groups, an increase of 100 mm of rainfall was associated with a 1% change in the SOC response to CA.

The temperature cannot explain the groups variability ($P > 0.05$, Table 4), with a R^2 always lower than 10%.

Table 4 shows that the effect of CA strongly depended on geographical locations as indicated by the large proportion of heterogeneity (25-39%) accounted for by latitude (degrees absolute value). In “Low” SOC group, with increasing latitude the impact of CA sharply increased, whereas, in “High” SOC group, CA had an opposite trend (Fig. 3C).

The SOC responses to CA did not reveal any differences across continents (Fig. 4A/B). However, the number of studies in South America and in Asia for the "Low" group and in Europe for the "High" group was limited, and thus, the 95% CIs were large and overlapping.

No differences in the effect of CA adoption were found between Csa and Cfa Köppen climate categories, since the 95% CI were large and overlapping (Table 4; Fig. 4C/D). The Csb climate was excluded from the analysis since only one study was found.

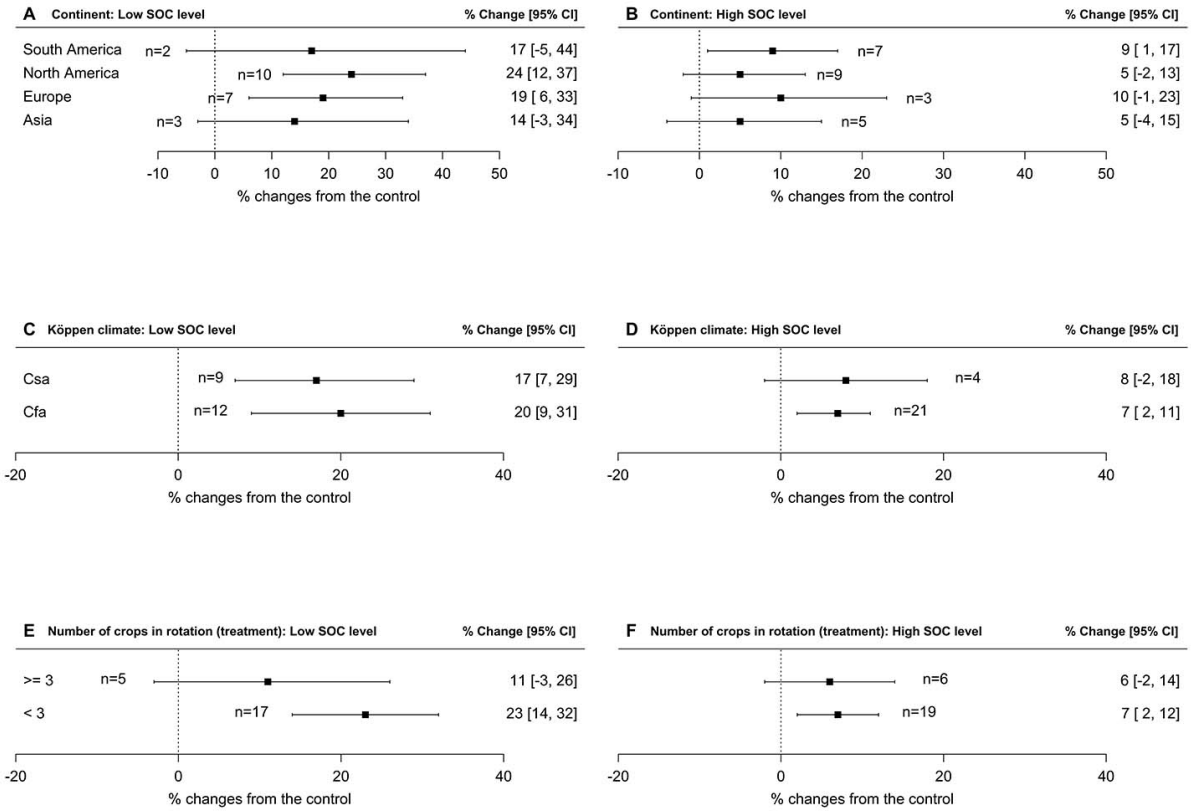

Figure 4*. SOC percentage changes due to conservation agriculture as effected by continents (A and B) and Köppen climate groups (C and D), the number of crops in treatment rotation (E and F), in the soils with "Low" and "High" SOC levels under conventional agriculture. The symbols indicate weighted average with 95% confidence intervals (CIs) and "n" represents the number of studies. Numbers in the right columns are summary effect estimates [lower 95% CI, upper 95% CI]. The dashed line indicates conventional agriculture (control). The effect of conservation agriculture on SOC was considered significantly different from the control if the 95% CIs do not overlap with zero, and significantly different between the groups of explanatory variables if their 95% CIs do not overlap. Groups with only one study were excluded from the analysis.*

1.3.4 Agronomic management practices

In most of the studies, the duration of experiments ranged from 2 to 30 years. Fig. 5A displays the significant positive relationship between experiment duration and SOC response due to CA adoption in both SOC level groups (Table 4). The regression slope was greater in the "Low" group; in particular, after ten years of CA implementation, the percentage change from conventional agriculture was 20% in the "Low" group ($\ln(r) = 0.17$), and 5% in the "High" group ($\ln(r) = 0.04$).

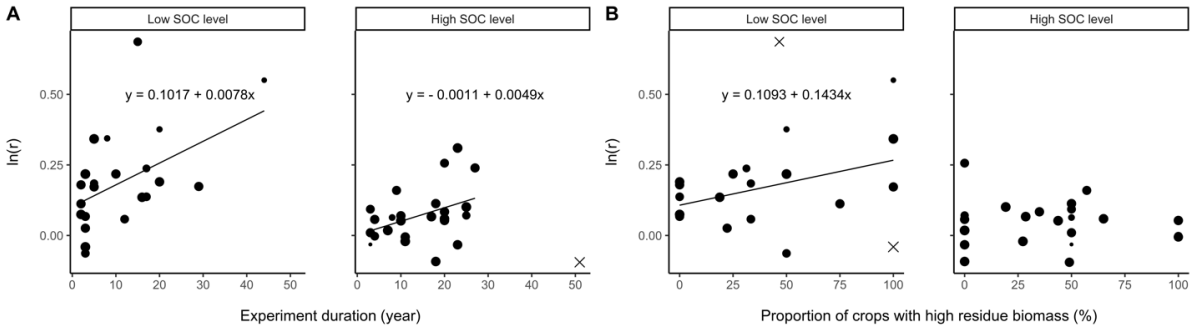

Figure 5*. Weighted meta-regressions between SOC changes due to conservation agriculture expressed as ln(r) and experiment duration (A) and proportion of crop with high residue biomass (B) in the soils with "Low" and "High" SOC levels under conventional agriculture. The point size represents the study weight in the analysis as expressed in eq. [5]. Statistics for meta-regressions and ID of studies identified as outliers (crosses) appear in Table 4. For back-transformation of ln(r), see Eq.10.*

The proportion of crops with high residue biomass in a rotation significantly affected C sequestration under CA only in the "Low" group (Table 4 and Fig. 5B). If all the crops in a rotation produced a large amount of residue, the SOC increase was about 29% ($\ln(r) = 0.25$). In a rotation in which only half of the crops left a high amount of residue on the soil, the SOC increase due to CA adoption was about 20% ($\ln(r) = 0.18$) compared to conventional agriculture. In the "High" group, the amount of residues did not modify the SOC response to CA (Table 4, Fig. 5B).

In both groups, the introduction of three or more crops in a treatment rotation and the nitrogen fertilization level did not have a significant impact (Table 4, Fig. 4E/F).

1.3.5 Publication bias

Although the funnel plots indicated some asymmetry, the Egger's regression test did not indicate a significant asymmetry ($P = 0.64$) when the sample size is present on the y-axis (Fig. S2 A, Supplemental file 1). When the SE appeared in the y-axis (Fig. S2 B, Supplemental file

1), some points fell outside the 95% CI, but the regression test still confirmed a non-significant asymmetry (P = 0.051). We concluded that our research does not suffer from publication bias. In addition, the fail-safe number indicated that the results are robust for both "Low" and "High" groups. In fact, the fail-safe number is 280 and 62 for the "Low" and "High" groups respectively, suggesting that there would need to be a consistent number of studies for each group before the cumulative effect would become statistically non-significant (Supplemental file 1).

1.4 Discussion

This meta-analysis summarizes the results of 47 studies published over a period of 20 years on the effects of CA practices on SOC sequestration in the plough layer under the Mediterranean and humid subtropical climates in five continents. Since our database included numerous different crops (n = 23) and rotations (n = 31) this allowed us to explore different agronomic conditions (Supplemental file 3). Previous meta-analysis on similar topic and climatic conditions summarized 33 studies on herbaceous crops (Aguilera et al., 2013 REF). Other meta-analyses reached greater number of studies including deeper soil layers (Luo et al., 2010, Mondal et al., 2020) or they were conducted on a global scale (e.g., Li et al., 2010, Sun et al., 2020, West and Post, 2002). Although our initial database was larger, many studies were not included to the database due to (1) the variability of management practices (e.g., minimum tillage in place of no-till, agronomic management change during the experiment's duration), or cover crop inclusion in control treatments; (2) incomplete and poor reporting of the results, such as missing means, SDs or sample sizes for controls and treatments; (3) utilization of pedotransfer functions or lack of reported bulk density. Despite such constrains, the number of studies included in the final database is comparable with other similar meta-analyses (Table 1). This number was sufficient to perform a robust, weighted meta-analysis to calculate a summarized effect size across the studies, as well as the means for the different categories of explanatory variables, and to determine the CIs around the means.

1.4.1 Overall effect and the role of SOC levels

This meta-analysis clearly indicates that under Mediterranean and humid subtropical climates, CA adoption had an overall positive effect on SOC sequestration amounting to an overall mean increase of 12% in the plough layer compared to conventional agriculture. This meta-analysis also gives the first evidence that the magnitude of SOC gain due to CA adoption was strongly

influenced by the SOC level under conventional agriculture. In soils which stored a low SOC amount, the impact of CA adoption was three times larger (20%, 95% CI 12-28%, n = 22) than in soils which stored the higher SOC (7%, 95% CI 3-11%, n = 25). In our database, the level of SOC under conventional agriculture varied from 18 to 102 Mg C ha^{-1} in the plough layer, which includes the average value of 63.5 Mg ha^{-1} reported by FAO (2020) for the warm temperate climate. The evidence of distinct responses between the "Low" and "High" SOC level groups (Fig. 2) became important to better understand the variability of CA impacts across Mediterranean and humid subtropical climates. As a rule, the carbon content achieved under conventional agriculture must be considered to estimate whether SOC sequestration can be increased by CA adoption. This can be explained by the fact that SOC sequestration rates have been found to be greater in soils that are far from their potential steady state (Tiefenbacher et al., 2021). On the contrary, when SOC is already close reaching to a steady state, the SOC gains are lower (Corsi, 2012; Kämpf et al., 2016).

Previous meta-analyses on this topic which summarized studies in Mediterranean (Aguilera et al., 2013) and temperate climates (Ogle et al., 2005) did not explicitly consider the SOC level under conventional tillage as a moderator: however, they demonstrated a 17-18% of SOC increase as an overall effect, which is somewhat larger than we found in this meta-analysis (12%) for the entire database. These larger responses very likely stem from the use of weighting by sample size or no weighting. In this meta-analysis however, the weighting by the inverse of the variance was used, which usually gives smaller effect size estimates (Hungate et al., 2009). Our results of the overall effects agree with the global meta-analysis by Li et al. (2020), who also used same metrics of effect size and weighting function (Table 1).

During the last two decades, no-till management has also been recommended as a practice to mitigate greenhouse gas emissions through soil C sequestration (Ogle et al., 2012) and lower fuel consumption (Aguilera et al., 2013). The present meta-analysis defines that, under Mediterranean and humid subtropical climates, CA produce positive carbon sequestration regardless of the initial carbon content (i.e., positive effect in both "Low" and "High" SOC level groups). This finding confirms that CA must be considered by the lawmakers to mitigate greenhouse gas emissions. In addition, Powlson et al. (2016) suggested to evaluate the SOC increase considering the management practices involved (e.g., crop rotation, residue management, soil characteristic).

1.4.2 Source of variation across studies

The final distribution of the effects size (Fig. 1) describes a wide range of SOC change in response to conservation agriculture (from -9% to 99% change from the control). The heterogeneity of the effect size, as quantified by the high I^2 value (94.6%, 95% CI 92.4-97.2%, n = 47) justifies the random model utilization (since the different studies do not share a common effect size). Similar I^2 value was reported by other agronomic (Kim et al., 2020; Tremblay et al., 2012; Zhao et al., 2020) or ecological meta-analyses (Senior et al., 2016). The large I^2 allows us to investigate reasons for the variability, applying subgroup analysis or meta-regression (Nakagawa et al., 2017).

Our results proved that splitting the database up into two groups based on the amount of SOC under conventional agriculture (i.e., “Low” SOC level and “High” SOC level) allowed us to detect contrasting effects of the pedoclimatic and management factors on SOC sequestration. In fact, the analysis of the whole database would have masked the moderators' impacts on SOC sequestration, since the effect of the two groups would have been averaged. Conversely, with this approach we can give agronomic explanations of the moderator impact, separately for the soils with low and high SOC stocks under conventional agriculture.

1.4.3 Pedo-climatic and geographical factors

Our results suggest a significant positive effect of CA due to the clay percentage only in soils with "High" SOC level (Fig. 3A). Several authors acknowledge the positive effect of the clay percentage on the SOC adsorption by the mineral fraction and the resulting SOC accumulation (Du et al., 2017; Haddaway et al., 2017; Xu et al., 2016). This is related to the fact that clay soils exhibit strong aggregate formation and stability that prevent SOM decomposition (Lorenz and Lal, 2018). Since C sequestration is constrained mainly by the availability of reactive surfaces (Churchman et al., 2020), high C amount (i.e., "High" SOC level group) still leads to increase in SOC response, if supported by greater clay content in the soil (Fig. 3A). In contrast, in the soils with "Low" SOC level all the C available is likely to be adsorbed by the clay minerals, making this factor irrelevant for further SOC increase.

In our study, the amount of rainfall showed a significant effect on SOC sequestration due to CA in both groups (Table 4, Fig. 3B), while some previous meta-analyses failed to detect the rainfall effect (Du et al., 2017; Luo et al, 2010). Sun et al. (2020) indicated that higher SOC gain with the CA adoption is expected with a decrement of the humidity index (ratio of annual mean precipitation to mean temperature). It is likely that, in our meta-analysis, the enhanced

soil water retention due to CA practices (Lal, 2020) occurred in soils with low SOC levels, which gave a visible advantage only in dry conditions (the left side of the regression shown in Fig. 3B), while in geographical areas where water is not limited, C sequestration improvement had only a small increment. Another possible explanation for the good CA performance in C depleted areas is associated with the irrigation technique: in some agricultural regions the irrigation counterbalances the negative effect of scant precipitation on carbon sequestration (Lorenz and Lal, 2018). In contrast, we found a positive trend in the “High” group, although the low slope indicated a weak impact of rainfall on CA effect. This finding agrees with the result by Post et al. (1982), who linked a high rainfall regime with SOC accumulation in soils.

Our meta-regressions clearly indicate that the geographical location of an experiment determined to what extent CA influenced SOC sequestration. Moving from the lower latitudes towards the middle latitudes suggests an increasing advantage of CA in soils with initially low SOC levels, as indicated by the positive meta-regression in the “Low” SOC level group (Fig. 3C). In this group, CA showed a small positive contribution at low latitude where the high temperature hastens the mineralization of the limited SOC stock. Conversely, moving to middle latitudes with lower temperatures, the CA effect increased, probably, due to slower mineralization. From the agronomic point of view, conservation agriculture practices are not enough to increase C sequestration in conditions with low carbon content and a warm climate (i.e., low latitude absolute value). In soils with high SOC levels, we found an opposite trend (Fig. 3C). This suggests that the higher effect size is found at low latitudes which are characterized by high temperature, where SOC stock is not a limiting driver, and it can be mineralized without decreasing the SOC stock accumulation in soil. Conversely, with higher latitudes, probably the introduction of CA practices in soil with an already high SOC level is not enough to lead to an increment in SOC stock accumulation. However, no significant effect of temperature was found for both "Low" and "High" groups (Table 4), indicating that even if temperature is certainly a driver of the SOC mineralization, other factors can influence the SOC accumulation. Therefore, these findings highlight the fact that conservation agriculture is not a "standardized solution" to explain the carbon accumulation problems in agricultural soils, and the benefits of its application should be evaluated by considering other agronomic and climatic variables.

The peculiar behaviors of the "Low" and "High" groups provide a novel contribution about the CA effect on SOC sequestration at different latitudes, due to the lack of previous findings

related to this topic or for results limited to specific soil layers. For example, Haddaway et al., (2017), who studied SOC response regardless of the C stock in conventional tillage (control), found that latitude was positively correlated to C stocks' mean differences in full profile C stocks.

Other geographical moderators were not useful to explain heterogeneity of the effect sizes across the studies. In fact, the continent moderator had no impact to explain the heterogeneity, probably, because the studies from different continents had the same climate conditions (i.e., Cfa, Csa). Therefore, in the present meta-analysis, the evidence that Cfa and Csa subgroups of the Köppen climate classification did not show significant differences could be partially explained by the similar average temperature and rainfall during the year. Ogle et al. (2005) confirmed that large differences occur with contrasting climates, finding that no-till implementation led to the largest increases in SOC storage under tropical moist conditions and the smallest under temperate dry conditions.

1.4.4 Agronomic management

Our results support the results of many other meta-analyses on the same topic (Angers and Eriksen-Hamel, 2008; Haddaway et al., 2017), which reported that experiment duration positively influences SOC accumulation in soil (Table 1). Moreover, our results indicate that in soils with low SOC content there was a quick temporal response to CA (i.e., a greater response starting from the beginning of the CA implementation). In addition, the SOC stock accumulation in soils with low SOC content throughout the years was faster, as confirmed by the higher regression slope compared to that of the "High" SOC level group.

Another critical aspect related to SOC sequestration is the crop residues management. Differences in the amounts of yields and, thus, crop residues, directly influence the amount of C inputs to the soil (Meurer et al., 2018; Poeplau and Don, 2015). On the other hand, when with ploughed soil the residues are expected to be in contact with deeper soil layers, CA management leaves them on the soil surface. In the latter case, CA leads to positive effects, such as soil temperature control, the limitation of soil erosion and the reduction of soil water evaporation, which are all associated with the reduction of SOC decomposition in soil (Duiker and Lal, 2000; Luo et al., 2010). In literature, the SOC stock in CA is known to positively respond to crop residues retention, as supported by the meta-analysis by Virto et al. (2012), who found a significant ($P = 0.001$, $n = 35$) relation between SOC accumulation in 0-0.3 m soil depth and organic input (i.e., crop residue), considering NT (with residues) as a treatment and

inversion tillage as a control. Our result supported this previous finding, but with a positive relationship limited to soils with scarce SOC stock. In fact, we found out that increasing the proportion of crops with high residue production in the rotation results in a SOC increase only in soils with the "Low" SOC level, reaching 29% change from the control when all the crops in the rotation produce high residue amounts.

Even if the positive relationship between SOC sequestration and the amount of crop residues retained on the soil has been highlighted in different studies, the different quality of the crop residue also plays a role in the C stock accumulation. For example, in the meta-analysis by Sun et al. (2020), they found that in most Mediterranean and temperate climates, SOC sequestration increased when crop residue retention and crop rotation are applied together. The number of crops in the rotation indeed plays a role in SOC accumulation, since monoculture produces the worst quality and quantity of dry matter (Copeland and Crookston, 1992). The study by González-Sánchez et al. (2012) demonstrated that, in general, the higher C soil fixation values were found in soils in which crops were rotated, with on average C sequestration rate 19% higher in the case of crop rotation and NT rather than monoculture. In the present meta-analysis, however, the number of crops in the CA treatment rotation did not significantly impact the SOC accumulation in the plough layer (Table 4). This result is likely due to the unbalanced number of studies between the two levels considered (i.e., rotations with three or more crops or with less than three, Fig. 4 E/F).

1.4.5 Perspectives

The current carbon stock data availability under our studies selection criteria did not allow us to obtain enough studies to consider the deeper layers (> 0.3 m depth). However, other authors highlighted the importance of also engaging the deeper layers for a complete evaluation of the soil carbon storage (Luo et al., 2010; Meurer et al., 2018; Piccoli et al., 2016). Sun et al. (2020) noted that, for the cases when SOC under no-till relative to conventional tillage increased in the top 0.3 m, the 0.3-0.6 m layer was also likely to increase its SOC. In the same way, the meta-analysis by Luo et al. (2010) showed that the total soil C content was almost stable in the deep layers (> 0.4 m depth). However, Du et al. (2017) reported that no-till management showed slightly lower SOC storage rates against conventional till in the subsoil layers (> 0.4 m).

Further research synthesis should address the SOC response to CA in the deeper soil layers, focus on specific climatic zones and different management practices. In this sense, the present work is useful since a reliable and replicable procedure is clearly presented.

Lastly, we should note that within this topic, the information regarding irrigation was rarely reported. The final low number of studies handling irrigation did not allow us to include this moderator in the meta-analysis.

1.5 Conclusions

The present meta-analysis evaluated the SOC response to CA practices in Mediterranean and humid subtropical climates. Limiting the analysis to specific climates offered the possibility to detect more precisely the effects of pedo-climatic and management practices, which otherwise would have been masked. Therefore, we have provided a novel contribution to understanding the actual impact of CA in the SOC stock accumulation.

The meta-analysis showed an overall positive effect of CA on SOC sequestration (12%). By dividing the whole database into two separate groups based on the SOC levels (with 40 Mg C ha^{-1} as the threshold) under conventional agriculture allowed us to better explain the variability of SOC responses to CA management. This meta-analysis highlighted that, under the climates considered, the effect of CA adoption on SOC accumulation in the plough layer reached 20% in soils with low SOC levels, while it only averaged 7% in soils with the high SOC levels.

The effect of CA on SOC accumulation depended on clay content solely in soils with more than 40 Mg C ha^{-1} under conventional agriculture, while it was not relevant in soils with low SOC levels. In both soil groups, experiment duration positively impacted SOC sequestration, with a greater effect found in the soils with low SOC content. In addition, in these soils, the retention of crop residues enhanced the CA positive contribution.

We conclude that in Mediterranean and humid subtropical climates, the most benefits from CA application in terms of SOC increase apply to agricultural soils with low SOC content and located in the middle latitudes and/or in dry areas.

Declaration of Competing Interest

The authors declare that they have no known competing financial interests or personal relationships that could have appeared to influence the work reported in this paper.

Acknowledgements

This work is funded by the Agriculture, Environment and Bioenergy PhD school of the University of Milan.

This study is also funded by the European Union's Horizon 2020 Framework Programme for Research and Innovation (H2020-RUR-2017-2) as part of the LANDSUPPORT project (grant agreement No. 774234), which aims at developing a decision support system for optimizing soil management in Europe.

This study is a part of the project "Carbon Market - Innovative cropping systems for carbon market" funded by Natural Resources Institute Finland (Luke). This study is also a part of the project SOMMIT: Sustainable management of soil organic matter to mitigate trade-offs between C sequestration and nitrous oxide, methane, and nitrate losses that received funding from the European Joint Programme SOIL (grant agreement ID: 862695).

Supplementary material

1. Supplemental file 1: query for article searching, and publication bias;
2. Supplemental file 2: raw carbon data of all the articles included in the database;
3. Supplemental file 3: database for meta-analysis;
4. Supplemental file 4: R codes used for the analyses;
5. Supplemental file 5: reference list of the articles included in the database;

References

Acutis, M., Tadiello, T., Perego, A., Di Guardo, A., Schillaci, C., Valkama, E., 2021a. EXTRACT: an Excel tool for the estimation of standard deviations from published articles, Environ. Model. Soft. 10.1016/j.envsoft.2021.105236.

Acutis, M., Tadiello, T., Perego, A., Di Guardo, A., Schillaci, C., Valkama, E., 2021b. EXTRACT tool_1.0.xlsm. figshare. Software. https://doi.org/10.6084/m9.figshare.14987130.v6.

Aguilera, E., Lassaletta, L., Gattinger, A., Gimeno, B.S., 2013. Managing soil carbon for climate change mitigation and adaptation in Mediterranean cropping systems: A meta-analysis. Agr. Ecosyst. Environ. 168, 25–36. https://doi.org/10.1016/j.agee.2013.02.003.

Álvaro-Fuentes, J., Paustian, K., 2011. Potential soil carbon sequestration in a semiarid Mediterranean agroecosystem under climate change: Quantifying management and climate effects. Plant Soil. 338, 261–272. https://doi.org/10.1007/s11104-010-0304-7.

Angers, D.A., Eriksen-Hamel, N.S., 2008. Full-Inversion Tillage and Organic Carbon Distribution in Soil Profiles: A Meta-Analysis. Soil Sci. Soc. Am. J. 72, 1370–1374. https://doi.org/10.2136/sssaj2007.0342.

Aria, M. and Cuccurullo, C., 2017. Bibliometrix: An R-tool for comprehensive science mapping analysis. J. Informetr. 11(4), pp 959-975, Elsevier. https://doi.org/10.1016/j.joi.2017.08.007

Borenstein, M., Hedges, L., Higgins, J., Rothstein, H., 2009. Introduction to Meta-Analysis. John Wiley & Sons, Ltd.

Bouma, E., 2005. Development of comparable agro-climatic zones for the international exchange of data on the efficacy and crop safety of plant protection products. EPPO Bulletin 35, 233–238. https://doi.org/10.1111/j.1365-2338.2005.00830.x.

Chen, D., Chen H., 2013. Using the Köppen classification to quantify climate variation and change: An example for 1901–2010. Environmental Development. 6, 69–79, http://dx.doi.org/10.1016/j.envdev.2013.03.007.

Churchman, G.J., Singh, M., Schapel, A., Sarkar, B., Bolan, N., 2020. Clay minerals as the key to the sequestration of carbon in soils. Clays Clay Miner. 68, 135–143. https://doi.org/10.1007/s42860-020-00071-z.

Climate Change Knowledge Portal, for Development Practitioners and Policy makers (2021). https://climateknowledgeportal.worldbank.org/download-data

Copeland, P.J., Crookston, R.K., 1992. Crop sequence affects nutrient composition of corn and soybean grow under high fertility. Agron. J. 84, 503–509.

Corsi, S., Friedrich, T., Kassam, A., Pisante, M., and Moraes S.J., 2012. Soil organic carbon accumulation and greenhouse gas emisson reductions from conservation agriculture: a literature review, Integrated crop management. FAO (Eds.), Food and Agriculture Organization of the United Nations, Rome.

Du, Z., Angers, D.A., Ren, T., Zhang, Q., Li, G., 2017. The effect of no-till on organic C storage in Chinese soils should not be overemphasized: A meta-analysis. Agr. Ecosyst. Environ. 236, 1–11. https://doi.org/10.1016/j.agee.2016.11.007.

Duiker, S.W., Lal, R., 2000. Carbon budget study using CO2 flux measurements from a no till system in central Ohio. Soil Till. Res. 54, 21–30. https://doi.org/10.1016/S0167-1987(99)00101-4.

FAO, 2020, Global Soil Organic Carbon Map (GSOCmap) Version 1.5. https://doi.org/10.4060/ca7597en.

FAO, 2017a. Global Soil Organic Carbon Map - Leaflet. Global Soil Partnership, Rome, Italy. 5 pp.

FAO, 2017b. Conservation agriculture, Rome, Italy, 2pp.

FAO, 2016. Save and Grow in practice: Maize, rice and wheat. Rome.

Glass, G., 1976. Primary, Secondary, and Meta-Analysis of Research. Educ. Res. 5(10), 3-8. https://doi.org/10.2307/1174772.

González-Sánchez, E.J., Ordóñez-Fernández, R., Carbonell-Bojollo, R., Veroz-González, O., Gil-Ribes, J.A., 2012. Meta-analysis on atmospheric carbon capture in Spain through the use of conservation agriculture. Soil Till. Res. 122, 52–60. https://doi.org/10.1016/j.still.2012.03.001.

Gurevitch, J., Koricheva, J., Nakagawa, S., Gavin, S., 2018. Meta-analysis and the science of research synthesis. Nature. 555, 175–182. https://doi.org/10.1038/nature25753.

Gurevitch, J., Hedges, L.V., 1999. Statistical issues in ecological meta-analyses 80, 8.

Haddaway, N.R., Hedlund, K., Jackson, L.E., Kätterer, T., Lugato, E., Thomsen, I.K., Jørgensen, H.B., Isberg, P.E., 2017. How does tillage intensity affect soil organic carbon? A systematic review. Environ. Evid. 6, 30. https://doi.org/10.1186/s13750-017-0108-9.

Hedges, L.V., Gurevitch, J., Curtis, P.S., 1999. The meta-analysis of response ratios in experimental ecology. Ecology. 80(4):1150–1156. https://doi.org/10.2307/177062.

Hedges, L., Olkin, I., 1985. Statistical Methods for Meta-Analysis. Academic Press, San Diego, CA.

Hernandez-Ochoa, I., S. Asseng, 2018. Cropping Systems and Climate Change in Humid Subtropical Environments. Agronomy. 8, 19. https://doi.org/10.3390/agronomy8020019.

Hungate, B.A., van Groenigen, K.J., Six, J., Jastrow, J.D., Luo, Y., de Graaff, M.A., van Kessel, C., Osenberg, C.W., 2009. Assessing the effect of elevated carbon dioxide on soil carbon: a comparison of four meta-analyses. Global Change Biol. 15, 2020–2034. https://doi.org/10.1111/j.1365-2486.2009.01866.x.

Jones, R.J.A., Hiederer, R., Rusco, E., Montanarella, L., 2005. Estimating organic carbon in the soils of Europe for policy support. Eur. J. Soil Sci. 56, 655–671. https://doi.org/10.1111/j.1365-2389.2005.00728.x.

Kämpf, I., Hölzel, N., Störrle, M., Broll, G., Kiehl, K., 2016. Potential of temperate agricultural soils for carbon sequestration: A meta-analysis of land-use effects. Sci. Total Environ. 566–567, 428–435. https://doi.org/10.1016/j.scitotenv.2016.05.067.

Kim, N., Zabaloy, M.C., Guan, K., Villamil, M.B., 2020. Do cover crops benefit soil microbiome? A meta-analysis of current research. Soil Biol. Biochem. 142, 107701. https://doi.org/10.1016/j.soilbio.2019.107701.

Koricheva, J., Gurevitch, J., Mengersen, K. (Eds.), 2013. Handbook of meta-analysis in ecology and evolution. Princeton University Press, Princeton.

Lal, R., 2020. Soil organic matter and water retention. Agr. J., Volume 112, Issue 5, September/October 2020, pages 3265-3277. https://doi-org.pros.lib.unimi.it/10.1002/agj2.20282.

Lal, R., 2004. Soil carbon sequestration impacts on global climate change and food security. Science 304, 1623–1627. 10.1126/science.1097396.

Li, Y., Li, Z., Chang, S.X., Cui, S., Jagadamma, S., Zhang, Q., Cai, Y., 2020. Residue retention promotes soil carbon accumulation in minimum tillage systems: Implications for conservation agriculture. Sci. Total Environ. 740, 140147. https://doi.org/10.1016/j.scitotenv.2020.140147.

Lorenz, K., Lal, R., Carbon sequestration in agricultural ecosystems, 2018. Springer Berlin Heidelberg, New York, NY.

Lugato, E., Panagos, P., Bampa, F., Jones, A., Montanarella, L., 2014. A new baseline of organic carbon stock in European agricultural soils using a modelling approach. Glob. Change Biol. 20, 313–326. https://doi.org/10.1111/gcb.12292.

Luo, Z., Wang, E., Sun, O.J., 2010. Can no-tillage stimulate carbon sequestration in agricultural soils? A meta-analysis of paired experiments. Agr. Ecosyst. Environ. 139, 224–231. https://doi.org/10.1016/j.agee.2010.08.006.

Mavridis, D., Moustaki, I., Wall, M., Salanti, G., 2017. Detecting outlying studies in meta-regression models using a forward search algorithm: Forward Search in Meta-analysis. Res. Syn. Meth. 8, 199–211. https://doi.org/10.1002/jrsm.1197.

Mazzoncini, M., Antichi, D., Bene, C.D., Risaliti, R., Petri, M., Bonari, E., 2016. Soil carbon and nitrogen changes after 28 years of no-tillage management under Mediterranean conditions 10. Europ. J. Agronomy. 77, 156–165. https://doi.org/10.1016/j.eja.2016.02.011.

Meurer, K.H.E., Haddaway, N.R., Bolinder, M.A., Kätterer, T., 2018. Tillage intensity affects total SOC stocks in boreo-temperate regions only in the topsoil—A systematic review using an ESM approach. Earth-Science Reviews. 177, 613–622. https://doi.org/10.1016/j.earscirev.2017.12.015.

Mondal, S., Chakraborty, D., Bandyopadhyay, K., Aggarwal, P., Rana, D.S., 2020. A global analysis of the impact of zero-tillage on soil physical condition, organic carbon content, and plant root response. Land Degrad. Dev. 31, 557–567. https://doi.org/10.1002/ldr.3470.

Nakagawa, S., Lagisz, M., Jennions, M. D., Koricheva, J., Noble, D. W., Parker, T. H. O'Dea, R. E. (2021, April 8). Methods for testing publication bias in ecological and evolutionary meta-analyses. https://doi.org/10.32942/osf.io/k7pmz.

Nakagawa, S., Noble, D.W.A., Senior, A.M., Lagisz, M., 2017. Meta-evaluation of meta-analysis: ten appraisal questions for biologists. BMC Biol. 15, 18. https://doi.org/10.1186/s12915-017-0357-7.

Ogle, S.M., Alsaker, C., Baldock, J., Bernoux, M., Breidt, F.J., McConkey, B., Vazquez-Amabile, G.G., 2019. Climate and soil characteristics determine where no-till management can store carbon in soils and mitigate greenhouse gas emissions. Sci. Rep. 9, 1–8. https://doi.org/10.1038/s41598-019-47861-7.

Ogle, S.M., Swan, A., Paustian, K., 2012. No-till management impacts on crop pro- ductivity, carbon input and soil carbon sequestration. Agr. Ecosys. Environ. 149, 37–49. https://doi.org/10.1016/j.agee.2011.12.010.

Ogle, S.M., Breidt, F.J., Paustian, K., 2005. Agricultural management impacts on soil organic carbon storage under moist and dry climatic conditions of temperate and tropical regions. Biogeochemistry. 72, 87–121. https://doi.org/10.1007/s10533-004-0360-2.

Paul, E.A., Paustian, K., Elliott, E.T., Cole, C.V., 1997. Soil Organic Matter in Temperate Agroecosystems: Long-term Experiments in North America. CRC Press, Boca-Raton, Florida, pp. 15–42. https://doi.org/10.1201/9780367811693.

Peel, M.C., Finlayson, B.L., McMahon, T.A., 2007. Updated world map of the Köppen-Geiger climate classification. Hydrol. Earth Syst. Sci. 12. https://doi.org/10.5194/hess-11-1633-2007.

Piccoli, I., Chiarini, F., Carletti, P., Furlan, L., Lazzaro, B., Nardi, S., Berti, A., Sartori, L., Dalconi, M.C., Morari, F., 2016. Disentangling the effects of conservation agriculture practices on the vertical distribution of soil organic carbon. Evidence of poor carbon sequestration in North-Eastern Italy. Agr. Ecosyst. Environ. 230, 68–78. https://doi.org/10.1016/j.agee.2016.05.035.

Pisante, M., Stagnari, F., Acutis, M., Bindi, M., Brilli, L., Di Stefano, V., Carozzi, M., 2015. Conservation Agriculture and Climate Change, in: Farooq, M., Siddique, K.H.M. (Eds.), Conservation Agriculture. Springer International Publishing, Cham, pp. 579–620. https://doi.org/10.1007/978-3-319-11620-4_22.

Poeplau, C., Don, A., 2015. Carbon sequestration in agricultural soils via cultivation of cover crops – A meta-analysis. Agr. Ecosyst. Environ. 200, 33–41. https://doi.org/10.1016/j.agee.2014.10.024.

Post, W.M., Emanuel, W.R., Zinke, P.J., G.A., Stangenberger, 1982. Soil carbon pools and world life zones. Nature. 298, 156–159 (1982). https://doi.org/10.1038/298156a0.

Powlson, D.S., Stirling, C.M., Thierfelder, C., White, R.P., Jat, M.L., 2016. Does conservation agriculture deliver climate change mitigation through soil carbon sequestration in tropical agro-ecosystems? Agr. Ecosyst. Environ. 220, 164–174. https://doi.org/10.1016/j.agee.2016.01.005.

Pravalie, R., Patriche, C., Borrelli, P., Panagos, P., Rosca, B., Dumitrascu, M., Nita, I.A., Savulescu, I., Birsan, M.V., Bandoc, G., 2021. Arable lands under the pressure of multiple land degradation processes. A global perspective. Environmental Research. 194, 110697. https://doi.org/10.1016/j.envres.2020.110697.

R Core Team (2018). R: A language and environment for statistical computing. R Foundation for Statistical Computing, Vienna, Austria. Available online at https://www.R-project.org/.

Raudenbush, S.W., 2009. Analyzing Effect Sizes: Random Effects Models. In H Cooper, LV Hedges, JC Valentine (eds.), The Handbook of Research Synthesis and Meta-Analysis, 2nd edition, pp. 295–315. Russell Sage Foundation, New York.

Rohatgi A., 2020. WebPlotDigitizer, Website: https://automeris.io/WebPlotDigitizer, Version: 4.3, Location: Pacifica, California, USA.

Rosenthal R., 1979. The 'File drawer problem' and tolerance for null results. Psychol Bull 86: 638–641.

Ruiz, I., Almagro, M., García de Jalón, S., Solà, M. del M., Sanz, M.J., 2020. Assessment of sustainable land management practices in Mediterranean rural regions. J. Environ. Manage. 276, 111293. https://doi.org/10.1016/j.jenvman.2020.111293.

Schillaci, C., Perego, A., Valkama, E., Märker, M., Saia, S., Veronesi, F., Lipani, A., Lombardo, L., Tadiello, T., Gamper, H.A., Tedone, L., Moss, C., Pareja-Serrano, E., Amato, G., Kühl, K., Damatirca, C., Cogato, A., Mzid, N., Eeswaran, R., Rebelo, M., Sperandio, G., Bosino, A., Bufalini, M., Tunçay, T., Ding, J., Fiorentini, M., Tiscornia, G., Conradt, S., Botta, M., Acutis, M., 2021. New pedotransfer approaches to predict soil bulk density using WoSIS soil data and environmental covariates in Mediterranean agro-ecosystems. Sci. Total Environ. 146609. https://doi.org/10.1016/j.scitotenv.2021.146609.

Senior, A.M., Grueber, C.E., Kamiya, T., Lagisz, M., O'Dwyer, K., Santos, E.S.A. & Nakagawa, S., 2016. Heterogeneity in ecological and evolutionary meta-analyses: its magnitude and implications. Ecology, 97, 3293-3299. https://doi.org/10.1002/ecy.1591.

Sperow, M., 2020. Updated potential soil carbon sequestration rates on U.S. agricultural land based on the 2019 IPCC guidelines. Soil Till. Res. 204, 104719. https://doi.org/10.1016/j.still.2020.104719.

Spinoni, J., Vogt, J., Naumann, G., Carrao, H., Barbosa, P., 2015. Towards identifying areas at climatological risk of desertification using the Köppen-Geiger classification and FAO aridity index: towards identifying areas at climatological risk of desertification. Int. J. Climatol. 35, 2210–2222. https://doi.org/10.1002/joc.4124.

Sterne, J.A.C., Egger, M., 2001. Funnel plots for detecting bias in meta-analysis: Guidelines on choice of axis. J. Clin. Epidemiol. (10):1046-55. 10.1016/s0895-4356(01)00377-8.

Sun, W., Canadell, J.G., Yu, Lijun, Yu, Lingfei, Zhang, W., Smith, P., Fischer, T., Huang, Y., 2020. Climate drives global soil carbon sequestration and crop yield changes under conservation agriculture. Glob. Change Biol. 26, 3325–3335. https://doi.org/10.1111/gcb.15001.

Tadiello, T. Perego, A., Elena, V., Schillaci, C., Acutis, M., 2022. Computation of total soil organic carbon stock and its standard deviation from layered soils. [Manuscript submitted for publication]. Department of Agricultural and Environmental Sciences - Production, Landscape, Agroenergy, University of Milan.

Thornthwaite, C. W. 1948. An approach toward a rational classification of climate. Geogr. Rev.38. 55–94. https://doi.org/10.2307/210739.

Tiefenbacher, A., Sandén, T., Haslmayr, H.-P., Miloczki, J., Wenzel, W., Spiegel, H., 2021. Optimizing Carbon Sequestration in Croplands: A Synthesis. Agronomy. 11, 882. https://doi.org/10.3390/agronomy11050882.

Toledo, D.M., Galantini, J., Dalurzo, H., Vazquez, S., Bollero, G., 2013. Methods for Assessing the Effects of Land Use Changes on Carbon Stocks of Subtropical Oxisols. Soil Sci. Soc. Am. J. 77, 1542–1552. https://doi.org/10.2136/sssaj2013.03.0087.

Tremblay, N., Bouroubi, Y. M., Bélec, C., William, R.M., Kitchen, N.R., Thomason, W.E., Ebelhar, S., Mengel, D.B., Raun W.R., Francis, D.D., Vories, E.D., Monasterio I.O., 2012. Corn Response to Nitrogen is Influenced by Soil Texture and Weather. Agr. J. 104, 1658-1671. https://doi-org.pros.lib.unimi.it/10.2134/agronj2012.0184.

Underwood, E.C., Klausmeyer, K.R., Cox, R.L., Busby, S.M., Morrison, S.A., Shaw, M.R., 2009. Expanding the global network of protected areas to save the imperiled Mediterranean biome. Conserv. Biol. 23, 43–52. 10.1111/j.1523-1739.2008.01072.x.

Viechtbauer, W., 2010. Conducting meta-analyses in R with the metafor package. Journal Stat. Softw. 36(3):1–48. 10.18637/jss.v036.i03.

Virto, I., Barré, P., Burlot, A., Chenu, C., 2012. Carbon input differences as main factor explaining the variability in soil organic C storage in no-tilled compared to inversion tilled agrosystems. Biogeochemistry. 108, 17–26. http://dx.doi.org/10.1007/s10533- 011-9600-4.

West, T.O., Post, W.M., 2002. Soil organic carbon sequestration rates by tillage and crop rotation: a global data analysis. Soil Sci. Soc. Am. J. 66, 1930–1946. https://doi.org/10.2136/sssaj2002.1930.

World Bank Clime, 2020. Climate change knowledge Portal (CCKP), https://climateknowledgeportal.worldbank.org/download-data.

Xu, X., Shi, Z., Li, D., Rey, A., Ruan, H., Craine, J.M., Liang, J., Zhou, J., Luo, Y., 2016. Soil properties control decomposition of soil organic carbon: results from data assimilation analysis. Geoderma. 262:235–42. http://dx.doi.org/10.1016/j.geoderma.2015.08.038.

Zhao, J., Yang, Y., Zhang, K., Jeong, J., Zeng, Z., Zang, H., 2020. Does crop rotation yield more in China? A meta-analysis. Field Crops Res. 245, 107659. https://doi.org/10.1016/j.fcr.2019.

Chapter 2. Computation of total soil organic carbon stock and its standard deviation from layered soils

This is the author-produced copy of the article published in the MethodsX journal.
This article is available at: https://doi.org/10.6084/m9.figshare.15066402.v3

Authors:

Tommaso Tadiello[a*], Alessia Perego[a], Elena Valkama[b], Calogero Schillaci[c], Marco Acutis[a]

Affiliation:

[a]DiSAA, Department of Agricultural and Environmental Sciences, University of Milan, Italy

[b]Natural Resources Institute Finland (Luke), Bioeconomy and Environment, Sustainability Science and Indicators, Tietotie 4, 31600 Jokioinen, Finland

[c]European Commission, Joint Research Centre (JRC), Ispra, Italy

**Corresponding author (tommaso.tadiello@unimi.it, DiSAA, Department of Agricultural and Environmental Sciences, University of Milan, Italy)*

Abstract

To assess carbon sequestration in the agricultural and natural systems, it is usually required to report soil organic carbon (SOC) as mass per unit area (Mg ha^{-1}) for a single soil layer (e.g., the 0-0.3 m ploughing layer). However, if the SOC data are reported as relative concentration (g kg-1 or %), it is required to compute the SOC stock and its standard deviation (SD) for a given layer as the product of SOC concentration and bulk density (BD). For a proper computation, it is required to consider that these two variables are correlated. Moreover, if the data are already reported as SOC stock for multiple sub-layers (e.g., 0-0.15 m, 0.15-0.3 m) it is necessary to compute the SOC stock and its SD for a single soil layer (e.g., 0-0.3 m). The correlation between stocks values from adjacent and non-adjacent soil sub-layers must be accounted to compute the SD of the single soil layer.

The present work illustrates the methodology to compute SOC stock and its SD for a single soil layer based on SOC concentration and BD also from multiple sub-layers. An Excel workbook automatically computes the means of stocks and SD saving the results in a ready-to-use database.

- Computation of a carbon (SOC) stock and its standard deviation (SD) from the product between SOC concentration and bulk density (BD), being correlated variables.
- Computation of a SOC stock and its SD from the sum of SOC stocks of multiple correlated sub-layers.
- An Excel workbook automatically computes the means of SOC stocks and SD and saves the results in a ready-to-use database.

GRAPHICAL ABSTRACT

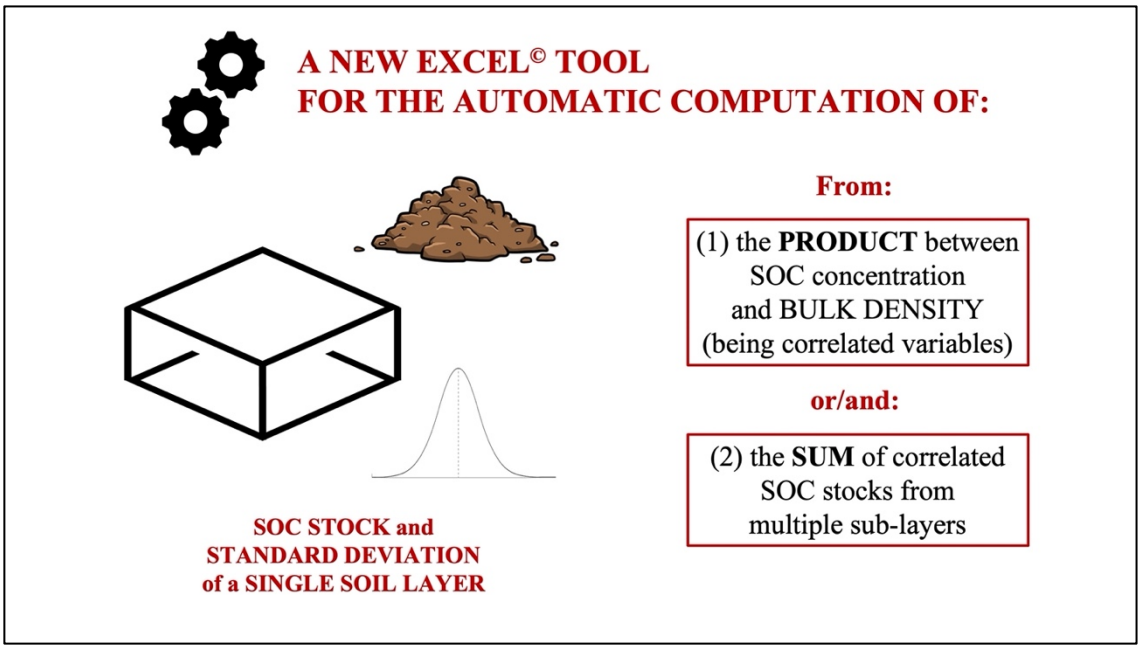

2.1 Method details

2.1.1 Background

Soil organic carbon (SOC) is regarded as the second most extensive carbon reservoir of the planet (Lugato et al., 2021). SOC stock (i.e., carbon stock expressed as Mg ha^{-1} or kg m^{-2}) can be increased by enhancing biomass production and retaining crop residues as an effective mitigation action against climate change, as stated by the 4 per 1000 international initiative (Minasny et al., 2017).

An exponential growth in numbers of experiments about SOC took place in the last decades (Smith et al., 2018): a literature search carried out on Scopus in 2020 revealed 5586 articles under the keywords searching "soil organic carbon" and 100 articles with "soil organic carbon meta-analysis". The significant attention around this topic is mainly due to the need for the definition of the best practices to enhance carbon sequestration for a specific agroecosystem.

Most of the articles yielded by the literature search report SOC as relative concentration (e.g., g kg^{-1}) and frequently for multiple soil layers or sampling depths. However, when SOC is the dependent variable in meta-analysis it is required to treat SOC as stock for a certain depth, for example, for ploughing soil layers (0-0.3 m).

If SOC data are not directly reported as stock, the following computation is needed:

$$SOC\ [Mg\ ha^{-1}] = OC\ \cdot LT\ \cdot BD\ \cdot (1 - RF)\ \cdot 10^4 \quad [1]$$

where OC is the organic carbon concentration (%), LT is the layer thickness (m), BD is the topsoil bulk density (Mg m^{-3}), and RF is the rock fragment content fraction (-) (Batjes, 1996). However, this formula does not take into account the correlation existing between OC and BD. It is also essential to compute the variability (i.e., standard deviation, SD) associated with the estimated SOC stock mean. The correct SD computation plays a role in two different situations: (1) when SOC stock is computed as the product between the OC and BD; (2) when SOC stock of different sub-layers is summed to obtain a single value for a total soil layer. In both cases, the SD must be computed considering the correlations existing between SOC stock and BD, and between these values of different sub-layers. This computation is essential to analyze unbiased data: the mean of SOC stock derived from equation 1 and its SD cannot be merely computed as the arithmetic mean (Van der Vaart, 1998), without considering the measurement error and the fact that they are correlated (Jensen et al., 2020).

This work aims to develop two different unbiased procedures to compute an SOC stock mean and its SD for a soil layer/horizon from the product of OC and BD (Case 1) or alternatively from the sum of SOC stocks of multiple sub-layers/horizons (Case 2). Both cases can occur when data came directly from field samplings or data extraction from scientific publications. An Excel© workbook was developed to compute the two procedures and to save the results as a final database, which can be further used in meta-analysis.

2.2 Soil organic carbon stock computation

The methodology is conceived to compute the SD of SOC for a control and a treatment that are compared in a meta-analysis for both Case 1 and Case 2. This is crucial for the correct computation of the effect-size.

Researchers usually compare the study variable means of a control and a treatment in experimental fields that differ in terms of tillage operations, crop residues management and other factors that can possibly affect SOC stock. Therefore, it is required a different computation of SD because the extent of correlation between the variables among soil layers depends on the control and treatment characteristics: for instance, the studied variables measured in the different soil layers under no-till management have a different correlation coefficient than that of under soil ploughing.

2.2.1 Case 1: product between OC and BD

The computation is based on OC relative concentration and BD; the resulting SOC stock is then considered a composite variable. For this reason, methodology considers both the correlation and the SDs of OC and BD to compute SOC stock and its SD.

The corresponding computation of SOC (expressed as Mg ha^{-1}) for a soil layer follows the next formula:

$$SOC_{\text{sub-layer}} = (\text{OC} \cdot \text{BD} + \text{Cov}(\text{OC}, \text{BD})) \cdot (\text{D}_\text{U} - \text{D}_\text{L}) \cdot 10^4 \quad [2]$$

where C is the carbon concentration [%], BD is the bulk density [Mg m^{-3}], D_U and D_L are the upper and lower layer depths [m] of the sub-layer. The covariance is computed as:

$$\text{Cov}(\text{C}, \text{BD}) = \sigma_\text{C} \cdot \sigma_\text{BD} \cdot \rho_{\text{C,BD}} \quad [3]$$

where σ is the SD. To calculate the correlation (ρ), the regression coefficient (-0.6) based on Manrique and Jones (1991) has been utilized, since they considered the OC as a predictor of BD.

The following formula computes SD between two variables (namely 1, 2, which are OC and BD in our computation) that are normally distributed (Bohrnstedt and Goldberger, 1969):

$$\text{SD} = \sqrt{\mu_1^2\sigma_2^2 + \mu_2^2\sigma_1^2 + 2\left(\mu_1\mu_2\text{Cov}(1,2)\right) + \sigma_1^2\sigma_2^2 + \text{Cov}^2(1,2)} \quad [4]$$

where σ and μ are respectively the SD and the mean of the two variables (i.e., OC and BD), while the covariance is computed as:

$$\text{Cov}(1,2) = \sigma_1 \cdot \sigma_2 \cdot \rho_{1,2} \quad [5]$$

The result of equation [4] has to be transformed according to the unit of the variable, in this case with a multiplicative factor of $[(D_U - D_L) \cdot 10^4]$ as reported in [2]. Equation 4 can be correctly applied to the SOC computation due to the normal distribution of OC and BD values (Jensen et al., 2020).

The OC and the BD are seldom measured on the same sample with independent replications. In this case, the best estimation of the SD of the carbon stock is the SD of the product (i.e., OC · BD) computed for each replication. When OC and BD are measured on samples separately taken, the equation 4 estimates the SD of the SOC stock.

2.2.2 Case 2: sum of stocks

This case applies when the SOC stock of a total soil layer is needed to be computed as the sum of SOC stocks of several sub-layers. In this case, SOC data from sampling or published studies are already expressed as stock (Mg ha^{-1} or kg m^{-2}). If data are reported as kg m^{-2}, they have to be expressed as Mg ha^{-1}. The SOC stock of the total soil layer is computed as:

$$SOC_{total\ soil\ layer} = \sum_{i=1}^{n} SOC_{stock} \quad [6]$$

where SOC_{stock} is the carbon stock of the i_{th} sub-layer.

The SD of the total soil layer is obtained from the the formula (Kenney and Keeping, 1951) of the variance (σ_z^2) of the sum of two correlated variables:

$$\sigma_z^2 = \sigma_x^2 + 2r\sigma_x\sigma_y + \sigma_y^2 \quad [7]$$

where x and y are the two correlated variables, σ the SD, and r is their correlation coefficient. The formula to compute the SD of the total soil layer is then:

$$SD = \sqrt{\sum_{i=1}^{n} \sigma^2(X_i) + 2\left(\sum_{i=1}^{n-1} Cov(X_i, X_{i+1}) + \sum_{i=1}^{n-2} Cov(X_i, X_{i+2}) + \sum_{i=1}^{n-3} Cov(X_i, X_{i+3})\right)} \quad [8]$$

where σ is the SD of the i_{th} sub-layer and n is the total number of layers analyzed. A single covariance term is computed as:

$$Cov(X_i, X_j) = \sigma_i \cdot \sigma_j \cdot \rho_{i,j} \quad [9]$$

where σ_i and σ_j are the SD of the X_i and X_j sub-layer, while ρ is the correlation between a pair of sub-layers according to their adjacent or non adjacent spatial disposition. Only layers that

are close to each other (adjacent) or at a maximum of three layer far away (non-adjacent) are considered in the correlation matrix.

The equation 8 is to be used when different layers are taken from the same undisturbed soil core. The covariance terms in the equation 8 reflect the correlation patters existing between soil depth layers also when they are sampled in different locations.

The correlation between layers depends on the control and treatment. For instance, let the control be conventional agriculture and the treatment be conservation agriculture. In control, soil is perturbed, and soil layers are mixed due to ploughing; the correlation can be assumed equal to zero. In the treatment, the correlation coefficient in the equation 9 could be empirically computed from the initial carbon data of each one of the different soil layers. In particular, it is assumed that two contiguous soil layers are more correlated than distant layers. In the Excel© Workbook, described in the next paragraph, the user can let the workbook automatically retrieve the correlation coefficients from the data entered, or manually set different correlation coefficients.

2.3 Excel© workbook

The Excel© workbook was developed for the SOC stock and SD computation under *Case 1* and *Case 2.* The code was developed in VBA language.

The users are allowed to let the Excel© workbook automatically retrieve the correlation coefficients (only for the Case 2 computations) from the different carbon stock data entered or manually insert them. This difference defines the computation type. In fact, in the Excel© workbook, the "SELECT COMPUTATION TYPE" list allows choosing the computation type between "Automatic" and "Manual".

The automatic and the manual computations are described below separately.

GENERAL INFO		Layer n°	Upper depth [cm]	Lower depth [cm]	CONTROL								TREATMENT							
					OC [%]	SE OC	SD OC	BD [Mg m3]	SE BD	SD BD	SOC stock [Mg ha]	SD SOC stock	OC [%]	SE OC	SD OC	BD [Mg m3]	SE BD	SD BD	SOC stock [Mg ha]	SD SOC stock
Study n°		1					0.00			0.00	0.00	0.00			0.00			0.00	0.00	0.00
Sample n°		2					0.00			0.00	0.00	0.00			0.00			0.00	0.00	0.00
Data source		3					0.00			0.00	0.00	0.00			0.00			0.00	0.00	0.00
Date [dd/mm/yy]		4					0.00			0.00	0.00	0.00			0.00			0.00	0.00	0.00
Sample size		5					0.00			0.00	0.00	0.00			0.00			0.00	0.00	0.00
ADDITIONAL NOTE:		6					0.00			0.00	0.00	0.00			0.00			0.00	0.00	0.00
		7					0.00			0.00	0.00	0.00			0.00			0.00	0.00	0.00
		8					0.00			0.00	0.00	0.00			0.00			0.00	0.00	0.00
		9					0.00			0.00	0.00	0.00			0.00			0.00	0.00	0.00
		10					0.00			0.00	0.00	0.00			0.00			0.00	0.00	0.00
		Total soil layer	0	0							0.00	0.00							0.00	0.00

Figure 1. *Example of a single template for the setting of the data input. The user is allowed to fill the green cells with all the information related to the sample/study selected.*

2.3.1 Automatic computation type

The user has first to insert the carbon data following the template showed in Figure 1. In each row of the template, and separately for control and treatment, the user can alternatively:

1. insert the OC % (and its SD) and the BD (and its SD) and leave the Excel© workbook to compute the SOC stock and its SD for a soil layer (Case 1);
2. directly insert the SOC stock and its SD of a sub-layers and leave the Excel© workbook to compute SOC stock and its SD for the total soil layer (Case 2).

Within each template (Figure 1), when the standard error is inserted, it is required to insert the sample size, being the number of replicates adopted in each sampling/study. In this way, the Excel© workbook can compute the standard deviation from the standard error. In this Excel© workbook it is assumed that the sample size does not vary within each template (i.e., each sub-layer has the same sample size). In addition, it is mandatory to insert the lower and the upper layer depth ("Lower depth [cm]", "Upper depth [cm]") values.

After all data have been inserted in one or more templates, press "COMPUTE AND SAVE" (Figure 2). The Excel© workbook will automatically retrieve the correlation coefficients and compute SOC stock for the total soil layer with the new correlation values. Then, the results are automatically saved in the "Database" sheet and the correlation values adopted in the computation appear in the automatic settings section, as showed in Figure 2.
In the Automatic computation type:

- before pressing "COMPUTE AND SAVE", all the values in each template will be temporarily computed assuming correlation equal to zero;
- the correlation coefficients are retrieved from all carbon data inserted in the "Data input" sheet separately for control and treatment;
- the correlation value for adjacent/non adjacent layers is retrieved only when at least three adjacent/non adjacent pair layers are inserted;
- the correlation value for non adjacent layers is computed as a unique value considering only layers that are two or three layers far from each other. For example, if a single sampling/study reports five layers (i.e., 1-2-3-4-5) from the top one (1) to the bottom (5), the Excel© workbook computes the non adjacent correlation coefficients, separately

for the control and treatment, considering the 1-3, 1-4, 2-4, 2-5, 3-5 non adjacent layers pairs;

- the SD value of the total soil layer (Case 2) is computed applying the "correlation between adjacent layers" coefficient to the layers that are close to each other, and the "correlation between non adjacent layers" to the layers that are two or three layers far away from each other (Figure 2);
- the correlation between OC and BD is always automatically set to -0.6.

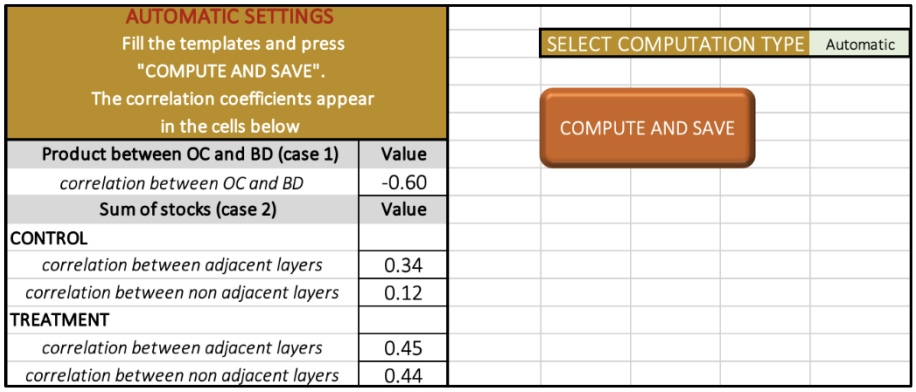

Figure 2. *Example of automatic setting of the correlation coefficients (product between OC and BD as Case 1, and sum of stocks as Case 2). In the Case 2, the correlation values are automatically retrieved separately for the control and treatment, and for the adjacent layers and non adjacent layers.*

2.3.2 Manual computation type

The user has to first insert the correlation coefficients for the product between OC and BD (Case 1) and the sum of stock (Case 2) for adjacent and non adjacent layers separately (Figure 3). Then, the user can insert the carbon data following the template shown in Figure 1. In each row of the template, and separately for control and treatment, the user can alternatively:

1. insert the OC % (and its SD) and the BD (and its SD) and leave the Excel© workbook to compute SOC stock and its SD for a soil layer (Case 1);
2. directly insert the SOC stock and its SD of the sub-layers and leave the Excel© workbook to compute SOC stock and its SD for the total soil layer (Case 2).

As for the automatic computation type, when the standard error is inserted (in the template shown in Figure 1), it is required to insert the sample size, being the number of replicates adopted in each sampling/study. In this way, the Excel© workbook can compute the standard deviation from the standard error. In this Excel© workbook it is assumed that the sample size

does not vary within each template (i.e., each sub-layer has the same sample size). In addition, it is mandatory to insert the lower and the upper layer depth ("Lower depth [cm]", "Upper depth [cm]") values.

After all the data have been inserted, press "SAVE" to let the Excel© workbook save all the results in the "Database" sheet.

In the Manual computation type:

- For those correlation values leaved empty, the correlation is set to zero;
- the SD value of the total soil layer (Case 2) is computed applying the "correlation between adjacent layers" coefficient to the layers that are close to each other, and the "correlation between non adjacent layers" to the layers that are two or three layers far away from each other.

MANUAL SETTINGS Fill the green cells below with the correlation values. If you want to save the results press "SAVE".		SELECT COMPUTATION TYPE	Manual
Product between OC and BD (case 1)	**Value**	SAVE	
correlation between OC and BD	-0.60		
Sum of stocks (case 2)	**Value**		
CONTROL			
correlation between adjacent layers	0.22		
correlation between non adjacent layers	0.12		
TREATMENT			
correlation between adjacent layers	0.87		
correlation between non adjacent layers	0.56		

Figure 3. *Example of manual setting of the correlation coefficients (product between OC and BD as Case 1, and sum of stocks as Case 2). In the Case 2, the correlation values have to be defined by the user separately for the control and treatment, and for the adjacent layers and non adjacent layers.*

As reported above, the Excel© workbook gives the possibility to store the results about SOC stock and SD for a total soil layer, also saving the general information (i.e., study number, or/and sample number as well as the data source, date of sampling and sample size). All this information is reported and ready to be used in the "Database" sheet (Figure 4), in which SOC stocks and SDs are given for all the total soil layers computed.

REFERENCE				CONTROL		TREATMENT		SINGLE LAYER		
Study n°	*Sample n°*	*Data source*	*Date [dd/mm/yy]*	*C stock [Mg ha]*	*SD C stock*	*C stock [Mg ha]*	*SD C stock*	*Layer LL [cm]*	*Layer UL [cm]*	*Sample size*
2	23	0	20/06/20	26	0.78	23.00	14.00	0	30	4.00
0	0	0	00/01/00	0	0.00	0.00	0.00	0	0	0.00
0	0	0	00/01/00	0	0.00	0.00	0.00	0	0	0.00
0	0	0	00/01/00	0	0.00	0.00	0.00	0	0	0.00
0	0	0	00/01/00	0	0.00	0.00	0.00	0	0	0.00
0	0	0	00/01/00	0	0.00	0.00	0.00	0	0	0.00
0	0	0	00/01/00	0	0.00	0.00	0.00	0	0	0.00
0	0	0	00/01/00	0	0.00	0.00	0.00	0	0	0.00

Figure 4. *Database sheet. For each sample/study, SOC stock and SD in the total soil layer are saved in a single row separately for control and treatment. In the first row of the example, SOC stock and SD of a total soil layer (0-0.3 m) are displayed for control and treatment. Ancillary data, such as study and sample number, data source, date, and sample size are shown in the same row.*

All the information required to compute the SD with the present Excel© workbook are summarized in a user manual directly in a workbook sheet (i.e., "Manual & Tips" sheet).
The Excel© workbook can be used to collect and elaborate data for meta-analysis or for re-elaborating data from field samples that have been measured as carbon concentration or in soil sub-layers.

Acknowledgements

The authors thank Dr Annachiara Colombi, PhD in Applied Mathematics, for supporting the mathematical formulation of the equations.
This work is funded by the Agriculture, Environment and Bioenergy PhD school of the University of Milan.
This study is also funded by the European Union's Horizon 2020 Framework Programme for Research and Innovation (H2020-RUR-2017-2) as part of the LANDSUPPORT project (grant agreement No. 774234), which aims at developing a decision support system for optimizing soil management in Europe.
This study is a part of the project "Carbon Market - Innovative cropping systems for carbon market" funded by Natural Resources Institute Finland (Luke). This study is also a part of the project SOMMIT: Sustainable management of soil organic matter to mitigate trade-offs between C sequestration and nitrous oxide, methane, and nitrate losses that received funding from the European Unions` Horizon 2020 research and innovation programme under grant agreement No. 862695 EJP SOIL.

Declaration of interests:

The authors declare that they have no known competing financial interests or personal relationships that could have appeared to influence the work reported in this paper.

Supplementary material *and/or* Additional information:

1. Excel© *workbook*

The tool for the computation of total soil organic carbon stock and its standard deviation from layered soils is freely available at:

https://doi.org/10.6084/m9.figshare.15066402.v3

References

Batjes, N.H., 1996. Total carbon and nitrogen in the soils of the world. Eur J Soil Science 47, 151–163. https://doi.org/10.1111/j.1365-2389.1996.tb01386.x.

Bohrnstedt, G., Goldberger, A., 1969. On the Exact Covariance of Products of Random Variables. Journal of the American Statistical Association, 64:328, 1439-1442. http://dx.doi.org/10.1080/01621459.1969.10501069.

Kenney, J.F. and Keeping, E. S., 1951. Mathematics of Statistics, Pt. 2, 2nd ed. Princeton, NJ: Van Nostrand.

Lugato, E., Lavallee, J.M., Haddix, M.L., Panagos, P., Cotrufo, M.F., 2021. Different climate sensitivity of particulate and mineral-associated soil organic matter. Nat. Geosci. 14, 295–300. https://doi.org/10.1038/s41561-021-00744-x.

Manrique, L. and Jones, C., 1991. Bulk density of soils in relation to soil physical and chemical properties. Soil Sci. Soc. Am. J. 55:476-481. https://doi.org/10.2136/sssaj1991.03615995005500020030x.

Minasny, B., Malone, B.P., McBratney, A.B., Angers, D.A., Arrouays, D., Chambers, A., Chaplot, V., Chen, Z.-S., Cheng, K., Das, B.S., Field, D.J., Gimona, A., Hedley, C.B., Hong, S.Y., Mandal, B., Marchant, B.P., Martin, M., McConkey, B.G., Mulder, V.L., O'Rourke, S., Richer-de-Forges, A.C., Odeh, I., Padarian, J., Paustian, K., Pan, G., Poggio, L., Savin, I., Stolbovoy, V., Stockmann, U., Sulaeman, Y., Tsui, C.-C., Vågen, T.-G., van Wesemael, B., Winowiecki, L., 2017. Soil carbon 4 per mille. Geoderma 292, 59–86. https://doi.org/10.1016/j.geoderma.2017.01.002.

Jensen, S. M., Svensgaard, J., Ritz, C., R., 2020. Estimation of the harvest index and the relative water content – Two examples of composite variables in agronomy. European Journal of Agronomy 112 (2020) 125962. https://doi.org/10.1016/j.eja.2019.125962.

Smith, P., Lutfalla, S., Riley, W.J., Torn, M.S., Schmidt, M.W.I., Soussana, J. F., 2018. The changing faces of soil organic matter research. Eur J Soil Sci 69, 23–30. https://doi.org/10.1111/ejss.12500.

Van der Vaart, A.W., 1998. Delta method. Asymptotic Statistics. Cambridge University Press, Cambridge, pp. 25–34. https://doi.org/10.1017/CBO9780511802256.

Chapter 3. A new module to simulate surface crop residue decomposition: description and sensitivity analysis

This is the official draft submitted to the Ecological Modelling and currently under peer review.

Authors:

Tommaso Tadiello[a], Mara Gabbrielli[a*], Marco Botta[a], Marco Acutis[a], Luca Bechini[a], Giorgio Ragaglini[a], Andrea Fiorini[b], Vincenzo Tabaglio[b], Alessia Perego[a]

Affiliation:

[a] Dipartimento di Scienze Agrarie e Ambientali Produzione, Territorio, Agroenergia, Università degli Studi di Milano, Milano, Italy

[b] Department of Sustainable Crop Production, Università Cattolica del Sacro Cuore, Via Emilia Parmense 84, 29122, Piacenza, Italy

[*] Corresponding author, mara.gabbrielli@unimi.it, tel. +39 02 5031 6612, via Celoria 2, 20133, Milan

**Corresponding author (tommaso.tadiello@unimi.it, DiSAA, Department of Agricultural and Environmental Sciences, University of Milan, Italy)*

Abstract

In the agroecosystem, the surface crop residues are widely recognized as affecting many processes such as soil water dynamics, crop growth, nitrogen and carbon cycling. For this reason, developing models that simulate the effect of the surface residues and their decomposition is crucial, especially while modelling conservation agriculture. To date, even though many cropping systems and C-oriented models differently simulate the evolution of the surface residue biomass, a comprehensive approach is still missing. In this study, we developed and new simulation module that explicitly simulates the decomposition of surface residues by including all variables and processes relevant to the agroecosystem's simulation. This module has been later integrated into the ARMOSA cropping system model. To quantify the contribution of each parameter to the simulated outputs (i.e., decomposed biomass), a sensitivity analysis (SA) was conducted, comparing the result with the APSIM model used as a benchmark. The SA was conducted on four different crop residues (maize, rye, soybean and wheat) over three different years. In addition, for each crop residues, the SA was performed for long and short simulation periods to verify whether parameters behaved differently according to the examined time period. The most critical parameters of the new module reflected the importance of the soil temperature, soil water content and residue biomass in the decomposition process. The potential decomposition rate had minor importance, highlighting that, when setting crop-specific values, other environment-related parameters are more relevant for the actual decomposition rate. In the case of APSIM model, the potential decomposition rate and the parameter related to soil temperature resulted in the first two ranks. Finally, concordance coefficients were used to compare SA outputs: compared to APSIM, the new model showed higher concordance passing from one crop residue to another even when comparing the short and long simulation periods within the same crop. In summary, this work presented a novelty in the surface residue representation and provided a deep survey of the module behaviour and characteristics.

Highlights

- A new simulation module has been developed to account surface residue decomposition;
- The new module has been later implemented into the ARMOSA model;
- A sensitivity analysis allowed to detect parameter/process importance;
- Soil temperature and water content, and residue mass mostly impact on decomposition;
- APSIM model has been used as a benchmark to test the new module.

3.1 Introduction

Surface crop residues represent a fraction of aboveground biomass lost by the crop through senescent organs or left on soil surface after harvest (for main crops) or termination (for cover crop). Permanent soil cover with surface crop residues is one of the main principles of conservation agriculture (FAO, 2016). Thus, the deliberate leaving of dead biomass on soil surface is considered as an important agronomic practice having a relevant impact on many processes such as soil water dynamics, soil erosion (Dietrich et al., 2019) and biodiversity, thus promoting crop growth and yield (Fiorini et al., 2020). Moreover, residue biomass retention and its subsequent decomposition has a significant effect on nitrogen and organic carbon dynamics (Chaves et al., 2021, Stella et al., 2019, Robertson et al., 2015, Iqbal et al., 2015, Coppens et al., 2007, Guérif et al., 2001).

For these reasons, the development of models that estimate simultaneously the decomposition of surface crop residues and their consequent transformation into soil organic matter along with the water and crop dynamics is crucial for a proper assessment of matter and energy flows in agroecosystems (Moreno-Cornejo et al., 2014). Another reason to specifically simulate the surface residue degradation is the slower decomposition rate of this residue pool compared to the one incorporated into the soil (Douglas et al. 1980).

To date, different cropping system models have been developed to simulate the decomposition of surface residues in response to pedoclimatic conditions and agronomic management. Besides the way they deal with the main environmental factors regulating the decomposition, each model differently focuses on specific biochemical or physical characteristics of the process. For example, the EPIC model considers the residue biochemical structure (through the lignin content), splitting the residues into metabolic and structural compartments (Izaurralde et al., 2006, Williams et al., 1984). The WEPP model carefully describes the effect of tillage operations on surface residues and considers standing and laying residues as two independent pools (Alberts et al., 1987). STICS is mainly based on nitrogen availability as regulating factor of residue decomposition rate (Justes et al., 2009, Brisson et al. 1998), while APSIM developed and improved different approaches to model the slower decomposition of the upper part of the surface residue layer (Holzworth et al., 2014, Thorburn et al. 2001). All the models mentioned above also simulate several other processes that directly involve surface residues or are affected by their presence (among which the most relevant are residues' water retention and evaporation, C and N fluxes deriving from residue decomposition and soil covering effect).

On the other hand, a more detailed simulation of residue decomposition is carried out by many C-oriented models (Dietrich et al., 2017, Nendel et al., 2011, Bruun et al., 2006). Even though they can simulate the decomposition process in detail, the fact that they usually do not simulate crop growth, as well as the effect of management operations on soil physico-chemical properties, makes them less suitable for assessing the contribution of residues to agroecosystem functioning.

To date, despite the richness of processes and the diversity of algorithms employed by both cropping system and C-oriented models, a comprehensive approach for the simulation of surface residue decomposition is still missing. A more exhaustive simulation of decomposition can improve the outputs of cropping system models and allows to better evaluate how the simulation of this process impacts on the whole agroecosystem. Thus, following a comprehensive approach, we developed a new simulation module that explicitly simulates the decomposition of surface residues by including all variables and processes that are relevant for agroecosystems simulation and that can be resumed as: (*i*) main crop residues decomposition after harvest, (*ii*) cover crop residues decomposition after mechanical termination, (*iii*) senescent leaves accumulation/decomposition during crop growth. This last process is essential since senescent leaves represent a possible source of soil C (Rumpel, 2011) and N that persists on the soil for a significant time. This module has been integrated and tested within the ARMOSA cropping system model (Valkama et al. 2020, Perego et al., 2013).

An assessment of models based on sensitivity analysis (SA) is needed to quantify the contribution of each parameter to the simulated outputs (Richter et al., 2010); for this reason, SA is an essential step before model calibration. Furthermore, SA is helpful to understand the behavior of the models itself (Confalonieri et al., 2012) by identifying where (i.e., for which parameters) a reduction of uncertainty leads to the biggest reduction of the respective output uncertainty (Diel and Franko, 2020). This indicates where further efforts for data quality shall be put to best use (Saltelli et al., 2007). In addition, to our knowledge, there is a lack of comparison studies among cropping system models that use different approaches to simulate surface residue decomposition. Comparing the results of SA of different models is a common way to highlight models' agreements and dissimilarities for a deeper analysis of the process under evaluation.

Therefore, the objectives of this work were: (i) to develop an integrated new module and assess it within the ARMOSA model to simulate surface residue decomposition and the processes

influenced by the residue presence; (ii) to assess the new module by analyzing its sensitivity to key parameters, in a case study with different crop residues and seasons; iii) to compare the sensitivity analysis of the new module with that of the APSIM model, based on the same case study.

3.2 Materials and Methods

3.2.1 The APSIM approach

APSIM is a comprehensive model developed to simulate biophysical processes in agricultural systems (Holzworth et al., 2014). Decomposition of surface residues in APSIM is implemented through the so-called SurfaceOM module. It models the kinetics of decomposition of organic materials left on soil surface until they are incorporated with tillage. The module simulates the flow of C to soil pools following the decomposition of dead aboveground biomass (Meier and Thorburn, 2016, Thorburn et al. 2001) using a first-order kinetics. The actual decomposition rate of the flat mass per unit area is obtained by the potential decomposition rate (unique for the whole mass) and the factors (0-1) accounting for the limitations imposed by residue moisture, temperature, C:N ratio and residue-soil contact. The moisture factor is estimated from the potential soil evaporation cumulated along the decomposition period. The effect of temperature on residue decomposition is described based on the average air temperature, while the CN limit factor is calculated for individual residue types. Lastly, the residue-soil contact factor operated where large amounts of surface residues are present, reducing the overall rates of decomposition.

3.2.2 The new surface residue decomposition module

The new surface residue decomposition module implemented in ARMOSA represents the most important processes regarding the dynamics of surface residue decomposition (biomass partitioning between standing and laying residues, decomposition rate and residue soil covering), and their influence on surface water balance (residue water retention and residue influence on soil evaporation) and soil properties (e.g., carbon and nitrogen balance). All the equations of the module are reported in Appendix A. After crop harvest or cover crop termination, the module simulates the actual decomposition rate of standing and flat residues separately. The decomposition process is based on different potential decomposition rates (PDR_s for standing residue biomass, PDR_f for flat residue biomass and PDR_f(leaves) specifically for leaves belonging to the flat biomass) and is affected by environmental and management conditions.

We adopted some key processes from the WEPP model for the simulation of: 1) the partitioning of crop residues at harvest in standing and flat components, based on crop and cutting height; 2) the decomposition of the standing biomass (as a function of rain and temperature) and its

conversion to the flat biomass (due to the action of wind and snow); 3) the soil covering level provided by standing and flat residues, possibly affected by soil tillage operations.

The decomposition of the flat component of surface biomass follows the APSIM approach, in that the potential decomposition rate of surface residues is limited by temperature, C:N ratio of the residues, soil-residues contact degree, and soil moisture. These regulating factors act separately on the actual decomposition rate of the three (stand, flat and leaves) pools. Unlike APSIM, however, the new module discriminates between leaf and stem biomass to account for their different susceptibility to decomposition. The effect of soil moisture was modelled based on the ARMOSA soil moisture simulation to be consistent with the algorithm already implemented for the residues incorporated into the soil. Carbon and nitrogen fluxes from surface residues decomposition are allocated into stable soil carbon and mineral soil nitrogen. Lastly, the STICS approach was adopted for estimating residue water retention (limited by incident rainfall and influenced by residue wettability), assessing residue evaporation demand (based on the flat residue soil cover) and subsequently adjusting soil evaporation to fulfil the unsatisfied evaporation request.

3.2.3 Case study for sensitivity analysis

The scenario used for sensitivity analysis spans between 2013 and 2017 and is based on a long-term field experiment (started in 2011) at the CERZOO research station, in Piacenza (45°00'18.0'' N, 9°42'12.7'' E; 68m above sea level), Po Valley, Northern Italy. The soil at the field site is a fine, mixed, mesic Udertic Haplustalfs (Soil Survey Staff, 2014). Main soil (0-30 cm) properties before the beginning of the experiment were: organic matter content 21 g kg^{-1}; pH (H_2O) 6.8; bulk density 1.36 g cm^{-3}; sand 122 g kg^{-1}; silt 462 g kg^{-1}; clay 416 g kg^{-1}; soil total N 1.2 g kg^{-1}; available P (Olsen) 32 mg kg^{-1}; exchangeable K (NH_4^+ Ac) 294 mg kg^{-1}, and cation exchange capacity 30 $cmol^+$ kg^{-1}. The climate is temperate (Cfa Köppen classification), with an average annual temperature of 14.2 °C and annual rainfall of 778 mm (last 20-years average). Daily weather inputs required by the models were obtained by the Agri4Cast Resources Portal (Biavetti et al., 2014).

Briefly, the crop sequence was a three-year crop rotation: maize (*Zea mays* L.), soybean (*Glycine max* (L.) Merr.) and winter wheat (*Triticum aestivum subsp. aestivum* L.). Rye (*Secale cereale* L.) was utilized as a cover crop after maize and winter wheat, in a no-tillage regime. The experimental design was a randomized block with 4 replicates. Approximately two weeks before sowing the cash crop, cover crops was terminated by spraying Glyphosate [N-

(phosphonomethyl) glycine] at the rate of 3 L ha^{-1}. Cash crop and cover crop residues, after harvesting and termination respectively, where left onto the soil surface without chopping.
In this experiment, a residue biomass decomposition assessment was conducted on surface residue biomass of the cash crop and on the whole surface cover crop biomass. The different residues biomasses were used to initialize the models under the present study. Thus, the residue biomass from the harvest of the cash crop and from the termination of the cover crop represent the dependent variable on which the present study is based. We will use the term "surface residue biomass" for the biomass laying on the soil surface regardless of its source (i.e., harvest or termination). Once the following crop was harvested or terminated, the previous residues (if still present on the surface) were removed from the soil, and the new residues were put on the soil surface. More details about the whole experiment are available in Boselli et al. (2020).

3.2.4 Sensitivity analysis

Sensitivity analysis (SA) was carried out on the amount of decomposed residue biomass, which is the dependent variable that is affected by all processes included in the new module. Therefore, all the parameters involved in biomass decomposition were considered in the sensitivity analysis. A complete parameter's list is reported in Table 1.
To better assess the role of the parameters on the decomposition dynamics under different pedo-climatic conditions, several SAs were conducted on residues of all crops in the rotation, in the periods of the year when they are on the soil surface. In addition, for each tested crop, two timespans of decomposition, hereafter reported as "simulation periods", were considered: (1) the "Long Simulation Period" (LSP), from crop harvest/termination to the following crop harvest/termination, and (2) the "Short Simulation Period" (SSP), that is half of the long simulation period and starts from the same crop harvest/termination date. The introduction of the LSP and SSP periods allowed us to detect possible patterns of parameter sensitivity in different stages of residue decomposition. In fact, the analysis of SSP and LSP can distinguish the parameters that are important only at the beginning of the decomposition process (when the environmental conditions might be different compared to the end of LSP), from the parameters that maintain their importance along the whole decomposition period.
For both the new module and APSIM, the total number of SAs (10) was equal to the combination of the number of crops in the rotation (i.e., maize, rye, soybean, wheat, and rye) multiplied by the number of simulation periods (LSP and SSP). For each SA, Table 2 shows the specific crop residues under decomposition and the period of the year involved. Table 2

also shows the initial residue biomass at the beginning of each SA, that was derived from Boselli et al. (2020).

Table 1. *Crop parameters selected for the sensitivity analysis. Equations related to the new module implementation are reported in appendix A.*

Model	Name	Unit	Mean (SD)				Definition	Source
			Maize	Wheat	Rye	Soybean		
New module implemented in ARMOSA	PDR_f	kg m^{-2} d^{-1}	0.0065 (0.00195)	0.0085 (0.00255)	0.0085 (0.00255)	0.0038 (0.0039)	Decomposition rate of the flat residue biomass	Calibrated starting from Stott et al., 1990 and Probert et al., 1998
	PDR_f (leaves)	kg m^{-2} d^{-1}	0.015 (0.0045)	0.015 (0.0045)	0.015 (0.0045)	0.013 (0.0045)	Decomposition rate of the flat residue biomass (leaves)	Calibrated starting from Stott et al., 1990
	CN_{opt}	-	25 (7.5)	25 (7.5)	25 (7.5)	25 (7.5)	Optimum C/N ratio of flat biomass for decomposition	Thorburn et al., 2001
	CN_{slope}	-	0.277 (0.0831)	0.277 (0.0831)	0.277 (0.0831)	0.277 (0.0831)	Slope of C/N ratio function curve	Thorburn et al., 2001
	T_{opt}	°C	20 (6)	20 (6)	20 (6)	20 (6)	Optimum temperature for decomposition	APSIM default values
	Cf_{rt}	m^2 kg^{-1}	2.1 (0.63)	6.4 (1.92)	6.4 (1.92)	5.2 (1.56)	Area to mass ratio of residue biomass	Stott et al, 1990
	B_{f_crit}	kg m^{-2}	0.2 (0.06)	0.2 (0.06)	0.2 (0.06)	0.2 (0.06)	Critical flat residue biomass above which the decomposition is slower	APSIM default values
	$Wett_{mulch}$	mm Mg^{-1} ha	2.6 (0.78)	2.6 (0.78)	2.6 (0.78)	2.6 (0.78)	Residue biomass water retention	Scopel et al., 1998
	SWC_{min}	-	0.2 (0.06)	0.2 (0.06)	0.2 (0.06)	0.2 (0.06)	Minimum residue water content for decomposition	Calibrated
	SWC_{optmin}	-	0.6 (0.18)	0.6 (0.18)	0.6 (0.18)	0.6 (0.18)	Minimum optimum residue water content for decomposition, expressed as a proportion of field capacity	Calibrated
	SWC_{optmax}	-	1.1 (0.33)	1.1 (0.33)	1.1 (0.33)	1.1 (0.33)	Maximum optimum residue water content for decomposition expressed as a proportion of field capacity	Calibrated
	MA_{optb}	-	1.5 (0.45)	1.5 (0.45)	1.5 (0.45)	1.5 (0.45)	First slope of the water limitation function	Calibrated
	MA_{opta}	-	1 (0.3)	1 (0.3)	1 (0.3)	1 (0.3)	Second slope of the water limitation function	Calibrated
	$Conv_{fct}$	-	0.99 (0.297)	0.99 (0.297)	0.99 (0.297)	0.99 (0.297)	Adjustment factor to account for the effect of wind and snow on the standing residue biomass	Stott et al., 1990
APSIM	B_{f_degr}	kg m^{-2} d^{-1}	0.1 (0.03)				Potential decomposition rate (for all biomass)	APSIM default values
	CN_{opt}	-	25 (7.5)				Optimum C/N ratio of residue biomass for decomposition	APSIM default values
	CN_{slope}	-	0.277 (0.0831)				Slope of C/N ratio function curve	APSIM default values
	T_{opt}	°C	20 (6)				Optimum temperature for decomposition	APSIM default values
	Cf_{rt}	ha kg^{-1}	0.0005 (0.00015)				Area to mass ratio of residue biomass	APSIM default values
	B_{f_crit}	kg ha^{-1}	2000 (600)				Critical mass of residue biomass above which the decomposition is slower	APSIM default values
	cum_eos_max	mm	20 (6)				Cumulative potential soil evaporation at which decomposition rate becomes zero	APSIM default values

Table 2. *Simulation starting and ending dates for each crop residue in the rotation. The ending dates are divided between short (SSP) and long (LSP) simulation period. For each crop the initial total residues biomass is reported.*

Crop residues	Simulation starting date (harvest or termination date)	Simulation ending date		Initial residue biomass (kg DM ha^{-1})
		SSP	LSP	
Maize	17/09/2014	07/01/2015	28/04/2015	11707
Rye (1)	21/04/2015	25/06/2015	28/08/2015	2850
Soybean	01/10/2015	29/01/2016	28/05/2016	3280
Wheat	08/07/2016	16/11/2016	27/03/2017	7577
Rye (2)	07/04/2017	13/06/2017	19/08/2017	2230

In addition, a comparison among crop residues decomposing in a similar period of the year was done to better evaluate the role of environmental conditions on decomposition: we have distinguished crop residues that decompose during the colder season (winter or fall) and residues that decompose during the warm season (spring or summer). Figure 1 shows for each crop in the rotation the season of decomposition, split by SSP and LSP, allowing an easier comparison among crops.

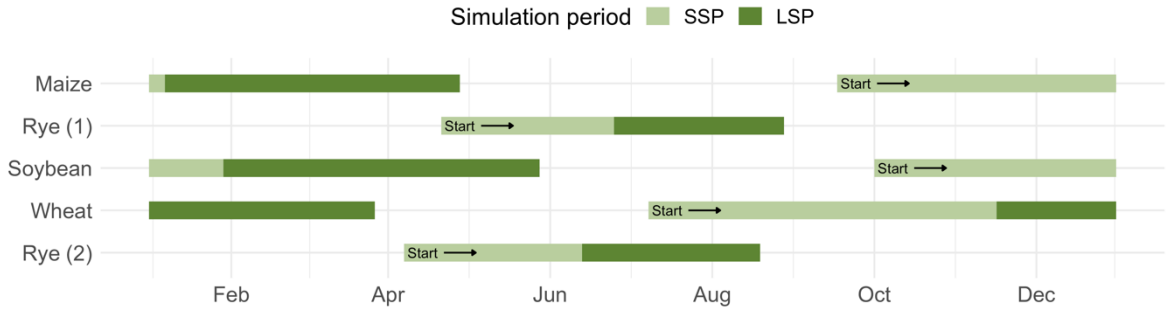

Figure 6. *Seasons of the year during which the crops residue decomposition occurred. The total green area is the length of the season when the residues were on the soil surface. "Start" indicates the harvest or termination date from which the decomposition process started. SSP, short simulation period; LSP, long simulation period. The LSP has to be graphically considered as the sum of the SSP and LSP (for more details see Table 2).*

Sensitivity analysis requires setting the average and standard deviation of the parameters. Parameters values were derived from the literature (Table 1). When no data were available, default or calibrated values were adopted. Standard deviation was set to 30% of the average for all parameters to prevent unrealistic values. All parameter distributions were assumed to be normal (Confalonieri et al., 2006).

Random variates of the same parameters were generated using the sampling technique for sensitivity analysis known as the Morris method (Morris, 1991) and further improved by

Campolongo et al. (2004). This technique deals efficiently with models containing a large number of input parameters without relying upon strict assumptions about the model such as additivity or monotonicity of the input-output relationship (Confalonieri, 2006). The study of Paleari et al. (2021) highlighted that the Morris method is a suitable alternative to more demanding SA methods (e.g., Sobol method) when ranking parameters or discriminating between influential and non-influential parameters.

The Morris method is based on a systematic sampling of the multidimensional space defined by the possible values of the parameters to generate a random set of OAT (i.e., once at time) experiments (Pianosi et al., 2016) and identifying the few crucial parameters based on the distribution (*Fi*) of the elementary effect associated with the i^{th} input factor. To estimate these quantities, Morris suggests sampling r elementary effects from each *Fi* via an efficient design that constructs r trajectories of (k + 1) points in the input space, each providing k elementary effects, one per input factor.

For each model input (X), the elementary effect is defined as:

$$d_i(X) = \left(\frac{y(X_i,\ldots,X_{i-1},X_i+\Delta,X_{i+1},\ldots,X_k)-y(X)}{\Delta}\right) \quad [1]$$

where (i) $X = (x_1,\ldots, x_k)$ as the k-dimensional vector of model studied parameters x_i; (ii) all variables are rescaled in the 0–1 range; (iii) x_i can take only P (the number of levels, using the Morris terminology) discrete values in the set {0, 1/(P - 1), 1/(P - 2),. . ..,1} and (iv) Δ is a multiple of 1/(P - 1).

The total cost of the experiment is thus r(k + 1) (Campolongo et al 2007). The Morris method requires the choice of the number of trajectories (sequences of points starting from a random base vector in which two consecutive elements differ only for one component) and levels. For both models, the sensitivity analysis was run using 10 trajectories and 4 levels.

The method samples values of X from the hyperspace Ω (identified by an k-dimensional P-level grid) and finally calculates the mean (μ, strength) assessing the overall influence of the parameter on y(X) and its standard deviation (σ, spread) estimating the totality of the higher order effects (Richter et al., 2010). In this work, μ is considered as absolute value (μ^*) as proposed by Campolongo et al. (2004). The μ^* value is successful in ranking parameters in order of importance and performs well when the goal is identifying non-influential parameters (Confalonieri et al., 2006). The second measure (σ) is useful to detect parameters involved in interaction with other parameters, or whose effect is non-linear (Saltelli et al., 2004). With this

convention the more “dangerous” (i.e., sensitive) parameters are in the top right quadrant of the σ versus μ^* plot (“danger zone”), where both sensitivity and strength are high (Confalonieri et al., 2006).

For the new module, the SA was conducted using the ARMOSA integrated feature that allows the model to easily interact with the Salib external library (Herman and Usher, 2017). This library implements many sensitivity analysis methods, including Morris. In the case of APSIM, the "sensitivity" package (Iooss et al., 2021) was used to setting the grid for the SA (i.e., a data frame with the combinations of parameters to be evaluated). To use this package the complementary "apsimx" package (Miguez, 2022) interface was utilized to set and run the SA. The functions belonging to the "apsimx" package also allow the user to open, inspect, read and edit the simulation file (".apsim"). In addition, this package allows editing the configuration files (".xml"), where the default setting of the parameters is stored. The code used to set the SA is available as supplemental material (Supplemental material 1).

3.2.5 Statistical analysis

To evaluate the agreement between the different sensitivity rankings within each model, the top-down concordance coefficient was applied, which allows to emphasize the agreement among rankings assigned to important parameters through the transformation of original data into Savage-scores (Savage, 1954). Savage-scores are calculated as follows:

$$S_i = \sum_{j=1}^{n} \frac{1}{j} \quad [2]$$

where *i* is the rank assigned to the rank ith order statistic in a sample of size n. The ith rank has been assigned to the different μ^* for each parameter in a single SA.

After the conversion into Savage-scores, the Kendall's coefficient of concordance was applied. This coefficient of concordance can be used to measure the agreement among *b* sets of rankings when $b > 2$ (Iman and Conover, 1987). It is also known as the top-down correlation coefficient because of its sensitivity to agreement among the top ranks. It can be computed as:

$$C_T = \frac{1}{b^2(n-S_1)} \sum_{i=1}^{n} S_i^2 - b^2 n \quad [3]$$

where S_i is the sum of the Savage-scores assigned to the ith object taken over all *b* sets of rankings. The coefficient of concordance is associated with a *p-value* under the Kendall null

hypothesis that the p judges or raters (i.e., set of SAs) produce independent rankings of the objects or subjects (i.e., parameters). To preserve the correct Type I error, Siegel and Castellan (1988) recommended the use of a permutation-based table of critical values for C_T only when the number of parameters is ≤ 7. When the number of parameters exceeds seven, they recommended using the χ^2 distribution approximation. Thus, according to the parameters number, the *p-value* of each coefficient of concordance was obtained with the χ^2 distribution for the new module (14 parameters evaluated) and with the permutation-based method for APSIM (7 parameters evaluated) (Legendre et al., 2005). Both the C_T and the *p-values* coefficients were automatically retrieved from all sets of ranks using the R package "synchrony" (Tarik, 2019) using the ranking ties correction when necessary.

3.3 Results

3.3.1 Models' parameters: similarities and differences between the new module and APSIM

The two modelling approaches (i.e., the new module and APSIM) utilized different parameters to simulate surface residue biomass decomposition (Table 1; Appendix A). Only five of them, CN_{opt} and CN_{slope} (accounting for the CN ratio of the residue biomass), T_{opt} (accounting for the optimal temperature for decomposition), Cf_{rt} (accounting for the area to mass ratio of residue biomass) and B_{f_crit} (accounting for the critical flat residue biomass above which the decomposition is slower) are in common since they have the same biological meaning and role within the simulated process.

Other parameters reflect the different approaches adopted. Starting from the potential decomposition rates, the new module uses two different parameters, one for leaves (PDR_f (leaves)) and one for the rest of flat biomass (PDR_f). These potential decomposition rates are further defined specifically for each crop. The third potential decomposition rate (PDR_s) was not used in this study because of the lack of standing residue. APSIM instead uses a single potential decomposition rate (B_{f_degr}) regardless the residue biomass component. The limitation of biomass decomposition due to soil water is represented by four parameters in the new module (SWC_{min}, SWC_{optmin}, SWC_{optmax}, MA_{optb} and MA_{opta}, Eq. 10, Appendix A, Table 1), whereas only by one parameter (cum_eos_max) in APSIM. Furthermore, the new module uses the $Wett_{mulch}$ and the $Conv_{fct}$ parameters to define the residue biomass water retention and to account for the effect of wind and snow on the standing residue biomass, respectively.

Other model parameters belonging to ARMOSA are not included in this analysis because they are not directly related to decomposition and were left at their default value.

3.3.2 Sensitivity analysis

Sensitivity analysis results are described separately for the new module and for APSIM. Within each of these approaches, SA results are presented for each crop in the rotation (Table 2).

3.3.2.1 New decomposition module implemented in ARMOSA

The results differed based on the crop and the period of the year in which residues decompose. In the case of maize, T_{opt}, B_{f_crit} and SWC_{min} had the highest effect on decomposition, with no differences between SSP and LSP (top right quadrant in Figure 2A/2B). Another important parameter involved in the process was CN_{opt}, while all the other parameters had μ^* equal or close to zero (Fig. 2A/2B).

For rye, a clear pattern was visible only in 2017 ("Rye (2)", Fig. 2I/2L) when the SWC_{min} (i.e., minimum residue water content for decomposition process expressed as a proportion of field water capacity) showed constantly a more relevant effect than all the other parameters. In 2015 (i.e., "Rye (1)"), the same pattern appeared only in LSP (Fig. 2D). In SSP (Fig. 2C) instead, B_{f_crit} and T_{opt} appeared in the top right quadrant together with SWC_{min}. The impact of these three parameters could be discriminated by ranking on the basis of σ: T_{opt} maintained an essential role but its interactions with other parameters were low.

In the case of soybean, T_{opt} still had the same importance as found in maize. No other parameters had a significant influence on model outputs as indicated by low μ^* (Fig. 2E/2F).

For wheat, SA showed a clear pattern in SSP, with SWC_{min} covering the largest μ^* percentage compared to all the other parameters (Fig. 2G). Values of μ^* decreased smoothly in LSP from right to left but with discontinuities, allowing to distinguish the most influential parameters. SWC_{min} ranked first, followed by B_{f_crit}, T_{opt}, SWC_{optmin} and PDR_f (Fig. 2H).

A valuable indication of the SA results can be retrieved by averaging the Savage-scores (Paleari et al., 2021) of the sensitivity metrics estimated for the different crops and simulation periods (data not shown). The average final ranking allowed us to identify the top parameters associated with surface residue decomposition, regardless of the crop and of the period of decomposition. Starting from the most relevant, the top five parameters were T_{opt}, SWC_{min}, B_{f_crit}, PDR_f and PDR_f (leaves).

Kendall's coefficient of concordance, computed on the whole set of ten SAs, showed a high concordance value ($C_T = 0.86, p\text{-}value < 0.001$) meaning that the ten different rankings significantly agreed in the definition of the most important parameters. Table 3 shows the coefficient of concordance and the associated *p-value* among all the SAs. On average, the concordance values within each crop between the short and long period were always high (C_T = 98-99, Table 3) and significant (*p-value* < 0.05). These values reflected the high concordance of the top ranks within every single crop, as shown in Figure 2, even though some differences were found for parameters with lower importance (i.e., lower values of μ^*).

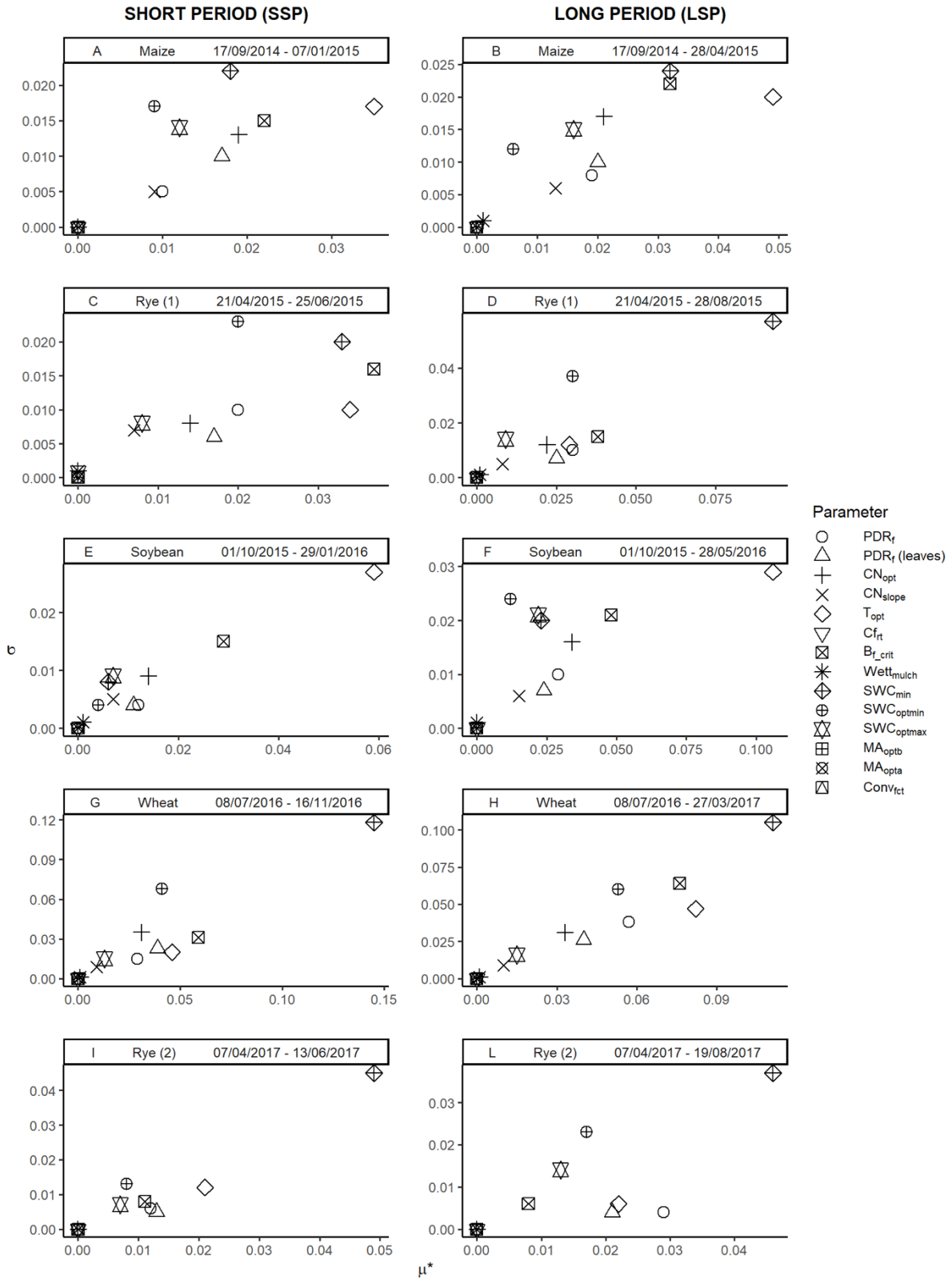

Figure 2. *The mean (μ*) and the standard deviation (σ) effects for the new module implemented into the ARMOSA model, calculated for the sensitivity analysis with the Morris method. The decomposed biomass was used as a dependent variable. Each graph label indicates the crop residue involved, the starting and ending dates of each SA for the short (SSP) and long (LSP) period respectively. Parameters shared between the two model approaches (CN_{opt}, CN_{slope}, T_{opt}, Cf_{rt}, B_{f_crit}) have the same symbol as in figure 3. More information on the parameters is given in Table 1.*

Table 3. Matrix summarizing ten sensitivity analyses (five crops and two simulation periods, the short simulation period, SSP, and the long simulation period, LSP) conducted with the new module implemented into ARMOSA. The top right quadrant reports the coefficients of concordance (Eq. 3, with 10 'raters' and 14 subjects), while the bottom left quadrant reports the associated p-values.

		Coefficient of concordance (C_T)									
		Maize (SSP)	**Maize (LSP)**	**Rye (1) (SSP)**	**Rye (1) (LSP)**	**Soybean (SSP)**	**Soybean (LSP)**	**Wheat (SSP)**	**Wheat (LSP)**	**Rye (2) (SSP)**	**Rye (2) (LSP)**
	Maize (SSP)		0.99	0.95	0.90	0.96	0.98	0.94	0.93	0.86	0.82
	Maize (LSP)	0.019		0.95	0.92	0.96	0.97	0.96	0.96	0.89	0.85
	Rye (1) (SSP)	0.026	0.025		0.98	0.91	0.94	0.98	0.98	0.93	0.9
	Rye (1) (LSP)	0.037	0.031	0.021		0.86	0.89	0.98	0.99	0.92	0.92
p-value	**Soybean (SSP)**	0.023	0.024	0.034	0.049		0.99	0.88	0.9	0.8	0.77
	Soybean (LSP)	0.019	0.021	0.027	0.04	0.019		0.91	0.92	0.85	0.82
	Wheat (SSP)	0.027	0.024	0.02	0.02	0.042	0.034		0.98	0.92	0.89
	Wheat (LSP)	0.029	0.023	0.019	0.019	0.038	0.031	0.019		0.95	0.93
	Rye (2) (SSP)	0.049	0.041	0.029	0.031	0.076	0.054	0.032	0.026		0.98
	Rye (2) (LSP)	0.068	0.055	0.036	0.033	0.094	0.069	0.041	0.029	0.019	

Based on the season during which the crop residue decomposition occurs (Fig. 1), different crop residues can be compared. Maize residues mostly degraded in the same season as soybean: indeed, the two SA conducted in the two SSP had high concordance (C_T = 0.96, *p-value* = 0.023, Table 3), confirming the significant effect of T_{opt} and B_{f_crit}. If we consider the LSP of the same crops, the coefficient of concordance is still significantly high (C_T = 0.97, *p-value* = 0.024, Table 3), emphasizing, again, the importance of the temperature and the critical residue biomass amount (i.e., B_{f_crit}, the critical level of flat residue biomass above which the decomposition is slower) for the surface decomposition process. In this specific crop rotation, the wheat residues had the longest time of decomposition (262 days overall) covering the soil, differently from the other crop residues, from late autumn to early summer seasons. For this reason, it seemed not reasonable to compare it with the other crops. The two rye cover crops instead, were terminated almost in the same period, and their residues remained on the soil surface until the end of August. Thus, the coefficients of concordance confirmed the relevance of the soil water content (with SWC_{min} being the most critical parameter) on the surface decomposition process, even if C_T was lower compared to those above (for the short simulation periods C_T = 0.93, *p-value* = 0.029, while for the long simulation period C_T = 0.92, *p-value* = 0.033). This is mainly due to the second and third positions (alternately belonging to T_{opt}, B_{f_crit} or PDR_f) in the parameter rankings of the two cover crops belonging to different parameters.

3.3.2.2 The APSIM model

Compared to ARMOSA, the APSIM model has a lower number of parameters, which cause a lower parameter overlapping in the diagnostic diagrams (Fig. 3).

As for maize SA outputs varied between the SSP and LSP. The T_{opt} parameter clearly had an important role in the surface decomposition process in both simulation periods, but the effect was variable for the other parameters (Fig. 3A/3B). In fact, B_{f_crit} played a key role in the SSP, while the potential decomposition rate (B_{f_degr}) assumed a crucial weight for the LSP. All the other parameters (i.e., CN_{opt}, CN_{slope}, Cf_{rt} and cum_eos_max), even with lower values of σ, also reported lower values of μ^*. Thus, they were far away from the top-right quadrant.

For the rye cover crop, the results showed a similar parameters response between SSP and LSP within a single year, but differences emerged when comparing 2015 (i.e., "Rye (1)") to 2017 (i.e., "Rye (2)"). In 2015, the most critical parameter was the cum_eos_max, which scored the highest value in both SSP and LSP (Fig. 3C/3D). In the second and third positions of the ranking, we found the B_{f_degr} and Cf_{rt}, varying between LSP and SSP. All the other parameters have μ^* values close to zero, not affecting the SA output. In 2017, the most sensitive parameters remained the same as in 2015, but their ranks became considerably different. The temperature had a significant effect on the decomposition process, increasing the weight of the T_{opt} parameter in the SA analysis (Fig. 3I/3L). The potential decomposition rate (B_{f_degr}) is in the middle of the diagram for both SSP and LSP, always followed by cum_eos_max. Similar results have been observed also in soybean, when T_{opt} had the most significant impact against all the other parameters (Fig. 3E/3F) in both simulation periods. Focusing on SSP, the SA evidenced B_{f_crit} and B_{f_degr} as essential parameters affecting the decomposition process, since they are located in the top-right quadrant. In the long period, the weight of B_{f_crit} and B_{f_degr} is less evident and it is comparable with the weight of CN_{opt}. In LSP, the clusters of these three last parameters can be easily distinguished for all the other parameters, even though their impact is negligible. Wheat is the only crop heavily influenced by the B_{f_degr} parameter, which is constantly at the top right angle of the diagram (Fig. 3G/3H). Nevertheless, the situation becomes different when comparing the SSP with LSP. B_{f_crit} had a higher μ^* value in LSP, with a high σ value too. In SSP B_{f_crit} maintained high μ^* value but decreased the interaction with other parameters (lower σ value). In the bottom-left quadrant, the other parameters are less sensitive. B_{f_crit} and T_{opt} had predominant roles in the LSP diagram compared to CN_{opt}, CN_{slope}, Cf_{rt} and cum_eos_max parameters.

Averaging the Savage-scores of the sensitivity metrics, estimated for the different crops and periods, led to an averaged ranking (data not shown). The optimum temperature for decomposition (T_{opt}) led the rank, followed by the potential decomposition rate (B_{f_degr}), the critical residue mass (B_{f_crit}) and the cumulative potential soil evaporation (cum_eos_max).

Kendall's coefficient of concordance computed on the whole set of ten SA was relatively low (C_T = 0.43). The ten different rankings do not greatly agree with each other in defining the most critical parameters involved in the residue decomposition process, even with a significative test (*p-value* < 0.001).

Table 4 shows the coefficient of concordance and the associated p-value between all the combinations of SA. In APSIM, within each crop, the concordance values between SSP and LSP were significant (P < 0.05) except for maize, and with values almost stable around 90% (Table 4).

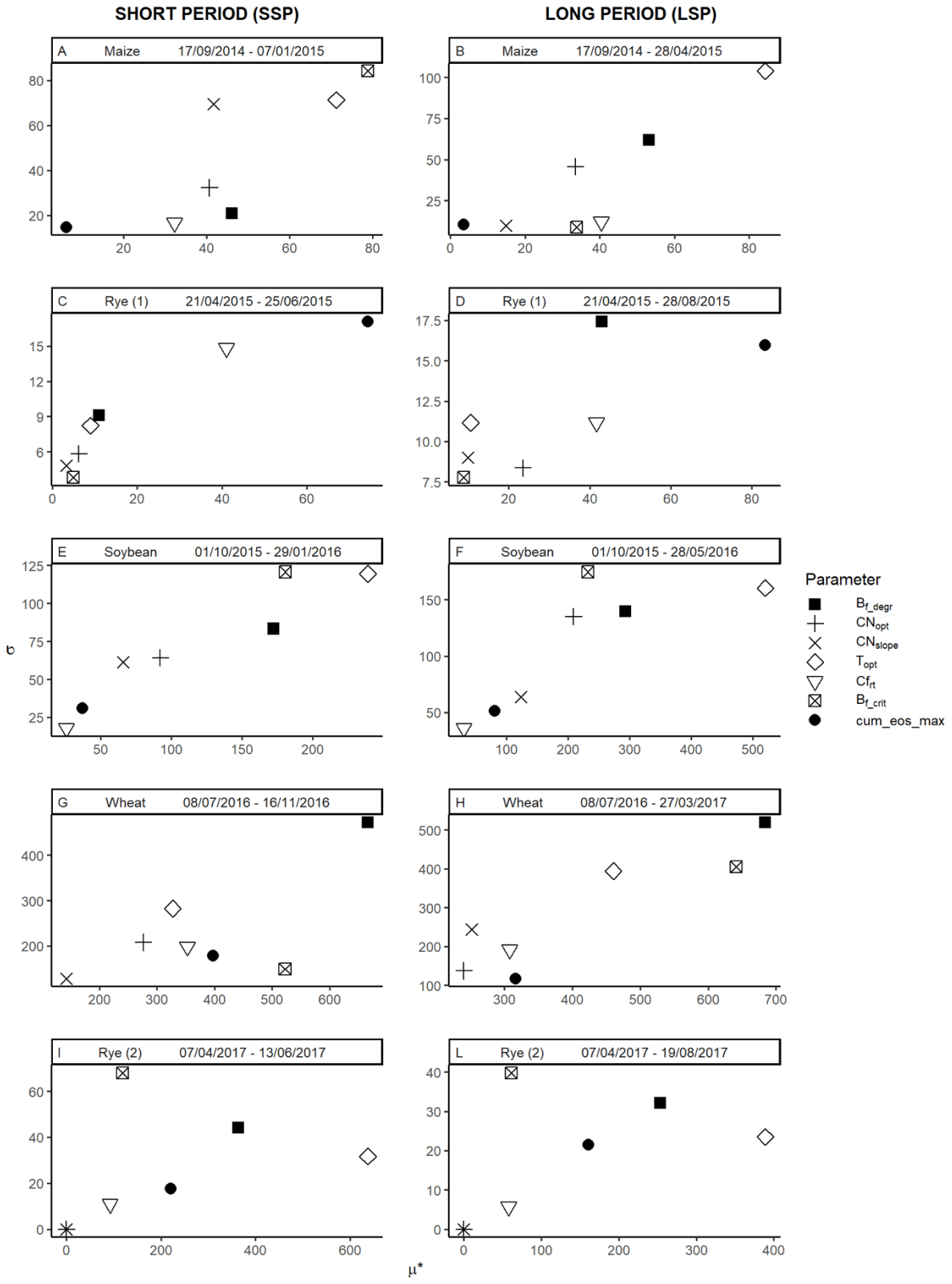

Figure 3. *The mean (μ^*) and the standard deviation (σ) effects for the APSIM model, calculated for the sensitivity analysis with the Morris method. The decomposed biomass was used as dependent variable. Each label indicates the crop residue involved, the starting and ending dates of each SA for the short (SSP) and long (LSP) period respectively. Parameters shared between the two models (CN_{opt}, CN_{slope}, T_{opt}, Cf_{rt}, B_{f_crit}) have the same symbol as in figure 2. More information on the parameters is given in Table 1.*

Table 4. *Matrix summarizing ten sensitivity analyses (five crops and two simulation periods, the short simulation period, SSP, and the long simulation period, LSP) conducted with the APSIM model. The top right quadrant reports the coefficients of concordance (eq. 3, with 10 raters and 7 subjects) while the bottom left quadrant reports the associate p-values.*

		Coefficient of concordance (C_T)									
		Maize (SSP)	**Maize (LSP)**	**Rye (1) (SSP)**	**Rye (1) (LSP)**	**Soybean (SSP)**	**Soybean (LSP)**	**Wheat (SSP)**	**Wheat (LSP)**	**Rye (2) (SSP)**	**Rye (2) (LSP)**
	Maize (SSP)		0.79	0.2	0.14	0.95	0.91	0.61	0.79	0.67	0.67
	Maize (LSP)	0.1		0.54	0.45	0.79	0.82	0.64	0.77	0.79	0.79
	Rye (1) (SSP)	0.935	0.456		0.95	0.29	0.34	0.73	0.61	0.73	0.73
	Rye (1) (LSP)	0.969	0.615	0.007		0.25	0.34	0.68	0.54	0.64	0.64
p-value	**Soybean (SSP)**	0.006	0.092	0.846	0.878		0.98	0.59	0.77	0.75	0.75
	Soybean (LSP)	0.017	0.069	0.773	0.771	0.002		0.61	0.79	0.79	0.79
	Wheat (SSP)	0.332	0.272	0.151	0.22	0.35	0.33		0.93	0.79	0.79
	Wheat (LSP)	0.1	0.117	0.331	0.455	0.116	0.101	0.012		0.9	0.9
	Rye (2) (SSP)	0.234	0.09	0.144	0.264	0.118	0.087	0.085	0.021		0.98
	Rye (2) (LSP)	0.226	0.09	0.144	0.268	0.118	0.088	0.085	0.019	0.001	

These values reflected the high concordance of the top ranks within every single crop. Based on the season under which the crop residue decomposition occurs (Fig. 1), as already shown with the new module implemented in ARMOSA, different crop residues can be compared to each other. Previously, maize was compared with soybean since the decomposition season of residue was almost the same. Also, in the case of APSIM, the two crop residues led to similar SA outputs. Both the comparisons between SA conducted on the short period (i.e., "Maize (S)" and "Soybean (S)") and long period (i.e., "Maize (L)" and "Soybean (L)") have high coefficients of concordance (C_T = 0.95 and C_T = 0.82, respectively), even if only the first was significant at the 5% threshold. These coefficients revealed that T_{opt}, B_{f_crit} and B_{f_degr} are the most influent parameters involved in the decomposition process of these crop residue. It is also worth comparing the two cover crops (i.e., "Rye (1)" and "Rye (2)") since their residues decompose in the same season and belong to the same crop species. Nevertheless, for APSIM the concordance coefficients were around 70% but not significant for the short and long period of decomposition (*p-value* > 0.10).

3.4 Discussion

Performing a set of ten different analyses, based on different crop residues, simulation periods (Table 2) and different seasons during the year (Fig. 1), allowed us to detect the sensitivity of the two models to the main parameters involved in surface residue decomposition. Moreover, since the SA results change according to the duration of the simulation (i.e., according to the value of the dependent variable at the last time step), the definition of different simulation periods (SSP and LSP) for each crop was useful to better define the parameters' role on residue decomposition kinetics. In fact, considering a single crop at the time and going thought SSP to LSP (i.e., increasing the simulation period), allowed us to detect if some parameters maintained their sensitivity regardless the different conditions.

The variation of parameter sensitivity between the two simulation periods within a single crop was usually lower in the new module (higher coefficients of concordance) than in APSIM, except for the "Rye (1)" crop. In this case, the impact of T_{opt} and B_{f_crit} was higher in SSP than in LSP (Fig. 2C). Probably, before the summer period (July and August 2015), when SWC_{min} was by far the most relevant parameter, the lower temperature and the initial amount of residues (2.85 Mg ha^{-1}) have contributed to slow the decomposition in the early stages, thus impacting the SA output. The parameters sensitivity under "Rye (2)" was more homogeneous comparing SSP and LSP. In fact, the temperature during April and May was on average slightly greater compared to 2015 (i.e., not strongly limiting the decomposition) and especially the initial amount of residues (2.23 Mg ha^{-1}) was closer to the B_{f_crit} threshold (2.00 Mg ha^{-1}).

Comparing crop residues that decomposed in the same season, the sensitivity analysis of the new module almost ended with the same parameter ranking (as in the case of maize vs soybean or rye (1) vs rye (2)). This is related to the high dependency of surface decomposition on the environmental factors rather than on biomass-specific characteristics (Iqbal et al., 2015, Lee et al., 2014, Marinari et al., 2014, Sanaullah et al., 2012). Even if these specific patterns were found when comparing crop residues having the same season of decomposition, the highly significant coefficients of concordance, for the whole set of ten SAs, highlighted the importance of the top-ranking parameters. Specifically, all the SAs conducted with the new module indicated that T_{opt} and SWC_{min} are the most influential parameters, as confirmed by the average ranking. The T_{opt} parameter, based on soil temperature (that is retrieved in ARMOSA from the simulated temperature of the 5 cm topsoil layer), reflects the optimum temperature for the activity of the microbial community that is primarily involved in residue decomposition

(Findeling et al., 2007), whose importance is well recognized (Findeling et al., 2007, Nicolardot et al., 2001) and gives the temperature a crucial role in the simulations.

When the temperature is not the limiting factor, the SWC_{min} became the most influential parameter, confirming that moisture limitation is also essential in this process (Coppens et al., 2007), especially if the residues are left on the soil surface (Lee et al., 2014). SWC_{min} is related to soil water retention; it defines the minimum residue water content for decomposition, expressed as a proportion of field water capacity. As expected, this parameter limited the decomposition mainly for crop residues laying on the soil surface during the dry period, such as in spring (in rye) or, even partially, in summer (in wheat). During the autumn/winter period, when soil water content is not limiting anymore, the importance of this parameter became lower (in maize) or even roughly negligible (in soybean). In the new module approach, SWC_{min} is used in the moisture factor equation (Eq. 10, Appendix A), representing the influence of soil water content on flat residue wetness and, consequently, on their decomposition rate. In ARMOSA, this parameter is based on the soil water content, while other modelling approaches are based on the biomass water content (Findeling et al., 2007). Even if the biomass water content rather than the soil water content is in principle more adequate, the soil water content of the top layer appears to be a good “proxy” of surface residue water content. In fact, the mass adjacent to the soil tends to adsorb water and to be rewetted by the underneath soil layer (Iqbal et al., 2015) in a phenomenon defined "sponge effect" (Kravchenko et al., 2017).

The role of the B_{f_crit} parameter (i.e., the critical flat residue biomass above which the decomposition is slower) in the new module is worth mentioning: for the new module, eight out of ten SAs included it in the list of the first three most influencing parameters. Even though B_{f_crit} is not explicitly related to the crop biomass properties, it is linked to the specific crop management. For example, in the cases of maize and wheat, the high amount of surface residues found after the harvest is a direct consequence of a farmer management choice. This parameter indirectly reflects the thickness of surface residue biomass, suggesting that the more residue biomass, the slower the decomposition process. Its importance was already reported by Thorburn et al. (2001) who stated that the "upper" mulch layer (i.e., the layer that is not in contact with the soil) has a negligible decomposition rate. The response of the model to this situation (i.e., when crop residue biomass is greater than 2 Mg ha^{-1}, Table 1, B_{f_crit}) is essential to avoid early overestimation of the carbon and nitrogen accumulation in soil due to the whole residue decomposition after a harvest/termination event (Fang et al., 2019). Further model improvements may consider recent findings that demonstrated that the upper mulch layer

slowly decomposes and that there is a gradient of moisture and decomposition rate (Dietrich et al., 2019).

We concluded that for the new module implementation into ARMOSA an accurate estimation of T_{opt}, SWC_{min} and B_{f_crit} is needed to properly simulate the residue decomposition.

On the other hand, it seems also reasonable to include the two potential decomposition rates (PDR_f and PDR_f (leaves)) within the set of most influential parameters. Nevertheless, even if μ^* for these parameters was always not null, they never appeared in the most critical top-right quadrant (Fig. 2). For the new module, this is probably due to the large impact of the environmental factors on decomposition, as indicated by T_{opt} and SWC_{min}. In addition, the fact that different PDR_f and PDR_f (leaves) values were assigned to each crop (Table 1) did not overestimate or underestimate the maximum rate of residue decomposition (i.e., making the parameters impacting more on the SA), leaving the other parameters to drive this process.

In APSIM, the SA concordance between short and long simulation periods within each crop was lower than in the new module. In other words, the APSIM parameter reacted more to the simulation period increment regardless the crop residues considered. This is evident by observing the SA results of maize (C_T = 0.79, *p-value* = 0.1, Table 4) and wheat (C_T = 0.93, *p-value* = 0.012, Table 4) showed in figure 3. In the case of maize, the initial amount of residues (11.7 Mg ha^{-1}) probably had a more considerable impact on the SSP SA output compared to the analysis "spreaded" between 17/09/2014 and 28/04/2015 (LSP). This is confirmed by the mathematical implementation shared with ARMOSA and reported in Eq. 13 (Appendix A): when $B_f > B_{f\_crit}$, then the decomposition is reduced exponentially. Moving away from the harvest date (i.e., increasing the duration of the decomposition), the B_{f_crit} lost its importance (as already noted with rye (1) with the new module), favoring the temperature (through T_{opt}) and the potential decomposition rate (B_{f_degr}) limitations (Fig. 3B). In the case of wheat instead (Fig. 3G/3H), the role of B_{f_crit}, together with T_{opt}, became higher in the long compared to the short period. This is probably due to the inclusion of the winter season in the long period, that decreased the B_{f_degr} impact compared to the other parameters. In other words, when temperature does not limit decomposition (as it frequently happens during the short period for wheat), the potential decomposition rate (B_{f_degr}) is the parameter that limit the process the most. Conversely, in the long period most of the decomposition occurs during the coldest months of the year, therefore the temperature interacts more with other parameters (higher value of σ, Fig. 3H), as showed in this case with B_{f_crit}.

Looking at the general trends found in APSIM, the impact of the different parameters partially reflected what was found in the new module implemented in ARMOSA. We found T_{opt} and B_{f_degr} in the first two ranking positions in almost all APSIM's SAs. Most of the SAs confirmed the high weight of these parameters except for the rye cover crop in 2015 ("Rye (1)", Fig. 3C/3D). This behavior in 2015 probably reflects the low water availability during summer (180 mm of rainfall between 21/04/2015 and 28/08/2015) limiting surface decomposition (through the *cum_eos_max* parameter) more than other factors. Thus, except for this specific situation, the only parameter related to water availability (*cum_eos_max*) did not influence the output as SWC_{min} did with the new module. The APSIM moisture factor considers the water availability using the cumulative potential soil evaporation (and thus the critical cumulative evaporation, *cum_eos_max*) to depict the effect that dry residues decompose more slowly than wet residues (Dietrich et al., 2019). Therefore, in this case, a soil property has been used as a proxy for surface residue moisture.

Contrary to the new module, the APSIM potential decomposition rate (B_{f_degr}) significantly impacted the SA output compared to the other parameters involved. The assumption of a unique default value for the decomposition rate (B_{f_degr} = 0.1 kg m^{-2} day^{-1}) in the APSIM model undoubtedly impacted the SA results more than the crop-specific rates employed in the new ARMOSA module. Specific calibration of this parameter is necessary to properly calibrate the model.

Another similarity in the behavior of the two approaches concerns the importance of B_{f_crit}. This parameter is taken from the APSIM equation that limits the decomposition based on the residue amount on the soil surface. Sharing the same equation, the two models gave comparable weight to the limitation of the decomposition rate above a 2 Mg ha^{-1} residue biomass threshold, confirming that the models responded in the same way to the amount of crop residue.

As a general trend, the two approaches gave comparable results for crop residue that share the same season of decomposition, highlighting the impact of environmental conditions. This agrees with Francos et al. (2003) and Richter et al. (2010), who stated that sensitivity analysis refers to specific conditions and it is not a general property of a model. At least for the new module, the high value of the concordance coefficient, computed on the whole set of SAs, highlighted that some parameters are the most important regardless the specific conditions of the crop biomass.

To better understand the model's behavior, the plasticity index ("*L*") has been computed on the whole set of SAs according to Confalonieri et al. (2012). This index (that ranges between 0 and 1, with the highest plasticity at 0) defines the tendency of the model to change its behavior

under different conditions. This index has to be intended only to compare models since specific minimum or maximum optimal plasticity values have not been defined. The low value obtained for APSIM (L = 0.14) describes a model with higher plasticity compared to the new module (L = 0.27). In other words, APSIM has more capability to react to an environmental change by altering the importance of its parameters (confirming the lower value of concordance coefficients). In the discussion above we highlighted that, in the new module, the T_{opt} and SWC_{min} had always a great impact on the SAs, probably leading to a lower plasticity compared to APSIM. Nevertheless, situations like rye (1) or wheat (comparing SSP and LSP in Fig. 2) still defined a module capable to change its parameters sensitivity to the environmental changes.

3.5 Conclusions

With this work a new module has been developed to explicitly include surface residue pools in many relevant modelling processes. In fact, the implementation of this new module into ARMOSA allowed to simulate many processes in which crop residues, laying on the soil surface, play a crucial role in water and nutrient cycling dynamics. Despite previous implementation of the surface residue decomposition, we developed a new module that simulates this process including all the important factors that give a complete representation of residue decomposition.

The APSIM model was used as a benchmark. This model was selected for its algorithm affinity to ARMOSA and for being a cropping system model widely cited in the literature.

A sensitivity analysis was conducted for each crop residue under analysis (i.e., maize, rye, soybean and wheat). In the present SA we distinguished between long and short simulation periods with the advantage of recognizing if some parameters, within single crop, impacted on the decomposition process regardless the different environmental conditions.

The most important parameters in the new module reflected the importance of the soil temperature (T_{opt}), the soil water content (SWC_{min}), and the residue biomass (B_{f_crit}) on the decomposition process. The two decomposition rates (PDRf and PDRf (leaves)) had minor importance, highlighting that, when setting crop specific values, other environment-related parameters are more relevant for the actual decomposition rate. The APSIM model, showed a lower concordance of SA results passing from a crop residue to another and even when comparing short and long simulation periods within the same crop. For maize and wheat, the SA output showed how the duration of the decomposition along different seasons could heavily influence the parameters impact. As a general trend, we always found T_{opt} and B_{f_degr} parameters in the first two rank positions. In addition, having assumed a unique default value for the decomposition rate, B_{f_degr} could have impacted the surface residue destiny more than the new module decomposition rates.

The outcome of this work allowed us to identify the most relevant parameters for a future work of the model calibration and to evaluate its behavior under variable conditions of the residue surface decomposition process.

Acknowledgments

This work was carried out under the project “Innovazioni per estendere l’uso delle colture di copertura in Lombardia - Innovations to extend the use of cover crops in Lombardy”, funded by the Rural Development Programme 2014-2020 of Regione Lombardia, Italy, Operation 16.1.01 (EIP-AGRI Operational Groups).

This study is also funded by the European Union’s Horizon 2020 Framework Programme for Research and Innovation (H2020-RUR-2017-2) as part of the LANDSUPPORT project (grant agreement No. 774234), which aims at developing a decision support system for optimizing soil management in Europe.

Sample Credit author statement

Tommaso Tadiello: Conceptualization, Software, Methodology, Formal Analysis, Investigation, Writing - Original draft, **Mara Gabbrielli**: Methodology, Software, Investigation, Writing - Original draft, **Marco Botta**: Methodology, Software, Writing- Reviewing and Editing, **Marco Acutis**: Conceptualization, Supervision, Writing- Reviewing and Editing, **Luca Bechini**: Conceptualization, Supervision, Writing- Reviewing and Editing, Funding acquisition, **Giorgio Ragaglini:** Conceptualization, Writing- Reviewing and Editing, **Andre Fiorini:** Resources**,** Conceptualization, Writing- Reviewing and Editing, **Vincenzo Tabaglio:** Resources, Conceptualization, Writing- Reviewing and Editing, **Alessia Perego:** Conceptualization, Writing- Reviewing and Editing, Supervision, Project administration, Funding acquisition.

References

Alberts, E. E., Holzhey, C. S., West L. T., Nordin, J. O, 1987. Soil Selection: USDA water erosion prediction project (WEPP). Paper No. 87-2542, Am. Soc. Agric. Eng., St. Joseph, MI.

Biavetti, I., Karetsos, S., Ceglar, A., Toreti, A., Panagos, P., 2014. European meteorological data: contribution to research, development, and policy support, in: Hadjimitsis, D.G., Themistocleous, K., Michaelides, S., Papadavid, G. (Eds.). Presented at the Second International Conference on Remote Sensing and Geoinformation of the Environment (RSCy2014), Paphos, Cyprus, p. 922907. https://doi.org/10.1117/12.2066286.

Boselli, R., Fiorini, A., Santelli, S., Ardenti, F., Capra, F., Maris, S.C., Tabaglio, V., 2020. Cover crops during transition to no-till maintain yield and enhance soil fertility in intensive agro-ecosystems. Field Crops Research 255, 107871. https://doi.org/10.1016/j.fcr.2020.107871.

Brisson, N., Itier, B., L'Hotel, J.C., Lorendeau, J.Y., 1998. Parameterisation of the Shuttleworth-Wallace model to estimate daily maximum transpiration for use in crop models. Ecological Modelling 107, 159–169. https://doi.org/10.1016/S0304-3800(97)00215-9.

Bruun, S., Luxhoi, J., Magid, J., Deneergaard, A., Jensen, L., 2006. A nitrogen mineralization model based on relationships for gross mineralization and immobilization. Soil Biology and Biochemistry 38, 2712–2721. https://doi.org/10.1016/j.soilbio.2006.04.023.

Campolongo, F., Cariboni, J., Saltelli, A., 2007. An effective screening design for sensitivity analysis of large models. Environmental Modelling & Software 22, 1509–1518. https://doi.org/10.1016/j.envsoft.2006.10.004.

Campolongo, F., Carboni, J., Saltelli, A., Schoutens, W., 2004. Enhancing the Morris method. In: Hanson, K.M., Hemez, F.M. (Eds.), Proceedings of the 4th International Conference on Sensitivity Analysis of Model Output. Santa Fe, New Mexico, March 8–11, pp. 369–379.

Chaves, B., Redin, M., Giacomini, S.J., Schmatz, R., Léonard, J., Ferchaud, F., Recous, S., 2021. The combination of residue quality, residue placement and soil mineral N content drives

C and N dynamics by modifying N availability to microbial decomposers. Soil Biology and Biochemistry 163, 108434. https://doi.org/10.1016/j.soilbio.2021.108434.

Confalonieri, R., Bregaglio, S., Acutis, M., 2012. Quantifying plasticity in simulation models. Ecological Modelling 225, 159–166. https://doi.org/10.1016/j.ecolmodel.2011.11.022.

Confalonieri, R., Acutis, M., Bellocchi, G., Cerrani, I., Tarantola, S., Donatelli, M., Genovese, G., 2006. Exploratory sensitivity analysis of cropsyst, warm and wofost: a case-study with rice biomass simulations. Italian Journal of Agrometeorology 17 - 25 (3).

Coppens, F., Garnier, P., Findeling, A., Merckx, R., Recous, S., 2007. Decomposition of mulched versus incorporated crop residues: Modelling with PASTIS clarifies interactions between residue quality and location. Soil Biology and Biochemistry 39, 2339–2350. https://doi.org/10.1016/j.soilbio.2007.04.005.

Diel, J., Franko, U., 2020. Sensitivity analysis of agricultural inputs for large-scale soil organic matter modelling. Geoderma 363, 114172. https://doi.org/10.1016/j.geoderma.2020.114172.

Dietrich, G., Recous, S., Pinheiro, P.L., Weiler, D.A., Schu, A.L., Rambo, M.R.L., Giacomini, S.J., 2019. Gradient of decomposition in sugarcane mulches of various thicknesses. Soil and Tillage Research 192, 66–75. https://doi.org/10.1016/j.still.2019.04.022.

Dietrich, G., Sauvadet, M., Recous, S., Redin, M., Pfeifer, I.C., Garlet, C.M., Bazzo, H., Giacomini, S.J., 2017. Sugarcane mulch C and N dynamics during decomposition under different rates of trash removal. Agriculture, Ecosystems & Environment 243, 123–131. https://doi.org/10.1016/j.agee.2017.04.013.

Douglas, C.L., Allmaras, R.R., Rasmussen, P.E., Ramig, R.E., Roager, N.C., 1980. Wheat straw composition and placement effects on decomposition in dryland agriculture of the Pacific Northwest. Soil Science Society of America Journal 44, 833–837. https://doi.org/10.2136/sssaj1980.03615995004400040035x.

Fang, Y., Singh, B.P., Cowie, A., Wang, W., Arachchi, M.H., Wang, H., Tavakkoli, E., 2019. Balancing nutrient stoichiometry facilitates the fate of wheat residue-carbon in physically defined soil organic matter fractions. Geoderma 354, 113883. https://doi.org/10.1016/j.geoderma.2019.113883.

FAO, 2016. Save and Grow in practice: Maize, rice and wheat. Rome. https://www.fao.org/3/i4009e/i4009e.pdf.

Findeling, A., Garnier, P., Coppens, F., Lafolie, F., Recous, S., 2007. Modelling water, carbon and nitrogen dynamics in soil covered with decomposing mulch. Eur J Soil Science 58, 196–206. https://doi.org/10.1111/j.1365-2389.2006.00826.x.

Fiorini, A., Boselli, R., Maris, S. C., Santelli, S., Perego, A., Acutis, M., ... & Tabaglio, V. (2020). Soil type and cropping system as drivers of soil quality indicators response to no-till: A 7-year field study. Applied Soil Ecology, 155, 103646. https://doi.org/10.1016/j.apsoil.2020.103646.

Francos, A., Elorza, F.J., Bouraoui, F., Bidoglio, G., Galbiati, L., 2003. Sensitivity analysis of distributed environmental simulation models: understanding the model behaviour in hydrological studies at the catchment scale. Reliability Engineering & System Safety 79, 205–218. https://doi.org/10.1016/S0951-8320(02)00231-4.

Guérif, J., Richard, G., Durr, C., Machet, J.M., Recous, S., Roger- Estrade, J., 2001. A review of tillage effects on crop residue management, seedbed conditions and seedling establishment. Soil and Tillage Research 61, 13–32. https://doi.org/10.1016/S0167-1987(01)00187-8.

Herman, J. and Usher, W., 2017. SALib: An open-source Python library for sensitivity analysis. Journal of Open Source Software, 2(9). Doi:10.21105/joss.00097.

Holzworth, D.P., Huth, N.I., deVoil, P.G., Zurcher, E.J., Herrmann, N.I., McLean, G., Chenu, K., van Oosterom, E.J., Snow, V., Murphy, C., Moore, A.D., Brown, H., Whish, J.P.M., Verrall, S., Fainges, J., Bell, L.W., Peake, A.S., Poulton, P.L., Hochman, Z., Thorburn, P.J., Gaydon, D.S., Dalgliesh, N.P., Rodriguez, D., Cox, H., Chapman, S., Doherty, A., Teixeira, E., Sharp, J., Cichota, R., Vogeler, I., Li, F.Y., Wang, E., Hammer, G.L., Robertson, M.J.,

Dimes, J.P., Whitbread, A.M., Hunt, J., van Rees, H., McClelland, T., Carberry, P.S., Hargreaves, J.N.G., MacLeod, N., McDonald, C., Harsdorf, J., Wedgwood, S., Keating, B.A., 2014. APSIM – evolution towards a new generation of agricultural systems simulation. Environ. Model. Softw. 62, 327–350. https://doi.org/10.1016/j.envsoft.2014.07.009.

Iman, R. L., and W. J. Conover. "A Measure of Top-Down Correlation." Technometrics, vol. 29, no. 3, 1987, pp. 351–57, https://doi.org/10.2307/1269344. Accessed 5 Apr. 2022.

Iooss, B., Da Veiga, S., Janon, A., and Gilles Pujol, 2021. sensitivity: Global Sensitivity Analysis of Model Outputs, https://CRAN.R-project.org/package=sensitivity to link to this page (version 1.27.0).

Iqbal, A., Aslam, S., Alavoine, G., Benoit, P., Garnier, P., Recous, S., 2015. Rain regime and soil type affect the C and N dynamics in soil columns that are covered with mixed-species mulches. Plant Soil 393, 319–334. https://doi.org/10.1007/s11104-015-2501-x.

Izaurralde, R.C., Williams, J.R., McGill, W.B., Rosenberg, N.J., Jakas, M.C.Q., 2006. Simulating soil C dynamics with EPIC: Model description and testing against long-term data. Ecological Modelling 192, 362–384. https://doi.org/10.1016/j.ecolmodel.2005.07.010.

Justes, E., Mary, B. & Nicolardot, B. Quantifying and modelling C and N mineralization kinetics of catch crop residues in soil: parameterization of the residue decomposition module of STICS model for mature and non mature residues. *Plant Soil* 325**,** 171–185 (2009). https://doi.org/10.1007/s11104-009-9966-4.

Kravchenko, A.N., Toosi, E.R., Guber, A.K., Ostrom, N.E., Yu, J., Azeem, K., Rivers, M.L., Robertson, G.P., 2017. Hotspots of soil N2O emission enhanced through water absorption by plant residue. Nature Geosci 10, 496–500. https://doi.org/10.1038/ngeo2963.

Lee H., Fitzgerald J., Hewins D.B., McCulley R.L., Archer S.R., Rahn T., Throop H.L., 2014. Soil moisture and soil-litter mixing effects on surface litter decomposition: a controlled environment assessment. Soil Biol Biochem 72:123–132. https://doi.org/10.1016/j.soilbio.2014.01.027.

Legendre, P., 2005. Species associations: the Kendall coefficient of concordance revisited. JABES 10, 226–245. https://doi.org/10.1198/108571105X46642.

Meier, E.A., Thorburn, P.J., 2016. Long Term Sugarcane Crop Residue Retention Offers Limited Potential to Reduce Nitrogen Fertilizer Rates in Australian Wet Tropical Environments. Front. Plant Sci. 7. https://doi.org/10.3389/fpls.2016.01017.

Marinari, S., Mancinelli, R., Brunetti, P., Campiglia, E., 2015. Soil quality, microbial functions and tomato yield under cover crop mulching in the Mediterranean environment. Soil and Tillage Research 145, 20–28. https://doi.org/10.1016/j.still.2014.08.002.

Miguez, F., 2022. apsimx: Inspect, Read, Edit and Run 'APSIM' "Next Generation" and 'APSIM' Classic. https://CRAN.R-project.org/package=apsimx (version 2.3.1).

Moreno-Cornejo, J., Zornoza, R., Faz, A., 2014. Carbon and nitrogen mineralization during decomposition of crop residues in a calcareous soil. Geoderma 230–231, 58–63. https://doi.org/10.1016/j.geoderma.2014.03.024.

Morris, M.D., 1991. Factorial sampling plans for preliminary computational experiments. Technometrics 33, 161–174.

Nicolardot, B., Recous, S. & Mary, B. Simulation of C and N mineralisation during crop residue decomposition: A simple dynamic model based on the C:N ratio of the residues. Plant and Soil 228, 83–103 (2001). https://doi.org/10.1023/A:1004813801728.

Paleari, L., Movedi, E., Zoli, M., Burato, A., Cecconi, I., Errahouly, J., Pecollo, E., Sorvillo, C., Confalonieri, R., 2021. Sensitivity analysis using Morris: Just screening or an effective ranking method? Ecological Modelling 455, 109648. https://doi.org/10.1016/j.ecolmodel.2021.109648.

Perego, A., Giussani, A., Sanna, M., Fumagalli, M., Carozzi, M., Alfieri, L., Brenna, S., Acutis, M., 2013. The ARMOSA simulation crop model: overall features, calibration and validation results. Italian Journal of Agrometeorology 3, 23–38.

Pianosi, F., Beven, K., Freer, J., Hall, J.W., Rougier, J., Stephenson, D.B., Wagener, T., 2016. Sensitivity analysis of environmental models: a systematic review with practical workflow. Environ. Model. Softw. 79, 214–232. https://doi.org/ 10.1016/j.envsoft.2016.02.008.

Probert, M.E., Dimes, J.P., Keating, B.A., Dalal, R.C., Strong, W.M., 1998. APSIM's water and nitrogen modules and simulation of the dynamics of water and nitrogen in fallow systems. Agricultural Systems 56, 1–28. https://doi.org/10.1016/S0308-521X(97)00028-0.

Richter, G.M., Acutis, M., Trevisiol, P., Latiri, K., Confalonieri, R., 2010. Sensitivity analysis for a complex crop model applied to Durum wheat in the Mediterranean. European Journal of Agronomy 32, 127–136. https://doi.org/10.1016/j.eja.2009.09.002.

Robertson, F.A., Armstrong, R., Partington, D., Perris, R., Oliver, I., Aumann, C., Crawford, D., Rees, D., 2015. Effect of cropping practices on soil organic carbon e evidence from long-term feld experiments in Victoria, Australia. Soil Research 53, 636-646. https://doi.org/10.1071/SR14227.

Rumpel, C., 2011. Carbon storage and organic matter dynamics in grassland soils. in: Lemaire, G., Hodgson, J., Chabbi, A. (eds). Grassland productivity and ecosystem services. CAB International, Wallingford, U.K., pp 65–72.

Saltelli, A., Ratto, M., Andres, T., Campolongo, F., Cariboni, J., Gatelli, D., Saisana, M., Tarantola, S., 2007. Global Sensitivity Analysis. The Primer. John Wiley & Sons Ltd, Chichester, UK.

Saltelli, A., Tarantola, S., Campolongo, F., Ratto, M., 2004. Sensitivity analysis in practice. Wiley, New York.

Sanaullah, M., Rumpel, C., Charrier, X., Chabbi, A., 2012. How does drought stress influence the decomposition of plant litter with contrasting quality in a grassland ecosystem? Plant Soil 352, 277–288. https://doi.org/10.1007/s11104-011-0995-4.

Savage, R., 1954. Contributions to the theory of rank order statistics - The two-sample case The Annals of Mathematical Statistics.

Scopel, E., B. Muller, J.M. Arreola Tostado, E. Chavez Guerra and F. Maraux. 1998. Quantifying and modeling the effects of light crop residue mulch on water balance: An application to rain-fed maize in western Mexico. Paper presented at the 16th International Congress of Soil Science, Montpellier, France, Aug. 20-26, 1998.

Soil Survey Staff, 2014. Key to Soil Taxonomy, 12th Edition. Natural Resources Conservation Service of the United States Department of Agriculture, Washington, DC, USA.

Stella, T., Mouratiadou, I., Gaiser, T., Berg-Mohnicke, M., Wallor, E., Ewert, F., Nendel, C., 2019. Estimating the contribution of crop residues to soil organic carbon conservation. Environ. Res. Lett. 14, 094008. https://doi.org/10.1088/1748-9326/ab395c.

Stott, H.F., Stroo, H.F., Elliot, L.F., Papendick, R.I., Unger, P.W., 1990. Wheat residue loss from fields under no-till management. Soil Sci. Soc. Am. J. 54, 92±98.

Tarik C. G., 2019. synchrony: Methods for Computing Spatial, Temporal, and Spatiotemporal Statistics. http://github.com/tgouhier/synchrony (version 0.3.8).

Thorburn, P.J., Probert, M.E., Robertson, F.A., 2001. Modelling decomposition of sugar cane surface residues with APSIM–Residue. Field Crops Research 70, 223–232. https://doi.org/10.1016/S0378-4290(01)00141-1.

Valkama, E., Kunypiyaeva, G., Zhapayev, R., Karabayev, M., Zhusupbekov, E., Perego, A., Schillaci, C., Sacco, D., Moretti, B., Grignani, C., Acutis, M., 2020. Can conservation agriculture increase soil carbon sequestration? A modelling approach. Geoderma 369, 114298. https://doi.org/10.1016/j.geoderma.2020.114298.

Williams, J.R., Jones, C.A., Dyke, P.T., 1984. A modeling approach to determining the relationship between erosion and soil productivity. Trans. ASAE 27, 129–144.

Appendix A

The module divides surface residues in a standing (B_s, kg DM m^{-2}) and a flat (B_f, kg DM m^{-2}) component. The flat component is further divided in two pools (stem and leaves) to better represent the specific characteristics of the plant fractions (in terms of C:N ratio and potential decomposition rate). Numerical integration is performed to calculate the values of B_s and B_f at each time step (Eq. 1 and 2).

$$B_{s(t)} = B_{s(t-1)} - dB_{s\_degr} + dB_{s\_part} - dB_{s\_conv} - dB_{s\_till} \quad [1]$$

$$B_{f(t)} = B_{f(t-1)} - dB_{f\_degr} + dB_{f\_part} + dB_{s\_conv} - dB_{f\_till} \quad [2]$$

The processes represented by the module rates are the following: residue decomposition (dB_{s_degr} and dB_{f_degr}, kg DM m^{-2} d^{-1}), residue partitioning at harvest (dB_{s_part} and dB_{f_degr}, kg DM m^{-2} d^{-1}), standing residue conversion into flat residue (dB_{s_conv}, kg DM m^{-2} d^{-1}) and residue incorporation into soil through tillage operation (dB_{s_till} and dB_{f_till}, kg DM m^{-2} d^{-1}).

Partitioning of the surface residue (B_{tot}, kg DM m^{-2}) in B_s and B_f is simulated using WEPP approach. The partitioning is estimated at harvest, before any other management operation, using the ratio between the cutting height (H_{cut}, m) and the crop height (H_{cm}, m) to determine the portion (F_{pc}, unitless, Eq. 3) of initial residue that becomes standing residue (Eq. 4). The portion of flat residue (Eq. 5) is determined as a complement (1-F_{pc}).

$$F_{pc} = \frac{\mathrm{H_{cut}}}{\mathrm{H_{cm}}} \quad [3]$$

$$dB_{s\_part} = B_{tot} F_{pc} \quad [4]$$

$$dB_{f\_part} = B_{tot}(1 - F_{pc}) \quad [5]$$

The decomposition of the standing residue (dB_{s_degr}, kg DM m^{-2} d^{-1}, Eq. 6) is also simulated adopting WEPP approach (Eq. 6).

$$dB_{s\_degr} = B_{s(t-1)} e^{-\mathrm{PDR_{stand}} fD_{stand} Size_i Fert_i} \quad [6]$$

The amount of remaining standing residue biomass at the end of the simulated time step depends on three limiting factors (fD_{stand}, $Size_i$ and $Fert_i$) that affect the optimal decomposition rate (PDR_{stand}, kg m^{-2} d^{-1}) of a specific residue type. fD_{stand}, $Size_i$ and $Fert_i$ consider respectively the limitations due to environment conditions, soil fertility and residue size.

The limiting factor that represents the environmental limitations that condition standing residue decomposition in field (fD_{stand}, unitless) considers the residue water content and the air temperature as independent limiting factors. The water limiting factor (fW_{stand}, unitless, Eq. 7) is obtained as the ratio between the rainfall of the considered time step ($Rain$, m) and a parameter representing the amount of rain that saturates the standing residue ($Rain_{sat}$, m) whose

default value is 0.004. The limiting factor ranges between 0 and 1 depending on the standing residue water content and on daily average temperature (T_{avg}, °C).

$$fW_{stand} = \begin{cases} \frac{Rain}{\mathrm{Rain_{sat}}} & if\ PRCP \leq \mathrm{Rain_{sat}} \\ 1 & if\ PRCP > \mathrm{Rain_{sat}} \\ 0 & if\ T_{avg} < 0 \end{cases} \quad [7]$$

The temperature limiting factor (fT_{stand}, unitless, Eq. 8) ranges between 0 and 1, and it is calculated as a function of daily average temperature (T_{avg}, °C) designed for temperate regions and defined by two parameters: the maximum (T_{max}, °C) and the minimum (T_{min}, °C) temperature for microbial decomposition of residues. This function is limited also by the temperature above which the microbial activity stops (T_{lim}, °C).

$$fT_{stand} = \begin{cases} \frac{2(T_{avg}+\mathrm{T_{min}})^2(\mathrm{T_{max}}+\mathrm{T_{min}})^2-(T_{avg}+\mathrm{T_{min}})^4}{(\mathrm{T_{max}}+\mathrm{T_{min}})^4} \\ 0\ \ if\ T_{avg} < \mathrm{T_{min}}\ or\ T_{avg} > \mathrm{T_{lim}} \end{cases} \quad [8]$$

The decomposition of flat residue biomass (dB_{f_degr}, kg DM m^{-2} d^{-1}) is simulated adopting APSIM approach that estimates the fraction of decayed biomass for each time step (Eq. 9). This approach is similar to the one adopted for the standing residue (WEPP model) but employs additional limiting factors. The decomposition rate is described as a function of: an optimal decomposition rate (PDR_{flat}, kg m^{-2} d^{-1}), environmental limiting factor such as a temperature (fT_{flat}, unitless) and a soil moisture (fW_{flat}, unitless) factor, and residue dependent limiting factors such as the C:N ratio (fCN_{flat}, unitless) and soil-residue contact degree ($fContact_{flat}$, unitless) factor.

$$dB_{f\_degr} = B_{f(t-1)} e^{-\mathrm{PDR_{flat}} fT_{flat} fW_{flat} fCN_{flat} fContact_{flat}} \quad [9]$$

All the limiting factors included are unitless and range between 0 and 1.

The moisture factor (Eq. 10) represents surface layer soil water content (SWC, m^3 m^{-3}) influence on flat residue wetness and therefore on their decomposition rate. The moisture factor included in the integrated mulch model of ARMOSA differs from the one employed in APSIM.

The modification was performed to use the moisture limiting factor equation both for flat surface and buried residue decomposition.

$$fW_{flat} = \begin{cases} 0 & when\ SWC < \mathrm{SWC_{min}} \\ \mathrm{MA_{min}} + (1-\mathrm{MA_{min}}) \frac{(SWC-\mathrm{SWC_{min}})}{(\mathrm{SWC_{optmin}}-\mathrm{SWC_{min}})^{\mathrm{MA_{optb}}}} & when\ SWC < \mathrm{SWC_{optmin}} \\ 1 & when\ SWC < \mathrm{SWC_{optmax}} \\ \mathrm{MA_{sat}} + (1-\mathrm{MA_{sat}})(\frac{(SWC_{sat}-SWC)}{(SWC_{sat}-\mathrm{SWC_{optmax}})^{\mathrm{MA_{opta}}}} & else \end{cases} \quad [10]$$

The temperature factor (Eq. 11) is obtained as a function or daily average air temperature (T_{avg}, °C) and is defined by a optimum decomposition temperature parameter (T_{opt}, °C).

$$fT_{flat} = \begin{cases} (\frac{T_{avg}}{T_{opt}})^2 \\ 0 \;\; if \; T_{avg} < 0 \end{cases} \quad [11]$$

The carbon to nitrogen ratio factor (Eq. 12) of a specific flat residue type is calculated as a function of the C:N ratio of the residue (*CN*, unitless) that is defined by three parameters: the optimum C:N ratio for decomposition (CN_{opt}, unitless), the function slope coefficient (CN_{slope}, unitless) and the C:N ratio value above which the decomposition stops (CN_{max}, unitless).

$$fCN_{flat} = \begin{cases} exp\frac{-CN_{slope}(CN-CN_{opt})}{CN_{opt}} \\ 1 \; if \; CN < CN_{opt} \\ 0 \; if \; CN > \; CN_{max} \end{cases} \quad [12]$$

The contact factor (Eq. 13) describes the effect of the flat residue biomass amount on the soil-residue contact degree and therefore on residue decomposition rate: it's based on the fact that lower amount of residue biomass decomposes faster due to their higher contact degree with soil. This limiting factor is estimated as a function of flat residue biomass (B_f, kg DM m^{-2}) defined by a critical residue biomass parameter (B_{f_crit}, kg DM m^{-2}) The critical residue biomass is the value above which the decomposition is slowed down by the "haystack effect" described by Thorburn et al. (2001), which does not consider standing residue contribute.

$$fContact_{flat} = \begin{cases} 1 & if \; B_f < B_{f\_crit} \\ \frac{B_{f\_crit}}{B_f} & if \; B_f > B_{f\_crit} \end{cases} \quad [13]$$

The conversion of standing residue to flat residue caused by weather events such as wind and snow respectively decreases standing residue (Eq. 14) and increases flat residue amounts. It is simulated by means of WEPP approach. that employs an adjustment factor ($Conv_{fct}$, unitless) representing the fraction of standing residue not converted to flat residue from wind and snow for the considered site.

$$dB_{s\_conv} = 1 - Conv_{fct}B_{s(t-1)} \quad [14]$$

Surface flat residue water dynamics are simulated adopting STICS approach, which estimates the amount of water both intercepted and directly evaporated by the mulch layer. The amount of water which is intercepted by the mulch layer (WC_{mulch}, Eq. 15) is the incident effective rainfall reaching the mulch layer (consisting in rainwater minus the amount intercepted by canopy of the crop). The intercepted water is simulated as a function of surface residue biomass (B_f, kg DM m^{-2}) defined by one parameter representing the residue wettability ($WETT_{mulch}$, mm Mg ha^{-1}). According to Scopel et al. (1998), the residue wettability depends on residue size

resulting from different management operations and ranges between 0.22 and 0.38 mm Mg ha^{-1}.

$$WC_{mulch(t)} = \mathrm{WETT}_{\mathrm{mulch}}\, B_{f(t)} \quad [15]$$

The mulch evaporation demand (Eq. 16) is estimated based on STICS approach multiplying the evaporation demand ($EVAP_d$, mm) by the actual soil fraction covered by flat residue (C_{total_actual}, unitless).

$$E_{mulch} = EVAP_d\, C_{total\_actual} \quad [16]$$

The soil evaporation is adjusted subsequently to fulfil the unsatisfied evaporation request.

The soil cover due to surface residue presence is simulated through WEPP approach, that estimates the total soil cover due to residue presence (C_{total}, Eq. 17) as the sum of two components: flat residue (C_{flat}, Eq. 18) and standing residue (C_{stand}, Eq. 19) soil cover. The soil covering effect is expressed as the fraction of surface covered by the residues and ranges from 0 to 1.

$$C_{total(t)} = C_{flat(t)} + C_{stand(t)} \quad [17]$$

Soil cover due to flat residue is simulated as a function of its biomass using a crop specific parameter (rtC_{flat}, m^2 kg^{-1}) representing the surface covered by a fixed amount of the specific crop residue.

$$C_{flat(t)} = 1 - e^{-rtC_{flat}\, B_{f(t)}} \quad [18]$$

Soil cover due to standing residue is estimated as a function of the ratio between the standing residue biomass at the considered time step and the standing residue at harvest ($B_{s(0)}$, kg DM m^{-2}). This function involves a crop specific parameter (A_{bm}, unitless) describing the surface occupied by stem basal area at maturity per square metre of soil.

$$C_{stand(t)} = \frac{B_{s(t)}}{B_{s(0)}}\, A_{bm} \quad [19]$$

Tillage operations have two main effects on the mulch biomass, both depending on the tillage type and intensity. The first one is to transfer a fraction of the standing residue to the flat residue. The second effect is the incorporation of a fraction of the flat residue into the soil; this process creates pools of organic matter that will evolve independently during the simulation.

The albedo of soil as influenced by both standing and flat surface residue presence is simulated adopting an approach derived from STICS. Soil albedo (ALB_s, unitless, Eq. [20]) is simulated as a function of the soil cover due to surface residue presence (C_{total}, unitless). The parameter involved in the function are the ones describing dry soil albedo (ALB_{bare}, unitless), mulch albedo (ALB_{mulch}, unitless).

$$ALB_{s(t)} = ALB_{bare} \times \left(1 - C_{total(t)}\right) + ALB_{mulch} \times C_{total(t)} \quad [20]$$

Chapter 4. Simulation of the new SOM fractions

4.1 Introduction

The implementation of the surface crop residue simulation into the ARMOSA model enabled a deep analysis of the link between the surface residue decomposition and SOM accumulation and decomposition in the bulk soil (i.e., belowground soil). As expressed in the previous chapter, the surface residue accumulation and the subsequent decomposition are extremely important to understand the SOM dynamic into the soil. Therefore, the effort to simulate "the surface decomposition" has to be coupled with a belowground SOM representation that can benefit from this improvement.

So far, the ARMOSA model represented the bulk soil organic matter with three different pools: stable, litter and manure. We refer hereafter to this classic ARMOSA version as ARMOSA 1.0. In ARMOSA 1.0, the litter pool describes "the fresh" SOM, that is the easiest degradable pool in the bulk soil; crop residues which are incorporated into soil become litter pools that will decompose in time according to specific rates. The stable pool represents the most durable SOM pool, so its rate of mineralization is slower. The manure pool is used to simulate all the different types of organic fertilizers or amendments that farmers add to the soil and usually have a rapid turnover. This representation allows the partition of the SOM into discrete pools based on turnover times, but it does not reflect the real composition of the organic matter. However, this concept has been widely adopted (SALUS, Basso and Ritchie, 2015, APSIM, Holzworth et al., 2014, EPIC, Izaurralde et al., 2006, RothC, Coleman and Jenkinson, 1996, Century, Parton et al., 1988) because of its simplicity to represent the different composition of the organic matter and to simulate its different decomposition rates (i.e., different mineralization rates). This modeling approach falls into the traditional pseudo first-order decay approaches with a range of SOM pools described based on their turnover times and decomposition pathways. These models have recently been shown to have very large parameter equifinality (i.e. different input parameters produce the same effect), which has been hypothesized to be the result of an incomplete representation of the processes (Smith et al., 2018, Luo et al., 2015). More recently, a new SOM modeling conceptualization has been adopted based on explicit microbial biomass, representations of mineral – surface interactions, vertical transport, nutrient controls and plant interactions (Smith et al., 2018).

This next generation of soil organic matter models is based on the very last scientific achievements about SOM that led to new ways to sample and describe the SOM composition.

In many different recent works (Lavallee et al., 2020, Haddix et al., 2020, Bongiorno et al., 2019, Cotrufo et al., 2019, Mitchell et al., 2018) the SOM composition is divided into dissolved (DOM), particulate (POM) and mineral-associated (MAOM) organic matter forms, three SOM components that are fundamentally different in terms of their formation, persistence, and functioning. The definition of these pools is based on their particle size and density as shown in Table 1.

Table 1. *Soil organic matter subdivision based on particle size and density of the single pool. Data retrieve from Lavallee et al. (2020).*

Pool	Description	Particle size	Density
DOM	Small particle water-extractable	< 45 μm	> 1.61-1.85 g/cm^3
POM	Lightweight fragments that are relatively undecomposed	> 50-63 μm	< 1.61-1.85 g/cm^3
MAOM	Formed by structure encapsulated by minerals, organo-mineral clusters, and primary organo-mineral complexes	< 20-63 μm	< 1.61-1.85 g/cm^3

In these studies, the authors provided evidence of the highly contrasting physical and chemical properties of the pools, mean residence times in soil, and responses to land use changes. Thus, these new DOM, POM and MAOM pools are easy to conceptualize and understand, relatively quick and inexpensive to separate, and are already incorporated into newer generation SOM models (Zhang et al., 2021, Woolf and Lehmann, 2019, Dwivedi et al., 2017, Campbell et al., 2016). In addition, large scale samplings campaigns (Orgiazzi et al., 2018) have been conducted by public scientific institutions and used to identify these new fractions (Lugato et al., 2021), which demonstrate the real interest about these new SOM frontiers.

Even though ARMOSA 1.0 is the result of continuous improving, thanks to the application and calibration of the model in over 50 locations, it does not represent the last scientific achievements presented above. Thus, ARMOSA 1.0:

1. it contains different organic matter pools that are not measurable since they do not represent the real SOM fractions that can be sampled in a soil;
2. as most of the full cropping system models it does not represent the last scientific achievements in the study of SOM;
3. it will be hardly comparable with the new generation models that account for the new organic matter pools.

Accordingly, I integrated the new knowledge into ARMOSA so that it can become a suitable cropping system model accounting for new generation SOM fractionation. In the next paragraph it will be explained how the new ARMOSA release, called ARMOSA 2.0, has been updated to account for these new pools.

4.2 New model release: conceptualization and main pools

This new model release has been developed to replace specifically the current ARMOSA 1.0 simulation of the soil organic matter dynamics.

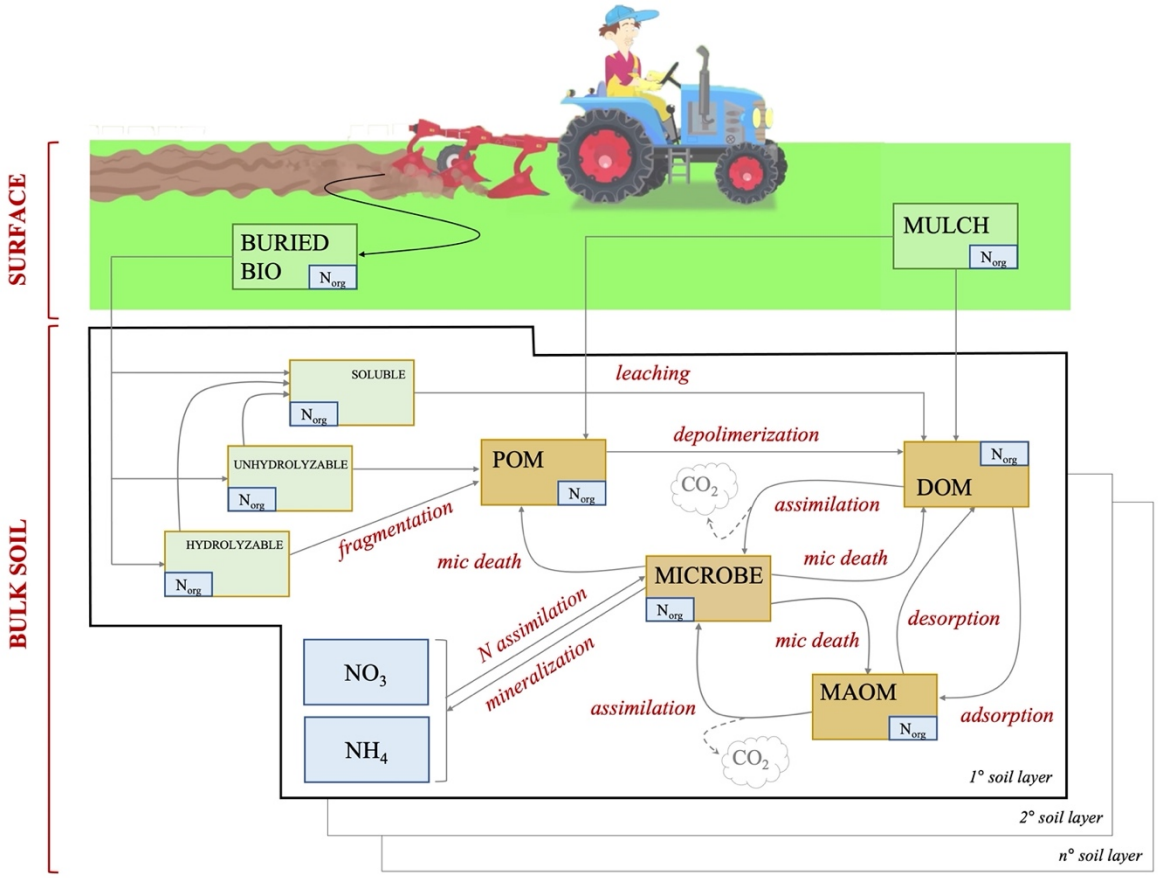

Figure 1. *Schematic representation of the new SOM conceptualization integrated into the ARMOSA 2.0 release.*

The new ARMOSA 2.0 simulates the bulk soil SOM dynamics through several processes that are illustrated in figure 1. This new way to interpret the SOM dynamic can be divided in two main parts (excluding the mulch layer that has been treated in the chapter 3). The first one describes the fate of the buried crop biomass through three pools called hydrolyzable, unhydrolyzable and soluble pools. The second part describes the dynamics of the organic matter already present in the bulk soil through the DOM, POM and MAOM pools belonging

to the new "organic matter approach" explained in the previous paragraph. The development of algorithms that specifically describe the buried biomass is due to the fact that it cannot be directly incorporated into the SOM pools because of its different decomposition process and turnover time. Nevertheless, as soon as this organic material decomposes, the carbon and nitrogen output go into the new SOM pools.

In addition to all these pools, ARMOSA 2.0 introduces the explicit representation of the microbiota growth and functions. As in the older ARMOSA version, the mineral nitrogen pool (which includes NO_3 and NH_4) is still present as state variable and it is split into NH_4 and NO_3 pools.

4.3 Main processes

All the main processes are represented in figure 1, where the square boxes represent the pools while the black lines are the carbon and nitrogen mass movements from one pool to another. As shown in figure 1, every single pool also presents a nitrogen component that reflects the specific pool C/N ratio. Likewise, all the biomass movements from a pool to another account also for a nitrogen movement that is computed based on the specific pool C/N ratio.

All the bulk soil processes are computed for each layer defined for a specific simulation. In addition, all the outputs (i.e., organic carbon and mineral nitrogen) from the mulch layer go to the first layer, and then can be potentially moved from a layer to another by the tillage events. On the contrary, once a tillage event moves the crop residue biomass from the soil surface (mulch) to a specific depth, the model creates the hydrolyzable, unhydrolyzable and soluble pools in the interested soil layers and split the biomass in these pools.

In the following sub-paragraphs, all the processes involved in the bulk soil will be described separately based in the main sections of this new model conceptualization.

4.3.1 The role of microbial biomass

With this new ARMOSA version, microbial biomass has a crucial role. The main difference between the previous ARMOSA approach and the new one is that a specific pool now represents the microbial biomass.

The scientific literature has debated for a long time about the possibility of accounting for microbial biomass or not. In particular, the scientific debate has been focused on whether or not the microbial biomass itself should work as a first limitation of the SOM decomposition. In other words, the microbial biomass can appear or not in the algorithms that simulate the

decomposition process making the process slightly different from one to another. Luo et al. (2016) stated that – although that models that explicitly consider the microbial biomass in the decomposition process might better explain priming effects, microbial acclimation, and pulse responses to some environmental changes – they tend to produce unrealistic oscillatory responses to perturbations, and their simulated C storage is not sensitive to C input. Conversely, Zhang et al. (2021) even with an explicitly microbial biomass simulation, did not limit the decomposition process using the microbial biomass itself. Nevertheless, their results captured the temporal dynamics of decomposition of the different pools. Wutzler and Reichstein (2008) reviewed different representations the SOM decomposition process, comparing non-explicit (i.e., the microbial biomass does not appear in the decomposition equations) with explicit (i.e., the microbial biomass appears in the decomposition equations) decomposition approaches and further divide them between linear or nonlinear equations. They argued that the formulations of SOM decomposition where the active decomposers are represented in a nonlinear manner are most suitable to describe long-term SOM dynamics. At the same time, Zhang et al. (2021) in their recent work stated that the "simplification" of the algorithm structure leads to a wider applicability of the models, suggesting that the non-explicit first order kinetic approach is the most suitable. Besides that, the first order kinetics remains the most widely applied formulation of substrate decomposition (Wutzler and Reichstein, 2008) where a linear decomposition d_S scales with available substrate *S*.

$$d_S = kS \quad [1]$$

This formulation assumes that substrate of each quality has it's own decomposer community associated with, and that this decomposer community is in equilibrium with the available substrate most of the time and therefore the decomposition is only limited by substrate (McGill and Myers, 2015). In this way, we assume that a minimum amount a microbial biomass always exists in the soil, allowing the decomposition process to start as soon as the organic carbon is available from the pools. The new ARMOSA release uses this last approach where the decomposition process is represented using the following equation:

$$d_S = C_{pool(i)} * K_{pool(i)} * T_{eff} * W_{eff} * CUE_{microbe} \quad [2]$$

where C_{pool} is the carbon mass belonging to the pool considered, K_{pool} is the maximum decay rate of the *i-th* pool considered at optimal temperature and moisture, while T_{eff} and W_{eff} represent the effect of temperature and moisture respectively. The $CUE_{microbe}$ coefficient is the decomposition efficiency based on the C/N ratio of the microbes and it will be explained in the 4.3.2 paragraph. This equation calculates the amount of carbon being decomposed but it does not represent the actual carbon assimilated by microbes. To obtain the real carbon mass assimilated by microbes to maintain their growth, the $CUE_{pool(i)}$ has to be applied. This value represents the decomposition efficiency due to the C/N ratio of the specific pool decomposed by microbes, and it defines the percentage of carbon assimilated versus respired (i.e., respired as CO_2). A deeper explanation of this efficiency can be found in the 4.3.2 paragraph. Thus, based on equation [2] the final equation representing the carbon assimilated is:

$$Microbial\_C_{assimilation} = C_{pool(i)} * K_{pool(i)} * T_{eff} * W_{eff} * CUE_{microbe} * CUE_{pool(i)} \quad [3]$$

Microbe assimilate carbon only from the DOM and MAOM pool, because the POM pool requires a further step of "depolymerization" to be assimilated (see paragraph 4.3.5). While microbes assimilate carbon, their biomass decreases due to its turnover, and the released carbon mass gets split between all the different pools (POM, DOM and MAOM). The module daily computes the death of microbes as:

$$Microbe\_C_{death} = C_{microbe} * K_{death} \quad [4]$$

where $C_{microbe}$ is the carbon mass belonging to the microbe pool and K_{death} is microbial death rate. After the $Microbe\_C_{death}$ computation, different coefficients are used to split the death carbon biomass between all the bulk soil pools.
All the coefficient value are listed in table 3.

4.3.2 Decomposition moderators

The decomposition dependency from the substrate is not the only key aspect because other factors, such as nutrient limitation and environmental condition, are involved to limit carbon sequestration (Wutzler and Reichstein, 2008). Usually, they are known as moderators of decomposition rates, and they include temperature, moisture, nitrogen availability and microbial C/N ratio controls.

The temperature moderator (T_{eff}) is obtained by a generalized Poisson function, which is the temperature response function of the CENTURY model (Burke et al., 2004).

$$T_{eff} = f_t \left(\frac{T_{max}-T}{T_{max}-T_{opt}}\right)^{0.2} e^{\frac{0.2}{2.63}\left(1-\left(\frac{T_{max}-T}{T_{max}-T_{opt}}\right)^{2.63}\right)} \quad [5]$$

where T is the soil temperature (°C), f_t= 4.99, T_{max}= 45°C and T_{opt}= 35°C.

The equation of the soil moisture moderator (W_{eff}) is taken from the ARMOSA model. It relies on a function that modifies the activity of the microbes based on the soil water content.

$$W_{eff}\begin{cases} 0 & if\ SWC < Min \\ \frac{(SWC-Min)}{OPT_{min}-Min)}^{MWC_1} & if\ Min \le SWC \le OPT_{min} \\ 1 & if\ OPT_{min} < SWC \le OPT_{max} \\ M_{SAT} + (1+M_{SAT}) * \left(\frac{Theta_{SAT}-SWC}{Theta_{SAT}-OPT_{max}}\right)^{MWC_2} & if\ SWC > OPT_{max} \end{cases} \quad [6]$$

in which SWC is the soil water content, $Theta_{SAT}$ is the soil water content at saturation, M_{SAT} is the is the microbial activity at saturation while Min, OPT_{min}, OPT_{max}, MWC_1 and MWC_2 are different coefficients to set the curve (see Table 3).

Lastly, two different efficiencies limiting the decomposition have been introduced to consider the C/N ratio of the microbes and the DOM and MAOM pools (i.e., the pools to be assimilated), respectively. In the last decade an intense debate has been done on the microbial decomposition efficiency CUE (Carbon Use Efficiency). Regarding the sensitivity of CUE to environmental conditions several scenarios and strategies have been proposed (Allison et al., 2010, Manzoni et al., 2012) but the uncertainty is still high (Wieder et al., 2013). For example, Campbell et al. (2016) suggested that microbial CUE is often variable during litter decomposition, depending on the decomposition environment, chemical characteristics of substrates being decomposed, and the physiological characteristics of microbes and microbial communities. Litter decomposition models that include variable microbial CUE more accurately represent partitioning of decomposed litter C to CO_2 versus microbial materials. These studies suggest that a dynamic CUE value would be the most reasonable way to represent the microbial activity fluctuation in response to different conditions. In the scientific literature the CUE ranges from low values (0.03-0.3, Soares and Rousk, 2019 or 0.26-0.3 or Woolf and Lehmann, 2019) to higher values (0.3-0.55, Sinsabaugh et al., 2016 and Soares and Rousk, 2019 or 0.25-0.75, Kyker-Snowman et al., 2020), making difficult to intend it as a unique immutable

value. The uncertainty of these values is another reason to define a dynamic CUE value rather than a unique one.

To represent this phenomenon two different CUE have been used. The first one represents the microbial response to the different pool composition (Zhang et al., 2021).

$$CUE_{pool} \begin{cases} \frac{CN_{microbe\_MAX}}{(CN_{pool}+CN_{CUE})} & if\ CUE < CUE_{MAX} \\ & else\ CUE_{MAX} \end{cases} \quad [7]$$

where $CN_{microbe\_MAX}$ is the maximum C/N allowed for the microbial biomass, CN_{pool} is the C/N of the pool considered, CN_{CUE} is a correction factor and CUE_{MAX} is the maximum CUE value allowed for microbes (see Table 3). This efficiency is maximum at low C/N values and decreases after the pool C/N reach the value of 20. This specific efficiency is a key point for the model since it defines the amount of carbon that cannot be assimilated by microbe and goes in the atmosphere as CO_2 emission (i.e., CO_2 respired).

The second CUE ($CUE_{microbe}$) has been introduced to account for the C/N of the microbial biomass itself, so it works as a second limitation beside the "classic" CUE_{pool}. Contrary to the CUE_{pool} this specific efficiency does not influence the amount of carbon respired and released as a CO_2 in the atmosphere. Many studies report that the optimal C/N ratio for microbe ranges between 8 and 11 (Kästner et al., 2021, Kyker-Snowman et al., 2020). We assume that the decomposition is greater around C/N=9.5 (i.e., the middle point of the range), decreasing towards the edge of the range and being zero out of the range. The equation that represents the decomposition moderator $CUE_{microbe}$ is the following:

$$CUE_{microbe} \begin{cases} \left(\frac{CN_{microbe}-CN_{microbe\_MIN}}{CN_{microbe\_OPTmin}-CN_{microbe\_MIN}}\right)^{S_1} & if \quad CN_{microbe\_MIN} < CN_{microbe} < CN_{microbe\_OPTmin} \\ 1 & if \quad CN_{microbe\_OPTmin} \le CN_{microbe} \le CN_{microbe\_OPTmax} \\ \left(\frac{CN_{microbe}-CN_{microbe\_MAX}}{CN_{microbe\_OPTmax}-CN_{microbe\_MAX}}\right)^{S_2} & if \quad CN_{microbe\_OPTmax} \le CN_{microbe} \le CN_{microbe\_MAX} \\ & else \quad 0 \end{cases} \quad [8]$$

where $CN_{microbe}$ is the microbes C/N and $CN_{microbe\_MIN}$, $CN_{microbe\_OPTmin}$, $CN_{microbe\_OPTmax}$, $CN_{microbe\_MAX}$ are four parameters used to set the curve (see Table 3). The microbial biomass dynamically changes its C/N in response to the carbon and nitrogen input received from all the different pools and thus the $CUE_{microbe}$ is recomputed every day accordingly to C/N changes. The model capability to represent the microbial biomass leads to the possibility that the microbial C/N could go out of range. For this reason, a specific

mechanism has been developed to deal with this possibility, keeping the microbial C/N in its biological range. The next paragraph illustrates how this mechanism works.

4.3.3 Microbial C/N control

The microbial C/N control mechanism (MCNC from hereon) has been developed to maintain the real biological C/N of the microbe in its specific range dealing with the microbial nitrogen incomes and outcomes. Even though this control mechanism has been specifically developed for the new ARMOSA model release, other models have a similar microbial C/N ratio control. For example, authors like Kaiser and Kalbitz (2012) or Zhang et al. (2021) developed algorithms that force microbes to spill the excess C or N to maintain their biomass stoichiometry through a carbon overflow respiration or a nitrogen excess mineralization.

The set of algorithms of the MCNC provide to the module two main features: (1) keeping the microbial C/N in the biological range, they provide a control on the microbe mass balance (i.e., the C and N composition) and, consequently, on the microbial CUE; (2) having the control on the microbial mass balance, they control the microbial C/N handling the possible N mineralization or immobilization. Here how this mechanism works:

1. since the MCNC needs to control the daily final microbial mass balance, all the different mass transfers to and from the microbial pool have to be done first;
2. at this point the MCNC computes the microbial C/N;
3. the MCNC is nitrogen based. This means that if the microbial C/N is lower than the $CN_{microbe\_MIN}$ the MCNC will produce a nitrogen "spilling" that moves nitrogen from the microbes to the N mineral pool (i.e., N mineralization). If the microbial C/N is higher than the $CN_{microbe\_MAX}$ the MCNC will produce a nitrogen "fishing" that captures nitrogen from the N mineral pool (i.e., N immobilization);
4. the precise amount of nitrogen mineralized or immobilized will be computed to restore an optimal C/N within the range (specifically to the $CN_{microbe\_OPT}$ value).

The MCNC equations are:

$$\begin{cases} if\ CN_{microbe} < CN_{microbe\_MIN} & N_{splilling} = (N_{microbe} + N_{ass} - N_{death}) - \left(\frac{C_{microbe}+C_{ass}-C_{death}}{CN_{microbe\_OPT}}\right) \\ if\ CN_{microbe} > CN_{microbe\_MAX} & N_{fishing} = \left(\frac{C_{microbe}+C_{ass}-C_{death}}{CN_{microbe\_OPT}}\right) - (N_{microbe} + N_{ass} - N_{death}) \end{cases} \quad [9]$$

where $CN_{microbe}$ is the microbes C/N, $N_{microbe}$ and $C_{microbe}$ are the N and C content of the microbes pool, N_{ass} and C_{ass} are the N and C assimilated from the microbes pool, N_{death} and

C_{death} are the N and C lost from the microbes pool as death biomass, while $CN_{microbe\_MIN}$, $CN_{microbe\_OPT}$ and $CN_{microbe\_MAX}$ are the four parameters used to set the curve (see Table 3). It has to be highlighted that after the daily carbon and nitrogen transfers from a pool to another, the MCNC works only if the microbial C/N ends up out of the fixed range.

4.3.4 Hydrolyzable, unhydrolyzable and soluble pools

Crop residues that are buried into the soil (i.e., due to a tillage event), are modeled using the "Soluble"", "Hydrolysable" and "Unhydrolyzable" biomass pools based on crop specific parameters. These parameters have been retrieved from the literature and are reported in Table 2. They reflect the different biomass components as a mass percentage. The "Soluble" pool is made of water-soluble components, while the other two pools represent the biomass structural component: the "Hydrolysable" pool represents polymers, such as proteins and cellulose and the "Unhydrolyzable" pool includes lignin, suberin, cutin, and microbial polysaccharide lignin complexes (Zhang et al., 2021). These litter fractions are commonly measured in decomposing litter or forage analyses (Van Soest et al., 1991).

Table 2. *Parameters used to define the "Soluble", "Hydrolyzable" and "Unhydrolyzable" pools. All the parameters are expressed as a percentage of the biomass mass.*

Crop	Soluble	Hydrolyzable	Unhydrolyzable	Source
GENERIC	10			Ahrens et al., 2020
GENERIC	59			Woolf and Lehmann et al., 2019
Grassland	35	50	15	Robertson et al., 2019
Alfalfa	70	22	8	Calpbell et al., 2016
Alfalfa (fresh)	diff	14.2	4.66	Soong et al., 2015
Alfalfa (hay)			25.3	Van Soest and Wine (1968)
Sugarcane	43.5			Bahadori et al., 2021
Grassland	55.6			Bahadori et al., 2021
Barley straw	58.4	32.5	9.1	Rowland and Roberts 1994
Barley straw	22	61.7	16.3	Vargas et al., 2012
Wheat straw			16.7	Van Soest and Wine (1986)
Wheat straw	12	70.3	17.7	Vargas et al., 2012
Maize straw	7.1	74.7	18.2	Vargas et al., 2012
Oat straw	7.8	75.6	16.6	Vargas et al., 2012
Rapeseed straw	9.3	73.5	17.2	Vargas et al., 2012

Once the model creates the hydrolyzable and unhydrolyzable pools, the decay process starts reducing the complex molecules into less complex water-soluble components. This process moves biomass from these two pools to the soluble one, and for the unhydrolyzable pool it is controlled by this equation:

$$Unhydro_{C_{decay}} = C_{unhydro} * K_{unhydro} * T_{eff} * W_{eff} * CUE_{microbe} \quad [10]$$

where $C_{unhydro}$ is the carbon belongs to the unhydrolyzable pool, $K_{unhydro}$ is the maximum decay rate at optimal temperature and moisture. T_{eff}, W_{eff} and $CUE_{microbe}$ are the temperature, moisture microbial C/N effect as describe in the equations [5], [6] and [8], respectively. In the same way the hydrolyzable decay is controlled by the following equation:

$$Hydro\_C_{decay} = C_{Hydro} * K_{hydro} * T_{eff} * W_{eff} * CUE_{microbe} * LCI_{eff} \quad [11]$$

where C_{hydro} is the carbon of the hydrolyzable pool, K_{hydro} is the maximum decay rate at optimal temperature and moisture, while all the other efficiencies are the same presented for the $Unhydro\_C_{decay}$. In addition, the hydrolyzable pool decay is controlled by the LCI_{eff}. This coefficient is dynamically computed on the base of the hydrolyzable and unhydrolyzable biomass ratio and it is a proxy of the lignocellulose index, the ratio between acid-insoluble an acid-soluble + acid-insoluble as described by (Soong et al., 2015).

The unhydrolyzable and hydrolyzable pools are involved also in a process called "fragmentation" that represents the starting point of the buried biomass degradation. Through this process these pools lose mass which get incorporated into the POM pool, and from there it will follow the process related to this specific pool. Both the fragmentation processes for unhydrolyzable and hydrolyzable pools work in the same way following the equations:

$$Unhydro\_C_{frag} = C_{unhydro} * K_{frag\_unhydro} * T_{eff} * W_{eff} \quad [12]$$

$$Hydro\_C_{frag} = C_{hydro} * K_{frag_{hydro}} * T_{eff} * W_{eff} \quad [13]$$

where $C_{unhydro}$ and C_{hydro} represent the carbon in the unhydrolyzable and hydrolyzable pools respectively, $K_{frag\_unhydro}$ and K_{frag_hydro} represent the maximum fragmentation rates (see

Table 3) to produce POM while T_{eff} and W_{eff} are the effect of temperature and moisture as described in equations [5] and [6], respectively.

The last process related to the buried biomass is related to the soluble pool. This pool, that account for the low mass and water-soluble molecule, decays with a rate defined by the following equation:

$$Soluble\_C_{decay} = C_{soluble} * K_{soluble} * T_{eff} * LCI_{eff} \quad [14]$$

where $C_{soluble}$ represents the carbon in the soluble pool, $K_{soluble}$ represents the maximum decay, while T_{eff} and W_{eff} are the effect of temperature and moisture as described in equations [5] and [6], respectively. The LCI_{eff} coefficient is the lignocellulose index as computed by equation [11]. The amount of carbon computed with equation [14] goes into the DOM pool and it will be available for the microbial assimilation.

4.3.5 POM

The particulate organic matter pool follows a depolymerization pathway that is needed before this pool can get assimilated by microbes. This pool is made of large, insoluble molecules with high activation energies (Williams et al., 2018). The process that transforms the POM mass into a lighter and more accessible SOC component is called "depolymerization". This process is led by microbes and move SOM mass from the POM to the DOM pool. Here the equation:

$$POM\_C_{depolymerized} = C_{POM} * K_{POM} * T_{eff} * W_{eff} * CUE_{microbe} \quad [15]$$

where C_{POM} is the carbon of the POM pool, K_{POM} is the maximum decay rate at optimal temperature and moisture. T_{eff}, W_{eff} and $CUE_{microbe}$ are the temperature, moisture and microbial C/N effect as described in the equations [5], [6] and [8], respectively.

4.3.6 DOM

This labile pool is involved in two processes that link it to the microbe biomass and to the MAOM pool. The first process is the microbial assimilation: due to its high accessibility this pool is primarily assimilated by microbes. The first process is based on the DOM carbon mass availability and the microbe efficiency. The equation reflects the eq. [3] structure:

$$DOM\_C_{assimilated} = C_{DOM} * K_{DOM} * T_{eff} * W_{eff} * CUE_{microbe} * CUE_{DOM} \quad [16]$$

where C_{DOM} is the carbon of the DOM pool, K_{DOM} is the maximum decay rate at optimal temperature and moisture. T_{eff}, W_{eff}, $CUE_{microbe}$ and CUE_{DOM} are the temperature, moisture, DOM C/N ratio and microbial C/N ratio effects as described in the equations [5], [6], [7] and [8], respectively. The amount of carbon that cannot be assimilated by microbes goes in the atmosphere as CO_2 emission. This amount corresponds to:

$$CO_{2fromDOM} = C_{DOM} * K_{DOM} * T_{eff} * W_{eff} * CUE_{microbe} * (1 - CUE_{DOM}) \quad [17]$$

At the same time the DOM molecules get adsorbed to the mineral structure becoming formally part of the MAOM pool. This pathway is called "adsorption" and consists of DOM molecules being adsorbed by the MAOM mineral structure. The amount of carbon adsorbed and incorporated in the MAOM pool is defined as:

$$DOM_{C_{adsorbed}} = C_{DOM} * K_{adsorb} * WFPS^2 \quad [18]$$

where C_{DOM} is the carbon of the DOM pool, K_{adsorb} is the maximum sorption rate of DOM to become MAOM at optimal temperature and moisture (see Table 3), while *WFPS* is the water filled pore space. The amount of carbon that can be adsorbed on the mineral surface is limited by the amount of clay present in the soil. Once the soil saturation threshold is reached the carbon adsorption process stops.

4.3.7 MAOM

The MAOM pool, formed by carbon particles encapsulated by minerals, get assimilated from microbes and exchange carbon with the DOM pool. The carbon assimilation by the microbe pool is modelled like the equation [3]. The maximum decay rate is lower than the DOM rate (see Table 3) and the CUE_{MAOM} represents the specific carbon use efficiency based on the MAOM C/N ratio:

$$MAOM_{C_{assimilated}} = C_{MAOM} * K_{MAOM} * T_{eff} * W_{eff} * CUE_{microbe} * CUE_{MAOM} \quad [19]$$

where C_{MAOM} is the carbon of the MAOM pool while T_{eff}, W_{eff}, $CUE_{microbe}$ and CUE_{MAOM} are the temperature, moisture, microbial and pool C/N effects as described in the equations [5], [6], [8] and [7], respectively. As the carbon molecules get adsorbed to the minerals, they also

get desorpted in a process called "desorption". In this way these molecules go back being part of the DOM pool following this equation:

$$MAOM\_C_{desorbed} = C_{MAOM} * K_{desorp} * WFPS^2 \quad [20]$$

where C_{MAOM} is the carbon of the MAOM pool, K_{desorp} is the maximum desorption rate of MAOM to become DOM at optimal temperature and moisture (see Table 3), while *WFPS* is the water filled pore space.

4.3.8 The role of nitrogen

Nitrogen plays an important role in controlling the organic matter dynamic into the bulk soil. The nitrogen movements across all the pools follow the same pathways described in the previous paragraphs. In fact, according to their C/N ratio all the different pools have a specific nitrogen percentage that allow to figure out the correct amount of nitrogen moving from a pool to another. The amount of nitrogen of the different organic pools can change during time due to the varying composition of the organic material coming from the top of the soil (i.e., crop residues) or to the different physical condition that led to an increase/decrease of the microbial assimilation. Other than that, the ammonium and nitrate pools (Fig. 1), which form the mineral nitrogen in the bulk soil, also interact with microbes.

Microbes daily request an amount of nitrogen based on the carbon assimilation. After the carbon mass to be assimilated by microbes has been defined, the module calculates the amount of nitrogen coming from the specific pool. Every single pool can deliver a different amount of nitrogen to the microbe pool based on its C/N ratio. Then, this amount is reduced by the nitrogen use efficiency (NUE). The remaining nitrogen part (i.e., the amount that is not directly assimilated by microbes) goes into the mineral ammonium pool. The equation that controls the amount of nitrogen assimilated by microbes from DOM and MAOM pools is:

$$Microbial\_N_{assimilation} = \frac{C_{pool(i)} * K_{pool(i)} * T_{eff} * W_{eff} * CUE_{microbe}}{C_{pool(i)} / N_{pool(i)}} * (NUE) \quad [21]$$

where $C_{pool(i)}$ and $C_{pool(i)}$ are the carbon mass of the pool considered, $K_{pool(i)}$ is the maximum decay rate of the *i-th* pool considered at optimal temperature and moisture, while T_{eff} and W_{eff} are the effect of temperature and moisture. The $CUE_{microbe}$ is computed by the equation

[8]. In this implementation the NUE value is equal to the efficiency applied to compute the assimilated carbon amount, so it varies with the C/N ratio of the pool considered. As described above, the amount of nitrogen that goes to the mineral pool is computed as:

$$Mineral\_N_{from\_microbes} = \frac{C_{pool(i)} * K_{pool(i)} * T_{eff} * W_{eff} * CUE_{microbe}}{C_{pool(i)}/N_{pool(i)}} * (1 - NUE) \qquad [22]$$

The bulk soil mineral pool can increase due to the $Mineral\_N_{from\_microbes}$ coming from the microbial activity, but it can also be modified by the MCNC mechanism described in the "microbial C/N control" paragraph. The net mineral nitrogen release from microbes, namely the net mineralization, is then computed as:

$$Net\_mineralization = Mineral\_N_{from\_microbes} + N_{splilling} - N_{fishing} \qquad [23]$$

where the three addends come from equation [22] and [9], respectively.

Table 3. *Parameter names, definitions, unit and optimal range values belonging to the ARMOSA 2.0 release. The list of acronyms is CUE (carbon use efficiency), DOM (dissolved organic matter), POM (particulate organic matter) and MAOM (mineral-associated organic matter). Calibrated parameters are highlight in bold.*

Parameter	Definition	Unit	Optimal value or range	Reference
$\boldsymbol{K_{death}}$	**Microbial death rate**	d^{-1}	0.1-0.8	Zhang et al., 2021
Min	Microbial activity at minimum saturation value (percentage of the saturation value)	-	0	ARMOSA
OPT_{min}	Coefficient used to set the optimal minimum value of the moisture effect on decomposition activity (percentage of the saturation value)	-	0.9	
OPT_{max}	Coefficient used to set the optimal maximum value of the moisture effect on decomposition activity (percentage of the saturation value)	-	1.1	
MWC_1	Coefficient used to set the curve of the moisture effect on decomposition activity	-	1.5	
MWC_2	Coefficient used to set the curve of the moisture effect on decomposition activity	-	1	
M_{SAT}	Microbial activity at saturation	-	0	
$CN_{microbe\_MAX}$	Maximum C/N of microbial biomass	g C g^{-1} N	11.4	Zhang et al., 2021
$\boldsymbol{CUE_{MAX}}$	**Maximum CUE of microbes**	g C g^{-1} N	0.46-0.8	
CN_{CUE}	Coefficient used to calculate CUE as a function of substrate C/N	g C g^{-1} N	5-15	
$CN_{microbe\_MIN}$	Minimum C/N of microbial biomass	g C g^{-1} N	6.6	Zhang et al., 2021, Kästner et al., 2021, Kyker-Snowman et al., 2020
$CN_{microbe\_OPTmin}$	Minimum optimal C/N of microbial biomass	g C g^{-1} N	8.5	ARMOSA
$CN_{microbe\_OPTmax}$	Maximum optimal C/N of microbial biomass	g C g^{-1} N	9.9	
CN_{OPT}	Microbial optimal C/N	g C g^{-1} N	9	Zhang et al., 2021
$K_{frag\_unhydro}$	Maximum decay of the unhydrolyzable pool at optimal temperature and moisture	d^{-1}	0.001-0.02	Zhang et al., 2021
K_{frag_hydro}	Maximum decay of the hydrolyzable pool at optimal temperature and moisture	d^{-1}	0.01-0.05	
$K_{soluble}$	Maximum decay of the soluble pool at optimal temperature and moisture	d^{-1}	0.01-0.05	
K_{POM}	Maximum depolymerization of the POM pool at optimal temperature and moisture	d^{-1}	0.001-0.01	
$\boldsymbol{K_{DOM}}$	**Maximum decay of the DOM pool at optimal temperature and moisture**	d^{-1}	0.1-1	
K_{MAOM}	Maximum decay of the MAOM pool at optimal temperature and moisture	d^{-1}	0.1-1	
K_{adsorb}	Maximum sorption rate of DOM too MAOM at optimal temperature and moisture	d^{-1}	0.01-0.5	
K_{desorp}	Maximum desorption rate of DOM too MAOM at optimal temperature and moisture	d^{-1}	0.025-0.125	

4.4 Numerical integration and model initialization

The numerical integration is performed to calculate the values of all the different bulk soil pools at daily time step. Here how the general integration of each pool looks like:

$$Pool_{C\,(i)(t)} = Pool\_C_{(i)(t-1)} + Pool\_C_{input} - Pool\_C_{output} \quad [24]$$

where $Pool_{C\,(i)(t-1)}$ is the carbon content of the *i-th* pool at the previous time step, $Pool\_C_{input}$ represents all the carbon inputs that a specific pool receive while $Pool\_C_{output}$ represents all the carbon outputs removed from the pool.

The numerical integration for the mineral nitrogen pool works as follow:

$$Mineral\_N_{(t)} = Mineral\_N_{(t-1)} + Net\_mineralization - N_{fishing} + N_{splilling} \quad [25]$$

where $Mineral\_N_{(t-1)}$ is the nitrogen content at the previous time step, $Net\_mineralization$ represents the net nitrogen input as in equation [23] while $N_{fishing}$ and $N_{splilling}$ represent the nitrogen immobilized or mineralized from microbes as expressed in equation [9].

The model initialization is necessary for the model to get the initial value of each pool both for the carbon and nitrogen amount. To set all the initial pool masses, the model needs the carbon content (%), the C/N ratio and the bulk density for each layer considered in the simulation. Then, based on the percentage in table 4, the masses values can be computed. The model calculates the initialization for each pool until 40 cm; below this layer, all the initial carbon stock gets stored in the MAOM pool.

***Table 4**. Carbon content and C/N value at the beginning of each simulation for each bulk soil pools. The initial carbon content is expressed as a percentage (%) of the total SOM mass. The initial C/N is the ratio between the carbon and the nitrogen masses at the beginning of the simulation.*

Pool	Initial C content	Initial C/N	Reference
Microbe	2	9.5	Kyker-Snowman et al., 2020
DOM	2	10	Lavallee et al., 2020
POM	20	25	Internal dataset
MAOM	76	12	Internal dataset
Soluble	0		-
Hydro	0		-
Not-Hydro	0		-

4.5 Model performance: calibration and comparison of models

The final release of the model has been testing several times to understand the behaviors of the different pools and to detect the pool's behavior. The pools evolution (Fig.2) is different mainly because of the different process the different pools deal with and their different turnover times. For instance, the DOM pool never exceeds the 2 t ha^{-1} due to its high decay rate (see Table 3), while both POM and MAOM tent to slightly increase due to the annual crop biomass inputs into the soil, or because of the slow turnover, respectively. On the other hand, the microbial

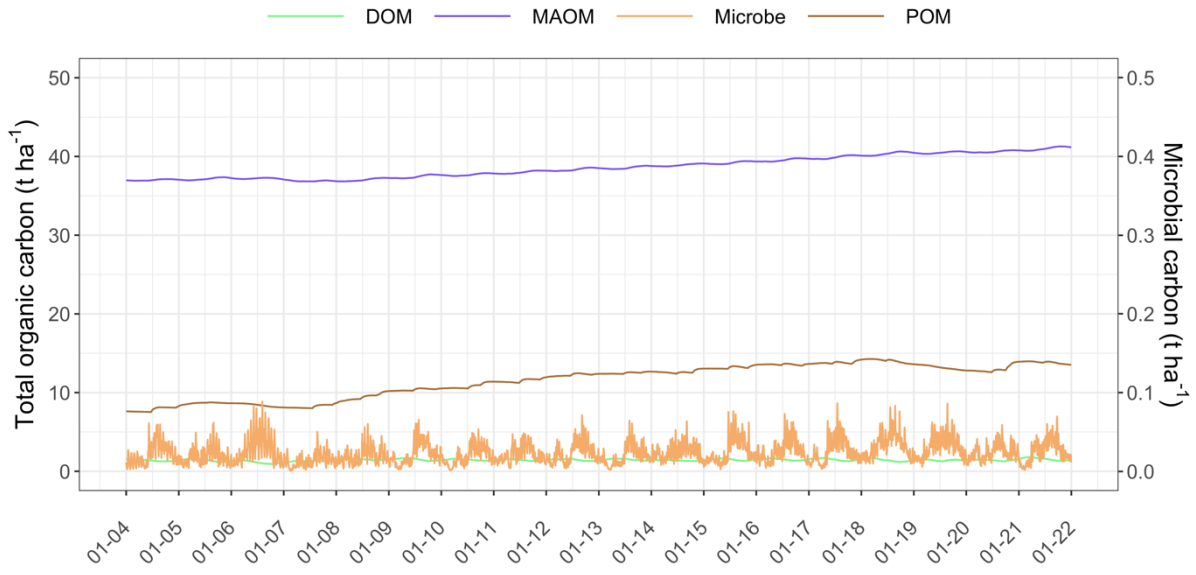

***Figure 2**. Evolution of the DOM, POM and MAOM pools in 20 years of minimum tillage management. The data shown in the graph refers to the top 30 cm layer.*

evolution in time is highly variable due to the high turnover rate of the microbial biomass. In fact, microbes tend to increase in response to a DOM or MAOM increase (i.e., the assimilation rate is proportional to the pool mass, as in equation [3]) but at the same time tent to reduce their biomass due to the high death rate when the assimilation is low (usually during the cold season). This initial test phase was conducted with default parameters, without a model calibration. To test the real model performance a set of four different carbon long-term experiment (LTE) datasets have been collected around Europe to increase the pedo-climatic variability to be represented by the model. Table 5 report the main characteristics of these four different locations.

***Table 5**. General information about the four locations considered to test the new ARMOSA release. Acronymous stand for CT, conventional till, MT, minimum till and NT, no till.*

Location	Country	Management	Texture	C (%)	Köppen Climate	LTE duration (year)
Canaleja	Spain	CT, MM, NT	loam	0.6	BSk	13
Changins (CA)	Switzerland	CT, MM	clay	2.9	Cfb	36
Changins (CL)	Switzerland	CT, MM	loam	1.1	Cfb	36
Foggia	Italy	MM, NT	clay	1	Csa	20

These locations were collected because (1) of the presence of different comparisons between soil managements and (2) a long-term SOC data collection.
To increase the model test quality we applied a multi-model comparison. This kind of model analysis belongs to a recent innovation in the use of crop models and it is based on a multi-models comparison on the same simulations (Ewert et al., 2015; Rosenzweig et al., 2013). In fact, these studies found that there is large variability in predictions between models, implying large uncertainty in predictions when a single model is used (Asseng et al., 2013; Bassu et al., 2014; Hasegawa et al., 2017; Rötter, Carter, Olesen, & Porter, 2011). The initial objective of these studies was to evaluate the uncertainty in the crop models predictions. Recently, it has been shown that the median of the models outputs was a good indicator of the central tendency of the models (Ehrhardt et al., 2018) and a better way to simulate a specific scenario instead of the single model utilization. In addition, the comparison of multiple models' output allows a greater comprehension of a single model behavior, because great differences between one model to another can be useful to detect any wrong model tendency.

Therefore, under the ARMOSA 2.0 testing process, the performance of this new release has been tested in comparison with the classical ARMOSA release (ARMOSA 1.0) and the SALUS

model. As described in the introduction, the ARMOSA 1.0 release shares with ARMOSA 2.0 all the algorithms except for those used for the new SOM dynamic simulation. This kind of comparison can be useful to understand if the new release is able to improve the actual SOM dynamic simulation, so the new algorithms have a real positive impact on the simulation. On the other hand, the SALUS (Systems Approach to Land-Use Sustainability) model is a cropping systems simulation platform that contains processed-based models derived from the well-validated CERES model, providing simulation of crop growth and development, and carbon, water, nitrogen (N), and phosphorus cycling dynamics on a daily time step (Martinez Feria and Basso, 2020). As ARMOSA, SALUS uses daily input values of incoming solar radiation (MJ/m2), maximum and minimum air temperature (°C), and rainfall (mm), as well as information on soil characteristics and management. SALUS has been tested extensively for simulating soil carbon dynamics (Basso et al., 2018, Senthilkumar et al., 2009) and for this reason has been selected as a benchmark to test the new ARMOSA 2.0 release performance.

Before the model comparison, all the three models have been calibrated with the trial-and-error procedure. This methodology is one of the most used one especially when few parameters are involved (Wallach et al., 2018). For each model no more than 4 parameters have been calibrated and their selection have been done based on previous modeling research paper. For the ARMOSA 2.0 model the calibrated parameters are shown in the table 3. As a first attempt, the use of physically defined, measurable pools allow for an easier model parameterization: the possibility to compare the same parameters with other models that already represents those SOM dynamics (i.e., DOM, POM and MAOM) allowed us to rank their importance on the SOC dependent variable.

The results of the model's simulations of the four different locations are represented in figure 3. All three models have generally followed SOC dynamics with a minimum calibration process. ARMOSA 2.0 had good performance having RMSE values almost equal to or better than other models (see Table 6). Analyzing one location at a time, we can denote that Spain has the lowest amount of carbon in the soil compared to the other sites. The SOC evolution over time (first 30 cm layer) is stable in conventional and minimum tillage. Probably, the climatic component (the site belongs to an arid area with low productivity) does not allow for an increase in the soil organic matter. Only the no-till management seems to have a higher SOC data variability. If in the first two cases, all the models reflected the linear SOC evolution, in the no-till management, none of the models succeeded in the SOC oscillations representation.

We had a different situation for the two locations in Switzerland, where the organic matter is much higher. Usually, this soil condition leads to a slow OM perturbation over time. This is true in the CL site, where the SOC stock did not vary in more than 30 years. The CA site seems slightly different, probably because of the high clay content that can support a possible SOC increase. In all these cases, ARMOSA 2.0 got good results regarding the capacity to represent the long-term SOC dynamic. The last site in Foggia (Italy) was the most controversial one. The measured data represented a high variability in a few years, a hard situation to be represented by any model and probably due to different sampling timing along the year or different sampling/analysis methodology. Besides, all the models were initialized more than ten years before the first measured point (because of a previous measurement taken years before). They could still simulate the positive trend due to the SOC delta between the measurements.

***Table 6**. RMSE values of the three models for each combination of location and management.*

Location	Management	RMSE		
		ARMOSA 1.0	**ARMOSA 2.0**	**SALUS**
Canaleja (Spain)	Conventional till	8.7	6.3	2.2
Canaleja (Spain)	Minimum till	2.7	3.7	2.4
Canaleja (Spain)	No till	8.5	12.2	4.9
Changins (CA) (Switzerland)	Conventional till	4.4	5.4	5.5
Changins (CA) (Switzerland)	Minimum till	3.1	2.6	3.6
Changins (CL) (Switzerland)	Conventional till	2.7	2.4	2.8
Changins (CL) (Switzerland)	Minimum till	4.9	2.8	6.0
Foggia (Italy)	Minimum till	8.4	8.8	3.5
Foggia (Italy)	No till	4.4	3.7	7.6

These general positive results are not exhaustive because of the previous calibration. Nevertheless, with few parameters calibrated, the model produced realistic outputs and got comparable results compared to the previous ARMOSA release and the SALUS model. The good results provided by ARMOSA 2.0 reflected the new pool's capability to represent the SOM dynamic. The inclusion of locations under conservation agriculture management (with minimum or no-till management) allowed us to focus our attention on how minimum soil disturbance or residue left on the surface can affect the SOC dynamics. In these locations, the topsoil directly receives aboveground residues, primary inputs to POM. In contrast, the deeper layers receive less residue biomass (because of null or superficial tillage events), more DOM

(from roots decomposition) and microbially derived compounds, which are primary inputs to MAOM. In addition, the SOC evaluation over long-term periods can depend on the MAOM saturation limit. ARMOSA 2.0 based this threshold on the soil texture (especially the clay content), so the capability to store highly persistent, stable, mineral associate carbon depends on the soil texture. This aspect can improve the final output in specific situation where the clay content plays a big role.

All these mechanisms captured the SOC evolution over time with a good accuracy and they will be the basis for future research or more detailed study on this topic.

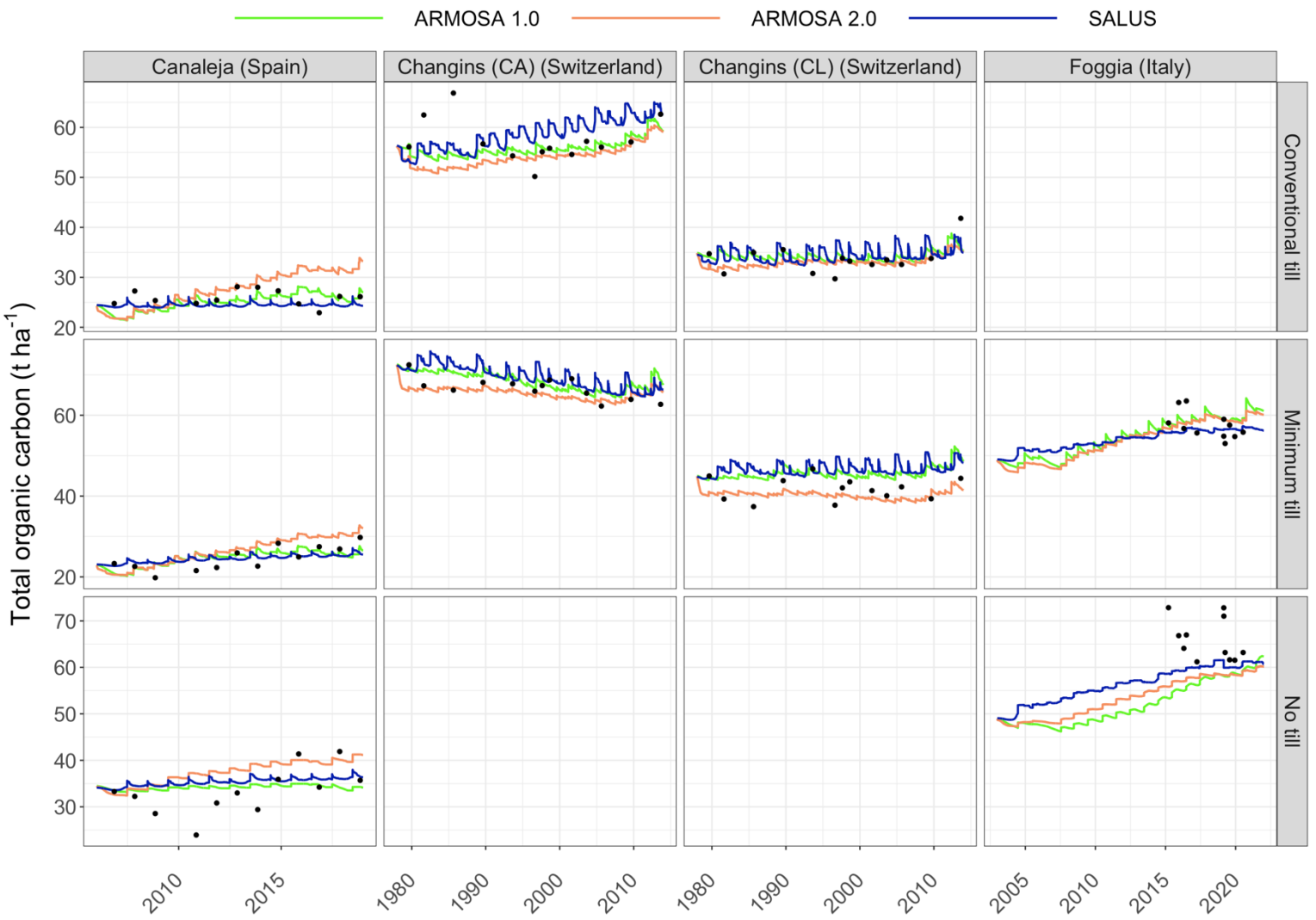

***Figure 3**. Temporal course of simulated (colored lines) and observed (black dots) SOC data in four locations (Canalaja, Spain, Changins CA, Switzerland, Changins CL, Switzerland and Foggia, Italy) and three different managements (conventional, minimum and no till). The three calibrated models are represented in green (ARMOSA 1.0), orange (ARMOSA 2.0) and blue (SALUS).*

Reference

Allison, S.D., Wallenstein, M.D., Bradford, M.A., 2010. Soil-carbon response to warming dependent on microbial physiology. Nature Geosci 3, 336–340. https://doi.org/10.1038/ngeo846

Andrieu, N., Howland, F., Acosta-Alba, I., Le Coq, J.-F., Osorio-Garcia, A.M., Martinez-Baron, D., Gamba-Trimiño, C., Loboguerrero, A.M., Chia, E., 2019. Co-designing Climate-Smart Farming Systems With Local Stakeholders: A Methodological Framework for Achieving Large-Scale Change. Front. Sustain. Food Syst. 3, 37. https://doi.org/10.3389/fsufs.2019.00037

Bahadori, M., Chen, C., Lewis, S., Boyd, S., Rashti, M.R., Esfandbod, M., Garzon-Garcia, A., Van Zwieten, L., Kuzyakov, Y., 2021. Soil organic matter formation is controlled by the chemistry and bioavailability of organic carbon inputs across different land uses. Science of The Total Environment 770, 145307. https://doi.org/10.1016/j.scitotenv.2021.145307

Baker, J.M., Ochsner, T.E., Venterea, R.T., Griffis, T.J., 2007. Tillage and soil carbon sequestration—What do we really know? Agriculture, Ecosystems & Environment 118, 1–5. https://doi.org/10.1016/j.agee.2006.05.014

Basso, B., Dumont, B., Maestrini, B., Shcherbak, I., Robertson, G.P., Porter, J.R., Smith, P., Paustian, K., Grace, P.R., Asseng, S., Bassu, S., Biernath, C., Boote, K.J., Cammarano, D., De Sanctis, G., Durand, J. □L., Ewert, F., Gayler, S., Hyndman, D.W., Kent, J., Martre, P., Nendel, C., Priesack, E., Ripoche, D., Ruane, A.C., Sharp, J., Thorburn, P.J., Hatfield, J.L., Jones, J.W., Rosenzweig, C., 2018. Soil Organic Carbon and Nitrogen Feedbacks on Crop Yields under Climate Change. Agric. environ. lett. 3, 180026. https://doi.org/10.2134/ael2018.05.0026

Basso, B., Hyndman, D.W., Kendall, A.D., Grace, P.R., Robertson, G.P., 2015. Can Impacts of Climate Change and Agricultural Adaptation Strategies Be Accurately Quantified if Crop Models Are Annually Re-Initialized? PLoS ONE 10, e0127333. https://doi.org/10.1371/journal.pone.0127333

Basso, B., Ritchie, J.T., n.d. Simulating Crop Growth and Biogeochemical Fluxes in Response to Land Management Using the SALUS Model 23.

Blanco-Canqui, H., Ruis, S.J., 2018. No-tillage and soil physical environment. Geoderma 326, 164–200. https://doi.org/10.1016/j.geoderma.2018.03.011

Bongiorno, G., Bünemann, E.K., Oguejiofor, C.U., Meier, J., Gort, G., Comans, R., Mäder, P., Brussaard, L., de Goede, R., 2019. Sensitivity of labile carbon fractions to tillage

and organic matter management and their potential as comprehensive soil quality indicators across pedoclimatic conditions in Europe. Ecological Indicators 99, 38–50. https://doi.org/10.1016/j.ecolind.2018.12.008

Burke, I.C., Kaye, J.P., Bird, S.P., Hall, S.A., McCulley, R.L., Sommerville, G.L., 2004. 13 Evaluating and Testing Models of Terrestrial Biogeochemistry: The Role of Temperature in Controlling Decomposition, in: Canham, C.D., Cole, J.J., Lauenroth, W.K. (Eds.), Models in Ecosystem Science. Princeton University Press, pp. 225–253. https://doi.org/10.1515/9780691228846-015

Campbell, E.E., Parton, W.J., Soong, J.L., Paustian, K., Hobbs, N.T., Cotrufo, M.F., 2016. Using litter chemistry controls on microbial processes to partition litter carbon □uxes with the Litter Decomposition and Leaching (LIDEL) model. Soil Biology 15.

Coleman, K., Jenkinson, D.S., 1996. RothC-26.3 - A Model for the turnover of carbon in soil, in: Powlson, D.S., Smith, P., Smith, J.U. (Eds.), Evaluation of Soil Organic Matter Models. Springer Berlin Heidelberg, Berlin, Heidelberg, pp. 237–246. https://doi.org/10.1007/978-3-642-61094-3_17

Cooper, J., Baranski, M., Stewart, G., Nobel-de Lange, M., Bàrberi, P., Fließbach, A., Peigné, J., Berner, A., Brock, C., Casagrande, M., Crowley, O., David, C., De Vliegher, A., Döring, T.F., Dupont, A., Entz, M., Grosse, M., Haase, T., Halde, C., Hammerl, V., Huiting, H., Leithold, G., Messmer, M., Schloter, M., Sukkel, W., van der Heijden, M.G.A., Willekens, K., Wittwer, R., Mäder, P., 2016. Shallow non-inversion tillage in organic farming maintains crop yields and increases soil C stocks: a meta-analysis. Agron. Sustain. Dev. 36, 22. https://doi.org/10.1007/s13593-016-0354-1

Cotrufo, M.F., Ranalli, M.G., Haddix, M.L., Six, J., Lugato, E., 2019. Soil carbon storage informed by particulate and mineral-associated organic matter. Nat. Geosci. 12, 989–994. https://doi.org/10.1038/s41561-019-0484-6

Cotrufo, M.F., Soong, J.L., Horton, A.J., Campbell, E.E., Haddix, M.L., Wall, D.H., Parton, W.J., 2015. Formation of soil organic matter via biochemical and physical pathways of litter mass loss. NATURE GEOSCIENCE 8, 6.

Dai, F., Zhou, Q., Lv, Z., Wang, X., Liu, G., 2014. Spatial prediction of soil organic matter content integrating artificial neural network and ordinary kriging in Tibetan Plateau. Ecological Indicators 45, 184–194. https://doi.org/10.1016/j.ecolind.2014.04.003

Dwivedi, D., Riley, W.J., Torn, M.S., Spycher, N., Maggi, F., Tang, J.Y., 2017. Mineral properties, microbes, transport, and plant-input pro□les control vertical distribution and age of soil carbon stocks. Soil Biology 16.

Ehrhardt, F., Soussana, J., Bellocchi, G., Grace, P., McAuliffe, R., Recous, S., Sándor, R., Smith, P., Snow, V., de Antoni Migliorati, M., Basso, B., Bhatia, A., Brilli, L., Doltra, J., Dorich, C.D., Doro, L., Fitton, N., Giacomini, S.J., Grant, B., Harrison, M.T., Jones, S.K., Kirschbaum, M.U.F., Klumpp, K., Laville, P., Léonard, J., Liebig, M., Lieffering, M., Martin, R., Massad, R.S., Meier, E., Merbold, L., Moore, A.D., Myrgiotis, V., Newton, P., Pattey, E., Rolinski, S., Sharp, J., Smith, W.N., Wu, L., Zhang, Q., 2018. Assessing uncertainties in crop and pasture ensemble model simulations of productivity and N 2 O emissions. Glob Change Biol 24, e603–e616. https://doi.org/10.1111/gcb.13965

Griscom, B.W., Adams, J., Ellis, P.W., Houghton, R.A., Lomax, G., Miteva, D.A., Schlesinger, W.H., Shoch, D., Siikamäki, J.V., Smith, P., Woodbury, P., Zganjar, C., Blackman, A., Campari, J., Conant, R.T., Delgado, C., Elias, P., Gopalakrishna, T., Hamsik, M.R., Herrero, M., Kiesecker, J., Landis, E., Laestadius, L., Leavitt, S.M., Minnemeyer, S., Polasky, S., Potapov, P., Putz, F.E., Sanderman, J., Silvius, M., Wollenberg, E., Fargione, J., 2017. Natural climate solutions. Proc. Natl. Acad. Sci. U.S.A. 114, 11645–11650. https://doi.org/10.1073/pnas.1710465114

Haddaway, N.R., Hedlund, K., Jackson, L.E., Kätterer, T., Lugato, E., Thomsen, I.K., Jørgensen, H.B., Isberg, P.-E., 2017. How does tillage intensity affect soil organic carbon? A systematic review. Environ Evid 6, 30. https://doi.org/10.1186/s13750-017-0108-9

Haddix, M.L., Gregorich, E.G., Helgason, B.L., Janzen, H., Ellert, B.H., Cotrufo, M.F., 2020. Climate, carbon content, and soil texture control the independent formation 7 and persistence of particulate and mineral-associated organic matter in soil 10.

Holzworth, D.P., Huth, N.I., deVoil, P.G., Zurcher, E.J., Herrmann, N.I., McLean, G., Chenu, K., van Oosterom, E.J., Snow, V., Murphy, C., Moore, A.D., Brown, H., Whish, J.P.M., Verrall, S., Fainges, J., Bell, L.W., Peake, A.S., Poulton, P.L., Hochman, Z., Thorburn, P.J., Gaydon, D.S., Dalgliesh, N.P., Rodriguez, D., Cox, H., Chapman, S., Doherty, A., Teixeira, E., Sharp, J., Cichota, R., Vogeler, I., Li, F.Y., Wang, E., Hammer, G.L., Robertson, M.J., Dimes, J.P., Whitbread, A.M., Hunt, J., van Rees, H., McClelland, T., Carberry, P.S., Hargreaves, J.N.G., MacLeod, N., McDonald, C., Harsdorf, J., Wedgwood, S., Keating, B.A., 2014. APSIM – Evolution towards a new generation of agricultural systems simulation. Environmental Modelling & Software 62, 327–350. https://doi.org/10.1016/j.envsoft.2014.07.009

Izaurralde, R.C., Williams, J.R., McGill, W.B., Rosenberg, N.J., Jakas, M.C.Q., 2006. Simulating soil C dynamics with EPIC: Model description and testing against long-term data. Ecological Modelling 192, 362–384. https://doi.org/10.1016/j.ecolmodel.2005.07.010

Jarecki, M., Grant, B., Smith, W., Deen, B., Drury, C., VanderZaag, A., Qian, B., Yang, J., Wagner-Riddle, C., 2018. Long-term Trends in Corn Yields and Soil Carbon under Diversified Crop Rotations. J. Environ. Qual. 47, 635–643. https://doi.org/10.2134/jeq2017.08.0317

Kaiser, K., Kalbitz, K., 2012. Cycling downwards – dissolved organic matter in soils. Soil Biology and Biochemistry 52, 29–32. https://doi.org/10.1016/j.soilbio.2012.04.002

Kästner, M., Miltner, A., Thiele-Bruhn, S., Liang, C., 2021. Microbial Necromass in Soils—Linking Microbes to Soil Processes and Carbon Turnover. Front. Environ. Sci. 9, 756378. https://doi.org/10.3389/fenvs.2021.756378

Kyker-Snowman, E., Wieder, W.R., Frey, S.D., Grandy, A.S., 2020. Stoichiometrically coupled carbon and nitrogen cycling in the MIcrobial-MIneral Carbon Stabilization model version 1.0 (MIMICS-CN v1.0). Geosci. Model Dev. 13, 4413–4434. https://doi.org/10.5194/gmd-13-4413-2020

Lavallee, J.M., Soong, J.L., Cotrufo, M.F., 2020. Conceptualizing soil organic matter into particulate and mineral□associated forms to address global change in the 21st century. Glob Change Biol 26, 261–273. https://doi.org/10.1111/gcb.14859

Lugato, E., Lavallee, J.M., Haddix, M.L., Panagos, P., Cotrufo, M.F., 2021. Different climate sensitivity of particulate and mineral-associated soil organic matter. Nat. Geosci. 14, 295–300. https://doi.org/10.1038/s41561-021-00744-x

Lugato, E., Panagos, P., Bampa, F., Jones, A., Montanarella, L., 2014. A new baseline of organic carbon stock in European agricultural soils using a modelling approach. Glob Change Biol 20, 313–326. https://doi.org/10.1111/gcb.12292

Luo, Y., Ahlström, A., Allison, S.D., Batjes, N.H., Brovkin, V., Carvalhais, N., Chappell, A., Ciais, P., Davidson, E.A., Finzi, A., Georgiou, K., Guenet, B., Hararuk, O., Harden, J.W., He, Y., Hopkins, F., Jiang, L., Koven, C., Jackson, R.B., Jones, C.D., Lara, M.J., Liang, J., McGuire, A.D., Parton, W., Peng, C., Randerson, J.T., Salazar, A., Sierra, C.A., Smith, M.J., Tian, H., Todd□Brown, K.E.O., Torn, M., Groenigen, K.J., Wang, Y.P., West, T.O., Wei, Y., Wieder, W.R., Xia, J., Xu, Xia, Xu, Xiaofeng, Zhou, T., 2016. Toward more realistic projections of soil carbon dynamics by Earth

system models. Global Biogeochem. Cycles 30, 40–56. https://doi.org/10.1002/2015GB005239

Luo, Z., Wang, E., Zheng, H., Baldock, J.A., Sun, O.J., Shao, Q., 2015. Convergent modelling of past soil organic carbon stocks but divergent projections. Biogeosciences 12, 4373–4383. https://doi.org/10.5194/bg-12-4373-2015

Manzoni, S., Taylor, P., Richter, A., Porporato, A., Ågren, G.I., 2012. Environmental and stoichiometric controls on microbial carbon□use efficiency in soils. New Phytologist 196, 79–91. https://doi.org/10.1111/j.1469-8137.2012.04225.x

Martinez□Feria, R., Basso, B., 2020. Predicting soil carbon changes in switchgrass grown on marginal lands under climate change and adaptation strategies. GCB Bioenergy 12, 742–755. https://doi.org/10.1111/gcbb.12726

Martre, P., Wallach, D., Asseng, S., Ewert, F., Jones, J.W., Rötter, R.P., Boote, K.J., Ruane, A.C., Thorburn, P.J., Cammarano, D., Hatfield, J.L., Rosenzweig, C., Aggarwal, P.K., Angulo, C., Basso, B., Bertuzzi, P., Biernath, C., Brisson, N., Challinor, A.J., Doltra, J., Gayler, S., Goldberg, R., Grant, R.F., Heng, L., Hooker, J., Hunt, L.A., Ingwersen, J., Izaurralde, R.C., Kersebaum, K.C., Müller, C., Kumar, S.N., Nendel, C., O'leary, G., Olesen, J.E., Osborne, T.M., Palosuo, T., Priesack, E., Ripoche, D., Semenov, M.A., Shcherbak, I., Steduto, P., Stöckle, C.O., Stratonovitch, P., Streck, T., Supit, I., Tao, F., Travasso, M., Waha, K., White, J.W., Wolf, J., 2015. Multimodel ensembles of wheat growth: many models are better than one. Glob Change Biol 21, 911–925. https://doi.org/10.1111/gcb.12768

McGill, W.B., Myers, R.J.K., 2015. Controls on Dynamics of Soil and Fertilizer Nitrogen, in: Follett, R.F., Stewart, J.W.B., Cole, C.V., Power, J.F. (Eds.), SSSA Special Publications. Soil Science Society of America and American Society of Agronomy, Madison, WI, USA, pp. 73–99. https://doi.org/10.2136/sssaspecpub19.c5

Minasny, B., Malone, B.P., McBratney, A.B., Angers, D.A., Arrouays, D., Chambers, A., Chaplot, V., Chen, Z.-S., Cheng, K., Das, B.S., Field, D.J., Gimona, A., Hedley, C.B., Hong, S.Y., Mandal, B., Marchant, B.P., Martin, M., McConkey, B.G., Mulder, V.L., O'Rourke, S., Richer-de-Forges, A.C., Odeh, I., Padarian, J., Paustian, K., Pan, G., Poggio, L., Savin, I., Stolbovoy, V., Stockmann, U., Sulaeman, Y., Tsui, C.-C., Vågen, T.-G., van Wesemael, B., Winowiecki, L., 2017. Soil carbon 4 per mille. Geoderma 292, 59–86. https://doi.org/10.1016/j.geoderma.2017.01.002

Mitchell, E., Scheer, C., Rowlings, D., Conant, R.T., Cotrufo, M.F., Grace, P., 2018. Amount and incorporation of plant residue inputs modify residue stabilisation dynamics in soil

organic matter fractions. Agriculture, Ecosystems & Environment 256, 82–91. https://doi.org/10.1016/j.agee.2017.12.006

Mondal, S., Chakraborty, D., Bandyopadhyay, K., Aggarwal, P., Rana, D.S., 2020. A global analysis of the impact of zero□tillage on soil physical condition, organic carbon content, and plant root response. Land Degrad Dev 31, 557–567. https://doi.org/10.1002/ldr.3470

Mueller, L., Schindler, U., Mirschel, W., Shepherd, T.G., Ball, B.C., Helming, K., Rogasik, J., Eulenstein, F., Wiggering, H., 2010. Assessing the productivity function of soils. A review. Agron. Sustain. Dev. 30, 601–614. https://doi.org/10.1051/agro/2009057

Ogle, S.M., Breidt, F.J., Easter, M., Williams, S., Killian, K., Paustian, K., 2010. Scale and uncertainty in modeled soil organic carbon stock changes for US croplands using a process-based model. Global Change Biology 16, 810–822. https://doi.org/10.1111/j.1365-2486.2009.01951.x

Ogle, S.M., Breidt, F.J., Paustian, K., 2005. Agricultural management impacts on soil organic carbon storage under moist and dry climatic conditions of temperate and tropical regions. Biogeochemistry 72, 87–121. https://doi.org/10.1007/s10533-004-0360-2

Orgiazzi, A., Ballabio, C., Panagos, P., Jones, A., Fernández□Ugalde, O., 2018. LUCAS Soil, the largest expandable soil dataset for Europe: a review. Eur J Soil Sci 69, 140–153. https://doi.org/10.1111/ejss.12499

Panagos, P., Hiederer, R., Van Liedekerke, M., Bampa, F., 2013. Estimating soil organic carbon in Europe based on data collected through an European network. Ecological Indicators 24, 439–450. https://doi.org/10.1016/j.ecolind.2012.07.020

Parton, W.J., Stewart, J.W.B., Cole, C.V., 1988. Dynamics of C, N, P and S in grassland soils: a model. Biogeochemistry 5, 109–131. https://doi.org/10.1007/BF02180320

Paustian, K., Lehmann, J., Ogle, S., Reay, D., Robertson, G.P., Smith, P., 2016. Climate-smart soils. Nature 532, 49–57. https://doi.org/10.1038/nature17174

Perego, A., Giussani, A., Sanna, M., Fumagalli, M., Carozzi, M., Brenna, S., Acutis, M., 2013. The ARMOSA simulation crop model: overall features, calibration and validation results 16.

Pr□v□lie, R., Patriche, C., Borrelli, P., Panagos, P., Ro□ca, B., Dumitra□cu, M., Nita, I.-A., S□vulescu, I., Birsan, M.-V., Bandoc, G., 2021. Arable lands under the pressure of multiple land degradation processes. A global perspective. Environmental Research 194, 110697. https://doi.org/10.1016/j.envres.2020.110697

Robertson, A.D., Paustian, K., Ogle, S., Wallenstein, M.D., Lugato, E., Cotrufo, M.F., 2019. Unifying soil organic matter formation and persistence frameworks: the MEMS model. Biogeosciences 16, 1225–1248. https://doi.org/10.5194/bg-16-1225-2019

Sándor, R., Barcza, Z., Hidy, D., Lellei-Kovács, E., Ma, S., Bellocchi, G., 2016. Modelling of grassland fluxes in Europe: Evaluation of two biogeochemical models. Agriculture, Ecosystems & Environment 215, 1–19. https://doi.org/10.1016/j.agee.2015.09.001

Sándor, R., Ehrhardt, F., Grace, P., Recous, S., Smith, P., Snow, V., Soussana, J.-F., Basso, B., Bhatia, A., Brilli, L., Doltra, J., Dorich, C.D., Doro, L., Fitton, N., Grant, B., Harrison, M.T., Kirschbaum, M.U.F., Klumpp, K., Laville, P., Léonard, J., Martin, R., Massad, R.-S., Moore, A., Myrgiotis, V., Pattey, E., Rolinski, S., Sharp, J., Skiba, U., Smith, W., Wu, L., Zhang, Q., Bellocchi, G., 2020. Ensemble modelling of carbon fluxes in grasslands and croplands. Field Crops Research 252, 107791. https://doi.org/10.1016/j.fcr.2020.107791

Senthilkumar, S., Basso, B., Kravchenko, A.N., Robertson, G.P., 2009. Contemporary Evidence of Soil Carbon Loss in the U.S. Corn Belt. Soil Sci. Soc. Am. J. 73, 2078–2086. https://doi.org/10.2136/sssaj2009.0044

Sinsabaugh, R.L., Turner, B.L., Talbot, J.M., Waring, B.G., Powers, J.S., Kuske, C.R., Moorhead, D.L., Follstad Shah, J.J., 2016. Stoichiometry of microbial carbon use efficiency in soils. Ecol Monogr 86, 172–189. https://doi.org/10.1890/15-2110.1

Smith, P., Cotrufo, M.F., Rumpel, C., Paustian, K., Kuikman, P.J., Elliott, J.A., McDowell, R., Griffiths, R.I., Asakawa, S., Bustamante, M., House, J.I., Sobocká, J., Harper, R., Pan, G., West, P.C., Gerber, J.S., Clark, J.M., Adhya, T., Scholes, R.J., Scholes, M.C., 2015. Biogeochemical cycles and biodiversity as key drivers of ecosystem services provided by soils. SOIL 1, 665–685. https://doi.org/10.5194/soil-1-665-2015

Smith, P., Davies, C.A., Ogle, S., Zanchi, G., Bellarby, J., Bird, N., Boddey, R.M., McNamara, N.P., Powlson, D., Cowie, A., Noordwijk, M., Davis, S.C., Richter, D.D.B., Kryzanowski, L., Wijk, M.T., Stuart, J., Kirton, A., Eggar, D., Newton-Cross, G., Adhya, T.K., Braimoh, A.K., 2012. Towards an integrated global framework to assess the impacts of land use and management change on soil carbon: current capability and future vision. Glob Change Biol 18, 2089–2101. https://doi.org/10.1111/j.1365-2486.2012.02689.x

Smith, P., Lutfalla, S., Riley, W.J., Torn, M.S., Schmidt, M.W.I., Soussana, J. □F., 2018. The changing faces of soil organic matter research. Eur J Soil Sci 69, 23–30. https://doi.org/10.1111/ejss.12500

Soares, M., Rousk, J., 2019. Microbial growth and carbon use efficiency in soil: Links to fungal-bacterial dominance, SOC-quality and stoichiometry. Soil Biology and Biochemistry 131, 195–205. https://doi.org/10.1016/j.soilbio.2019.01.010

Sokol, N.W., Sanderman, J., Bradford, M.A., 2019. Pathways of mineral□associated soil organic matter formation: Integrating the role of plant carbon source, chemistry, and point of entry. Glob Change Biol 25, 12–24. https://doi.org/10.1111/gcb.14482

Soong, J.L., Parton, W.J., Calderon, F., Campbell, E.E., Cotrufo, M.F., 2015. A new conceptual model on the fate and controls of fresh and pyrolized plant litter decomposition. Biogeochemistry 124, 27–44. https://doi.org/10.1007/s10533-015-0079-2

Sun, W., Canadell, J.G., Yu, Lijun, Yu, Lingfei, Zhang, W., Smith, P., Fischer, T., Huang, Y., 2020. Climate drives global soil carbon sequestration and crop yield changes under conservation agriculture. Glob Change Biol 26, 3325–3335. https://doi.org/10.1111/gcb.15001

Topa, D., Cara, I.G., Jit□reanu, G., 2021. Long term impact of different tillage systems on carbon pools and stocks, soil bulk density, aggregation and nutrients: A field meta-analysis. CATENA 199, 105102. https://doi.org/10.1016/j.catena.2020.105102

Valkama, E., Kunypiyaeva, G., Zhapayev, R., Karabayev, M., Zhusupbekov, E., Perego, A., Schillaci, C., Sacco, D., Moretti, B., Grignani, C., Acutis, M., 2020. Can conservation agriculture increase soil carbon sequestration? A modelling approach. Geoderma 369, 114298. https://doi.org/10.1016/j.geoderma.2020.114298

Van Soest, P.J., Robertson, J.B., Lewis, B.A., 1991. Methods for Dietary Fiber, Neutral Detergent Fiber, and Nonstarch Polysaccharides in Relation to Animal Nutrition. Journal of Dairy Science 74, 3583–3597. https://doi.org/10.3168/jds.S0022-0302(91)78551-2

Vargas, F., González, Z., Sánchez, R., Jiménez, L., Rodríguez, A., 2012. CELLULOSIC PULPS OF CEREAL STRAWS AS RAW MATERIAL FOR THE MANUFACTURE OF ECOLOGICAL PACKAGING 10.

Wallach, D., Martre, P., Liu, B., Asseng, S., Ewert, F., Thorburn, P.J., Ittersum, M., Aggarwal, P.K., Ahmed, M., Basso, B., Biernath, C., Cammarano, D., Challinor, A.J., De Sanctis, G., Dumont, B., Eyshi Rezaei, E., Fereres, E., Fitzgerald, G.J., Gao, Y., Garcia□Vila, M., Gayler, S., Girousse, C., Hoogenboom, G., Horan, H., Izaurralde, R.C., Jones, C.D., Kassie, B.T., Kersebaum, K.C., Klein, C., Koehler, A., Maiorano, A., Minoli, S., Müller, C., Naresh Kumar, S., Nendel, C., O'Leary, G.J., Palosuo, T.,

Priesack, E., Ripoche, D., Rötter, R.P., Semenov, M.A., Stöckle, C., Stratonovitch, P., Streck, T., Supit, I., Tao, F., Wolf, J., Zhang, Z., 2018. Multimodel ensembles improve predictions of crop–environment–management interactions. Glob Change Biol 24, 5072–5083. https://doi.org/10.1111/gcb.14411

Wallach, D., Palosuo, T., Thorburn, P., Hochman, Z., Gourdain, E., Andrianasolo, F., Asseng, S., Basso, B., Buis, S., Crout, N., Dibari, C., Dumont, B., Ferrise, R., Gaiser, T., Garcia, C., Gayler, S., Ghahramani, A., Hiremath, S., Hoek, S., Horan, H., Hoogenboom, G., Huang, M., Jabloun, M., Jansson, P.-E., Jing, Q., Justes, E., Kersebaum, K.C., Klosterhalfen, A., Launay, M., Lewan, E., Luo, Q., Maestrini, B., Mielenz, H., Moriondo, M., Nariman Zadeh, H., Padovan, G., Olesen, J.E., Poyda, A., Priesack, E., Pullens, J.W.M., Qian, B., Schütze, N., Shelia, V., Souissi, A., Specka, X., Srivastava, A.K., Stella, T., Streck, T., Trombi, G., Wallor, E., Wang, J., Weber, T.K.D., Weihermüller, L., de Wit, A., Wöhling, T., Xiao, L., Zhao, C., Zhu, Y., Seidel, S.J., 2021. The chaos in calibrating crop models: Lessons learned from a multi-model calibration exercise. Environmental Modelling & Software 145, 105206. https://doi.org/10.1016/j.envsoft.2021.105206

Wieder, W.R., Bonan, G.B., Allison, S.D., 2013. Global soil carbon projections are improved by modelling microbial processes. Nature Clim Change 3, 909–912. https://doi.org/10.1038/nclimate1951

Williams, E.K., Fogel, M.L., Berhe, A.A., Plante, A.F., 2018. Distinct bioenergetic signatures in particulate versus mineral-associated soil organic matter. Geoderma 330, 107–116. https://doi.org/10.1016/j.geoderma.2018.05.024

Woolf, D., Lehmann, J., 2019. Microbial models with minimal mineral protection can explain long-term soil organic carbon persistence. Sci Rep 9, 6522. https://doi.org/10.1038/s41598-019-43026-8

Wutzler, T., Reichstein, M., 2008. Colimitation of decomposition by substrate and decomposers – a comparison of model formulations 11.

Zhang, Y., Lavallee, J.M., Robertson, A.D., Even, R., Ogle, S.M., Paustian, K., Cotrufo, M.F., 2021. Simulating measurable ecosystem carbon and nitrogen dynamics with the mechanistically de□ned MEMS 2.0 model 25.

Chapter 5. General discussion

5.1 Introductory remarks

This thesis reports on the outcome of a research entitled "carbon sequestration under conservation agriculture: study and modelling of carbon dynamic". This PhD work aims to improve the existing modelling tools that allow quantifying and evaluating the conservation agriculture (CA) impact on SOC sequestration with a specific link to the ARMOSA cropping system model (Valkama et al., 2020, Perego et al., 2013). The specific objectives were:

1. provide an overview of the conservation agriculture impact on soil organic carbon;
2. provide a numerical tool that help SOC data collection through an automatic SOC stock and its SD computation;
3. develop a new module to be integrated into the ARMOSA model that explicitly include surface residue degradation;
4. develop and test a new ARMOSA release accounting for a new bulk soil SOM conceptualization based on measurable and physical defined pools.

The PhD intends to improve the ARMOSA capability to reproduce the effect of different soil management on soil organic carbon sequestration with particular attention to the CA practices. This chapter attempts to provide an overall synthesis of the work done, and to give an indication of how the research findings have contributed to a better understanding of the problems, to solving these problems, and to progressing science.

5.2 Discussion

5.2.1 Conservation agriculture as a beneficial practice for SOC sequestration

To define which conservation agriculture practices, impact the most on SOC sequestration and to quantify their single impact I reviewed the previous scientific research published between 1998 and 2020 with a meta-analytical approach. The research focus was related to the Mediterranean and humid sub-tropical areas. These areas would benefit the most from an organic matter increase because of the low soil fertility and dry climate. The results of this first analysis described that the conservation agriculture performance dramatically depends on multiple factors. In fact, based on a different initial SOC stock amount, the effect of CA on SOC accumulation can be much more correlated to crop residue retention (up to 20% more carbon stock under CA management), clay content (up to 12% more carbon stock with a 60%

of clay in the soil under CA management) or duration of the management application (up to 20% more carbon stock with a 10-year CA application). This first attempt to quantify the impact of CA on SOC sequestration based on previous works allowed me to focus my attention on those aspects that impact the most in the subsequent analysis and simulation models' improvement.

***Figure 1**. Remotely sensed image of a soybean field during harvest in Springport, MI (United States). The field has been farmed with conservation agriculture management. All the residues are left on the soil surface until the next sowing date. Photo credits: Richard Price, Bruno Basso lab (https://basso.ees.msu.edu/index.html).*

5.2.2 Are models an effective way to represent SOC dynamics?

Given the importance of SOC to crop productivity (Jarecki et al., 2018) and the potential for climate change to affect SOC stocks (Minasny et al., 2017), it is important to have the most reliable representation of the SOC dynamics into the agricultural soil through a full cropping system model (Basso et al., 2018). These models represent the whole system (i.e., soil, crop, atmosphere), so they can account for all the interactions between its different components.

The present work allowed us to define a new version of the ARMOSA full cropping system model that can represent different soil management scenarios across multiple pedo-climatic

conditions with an advanced SOC modelling approach. Developing this new ARMOSA release, specific attention has been devoted to improving the model to simulate conservation agriculture management. The model can now simulate different crop rotations, minimum tillage operations and continuous soil covering through surface crop residues in this scenario.

5.2.3 How can we improve the ARMOSA model SOC dynamic representation?

Based on the previous results and on the need to get reliable model outputs in the SOC simulation, I defined which were the ARMOSA requirements that would improve the general model reliability. For this reason, I developed a specific module that accounts for the surface crop residue degradation that was not previously considered. This module defines a more accurate way for the ARMOSA model to simulate the carbon dynamics in agricultural soils. In fact, in the previous ARMOSA version, the non-inclusion of the superficial carbon and nitrogen inputs to the soil (i.e., from the surface residue degradation) would allow other processes to compensate for this lack, disconnecting the model from the real process occurring at the field level. Besides that, the surface residue decomposition resulted highly dependent on the soil temperature and water content variation. Therefore, the model's capability to react to a variation of these conditions is a key improvement due to the rising temperatures and lack of water that will affect agriculture under the future climate change scenario (Basso et al., 2018). In addition, the new frontier of precision agriculture research is moving toward quantifying surface residue through the combination of productivity yield maps and satellite images. In the near future, models able to represent the surface residue evolution will be part of this quantification process. On the other hand, besides the carbon input from the surface, the core of the SOC dynamic representation occurs at the bulk soil level, where the atmospheric CO_2 concentrations can be stored, increasing the carbon stock (Griscom et al., 2017). Again, even though many carbon-oriented models represent in detail the bulk soil carbon dynamic, only the full cropping system model has the reliability to be identified as a decision support tool. This is due to their accuracy in predicting the C dynamics and to the ability to response to environmental and management drivers using the current scientific understanding (Cotrufo et al., 2015, Sokol et al., 2019). In addition, the very last scientific modelling guides suggested that these models should ideally be verifiable using physically defined and measurable pools (namely DOM, dissolved organic matter, POM, particulate organic matter and MAOM, mineral associated organic matter) rather than only with conceptual pools as for most historical ecosystem models (Zhang et al., 2021). For this reason, I developed a new ARMOSA 2.0 release that gathers the robustness of the

classical ARMOSA version, with a new SOM dynamic conceptualization accounting for these last scientific achievements. This new release has yielded promising results regarding the different pool representations and the evolution of the pools reflected in the data collected from the literature. In this last release, the central role of the microbe is worth mentioning as a "microbially explicit" approach has been integrated into th ARMOSA 2.0 version. Thus, microbial biomass now directly leads the decomposition process of the SOM pools. This improvement places ARMOSA 2.0 as a potential model candidate for several international projects where the capability of reproducing microbial activity is currently an essential requirement.

5.2.4 How does the new ARMOSA 2.0 release perform in comparison with other models?

As the last step of my Ph.D. activities, I tested the ARMOSA 2.0 release compared to the previous ARMOSA 1.0 version and the SALUS model. This comparison was based on measured carbon data collected across different countries and allowed me to test the performance of the new release in the simulation of conventional, minimum and no-till management. It has to be highlighted that the calibration procedure has been conducted on the minimum possible number of parameters for all the models. This intentional choice comes from the necessity of a new generation model to use the most parsimonious method in data calibration (Zhang et al., 2021). The current and future necessity to run models across countries on a large scale points out the need for models that can be run without a considerable calibration effort and using few high-impact parameters. The RMSE coefficients (5.3 for ARMOSA 1.0, 5.2 for ARMOSA 2.0 and 4.3 for SALUS, on average from all the simulations) retrieved from the three models are promising since ARMOSA 2.0 performed equal or, in specific cases, even better than the other two competitors. The specific behaviour of the different pools allowed to captured specific characteristic of the CA management. For instance, with a CA management the topsoil directly receives aboveground residues that are primary inputs to POM. In contrast, the deeper layers receive less residue biomass (because of null or superficial tillage events), more DOM (from roots decomposition) and microbially derived compounds, which are primary inputs to MAOM. In addition, in ARMOSA 2.0 the capability to store highly persistent, stable, mineral associate carbon (MAOM) depends on the soil texture. This aspect can improve the final output in specific situation highly contrasting soil type.

5.3 Conclusions

The capability of this new model release to capture the SOC pathways across different soil management practices will be extremely useful in predicting how conservation agriculture can impact SOC across different climates and locations. In the future, this improved understanding of the SOM dynamics will ultimately provide more reliable agronomic feedback for use in land management, global change mitigation, and food security. For this reason, it will be a priority for agronomists and policymakers across the globe.

Based on the results of this work, ARMOSA 2.0 would possibly improve in different ways. The DOM pool, for example, is known to be able to move from one soil layer to another with water movements. At the same time, the POM pool is continuously degraded by the soil microbiota and then moved between different layers in a phenomenon called "bioturbation". These two processes, related to DOM and POM, can provide even more reliability in the SOC stock estimation at different soil depths.

ARMOSA 2.0 was tested against carbon data expressed as total organic carbon in the model comparison work. The main reason was the difficulty of finding long-term datasets with SOM data measured by different pools (i.e., DOM, POM and MAOM). From a future perspective, it would be helpful to include datasets with pool measurements to get a clearer idea of each pool's behaviour.

A more extensive model ensemble procedure can be added to the model evaluation, especially with the inclusion of new models that explicitly account for these new SOM dynamics. That would allow a broader vision of the model performance compared to a larger model community.

Acknowledgements

During these three years, I had the opportunity to come across many different researchers and professors who helped me complete this work. I feel grateful to all of them because I have always met friendly and genuine people before scientists.

I want to start from Marco Acutis and Alessia Perego. If they didn't trust me, I wouldn't be at the end of this trip. Thanks for believing in me and supporting me every single day. Marco, I found in you a great example of how a scientist should be. Always curious, experienced and interested in improving science. I think every student should have a teacher like you. Alessia, thanks for being my everyday guide. You have been such a great friend, capable of understanding emotions underneath the tough science life.

Thanks to Mara Gabbrielli, a lovely friend and colleague sharing this trip with me. I think that this experience wouldn't be the same without you.

Thanks to Marco Botta for being such a nice office mate and friend. Your kindness and friendship are what make a day a better day.

Thanks to Elena Valkama, that guided me at the beginning of this experience. Your concreteness in science taught me a lot.

Thanks to Calogero Schillaci to be always available to debate and discuss about science with me.

Thanks to Bruno Basso, who nicely welcomed and guided me in the "New World" and will allow me to continue this trip with another incredible experience! And thanks to all the colleagues and friends I met in Lansing that helped me during such a unique experience abroad.

Thanks to Luca Bechini, Pietro Marino and Giorgio Ragaglini for your support and advice during this trip.

Thanks to my Mamma, Papà and sister for supporting me during this period and making me feel at home whenever I come back from abroad. I will need you all forever.

Thanks to all the other PhD colleagues (Chiara, Federico, Ermes, Roberta and all the others) for the reciprocal support during these three years!!